THE IMPACT OF CLIMATE VARIABILITY ON THE PRODUCTION OF BLACK SEA ANCHOVY: A MODELING STUDY

A THESIS SUBMITTED TO
GRADUATE SCHOOL OF MARINE SCIENCES
OF
MIDDLE EAST TECHNICAL UNIVERSITY

BY

CEREN GÜRASLAN

IN PARTIAL FULFILMENT OF THE REQUIREMENTS
FOR
THE DEGREE OF MASTER OF SCIENCE
IN
THE DEPARTMENT OF PHYSICAL OCEANOGRAPHY

SEPTEMBER 2010

THE IMPACT OF CLIMATE VARIABILITY ON THE PRODUCTION OF BLACK SEA ANCHOVY: A MODELING STUDY

submitted by **CEREN GÜRASLAN** in partial fulfilment of the requirements for the degree of **Master of Sciences in the Department of Physical Oceanography, Middle East Technical University** by,

Prof. Dr. Ferit Bingel _____
Director, **Graduate School of Marine Sciences**

Prof. Dr. Emin Özsoy _____
Head of Department, **Physical Oceanography**

Asst. Prof. Dr. Bettina Fach Salihoğlu _____
Supervisor, **Physical Oceanography Dept., METU**

Prof. Dr. Temel Oğuz _____
Co-Supervisor, **Physical Oceanography Dept., METU**

Examining Committee Members:

Asst. Prof. Dr. Bettina Fach Salihoğlu _____
Graduate School of Marine Sciences, METU

Prof. Dr. Temel Oğuz _____
Graduate School of Marine Sciences, METU

Asst. Prof. Dr. Barış Salihoğlu _____
Graduate School of Marine Sciences, METU

Prof. Dr. Ferit Bingel _____
Graduate School of Marine Sciences, METU

Prof. Dr. Zahit Uysal _____
Graduate School of Marine Sciences, METU

Date: _____

I hereby declare that all information in this document has been obtained and presented in accordance with academic rules and ethical conduct. I also declare that, as required by these rules and conduct, I have fully cited and referenced all material and results that are not original to this work.

Name, Last Name: CEREN GÜRASLAN

Signature :

ABSTRACT

THE IMPACT OF CLIMATE VARIABILITY ON THE PRODUCTION OF BLACK SEA ANCHOVY: A MODELING STUDY

Güraslan, Ceren
M. S., Department of Physical Oceanography
Supervisor: Asst. Prof. Dr. Bettina Fach Salihoğlu
Co-Supervisor: Prof. Dr. Temel Oğuz
September 2010, 101 pages

The influence of climate variability on anchovy eggs and larvae production and trophic interactions within the Black Sea ecosystem was studied with a one-dimensional, coupled lower trophic level and anchovy bioenergetics model that includes parameterizations for a gelatinous predator. Stochastic climate variability in the form of fifty-year interannual temperature and total mixing rate time series were used to simulate how climate-mediated effects cascade across different trophic levels and how the anchovy population responds to environmental disturbances. Model results reveal a high correlation of anchovy egg production and recruitment success in response to changes in temperature and complex and highly nonlinear interactions in the lower trophic level. Moreover, results indicated that temperature variation has a significant long-term control over egg production and larval survival rates. Thus, the results indicate that an increase of 2 °C in summer mean temperatures causes egg production to start 30 days earlier, whereas a 2 °C drop in summer mean temperatures causes a 45 days delay in egg production start with respect to baseline conditions. Further analyses suggest that daily temperatures in the spawning season have a stronger control over the intensity of egg production as compared to the amount of available spawners. Although, temperature has a direct effect on anchovy

egg and larvae production by influencing mortality as well as production and growth rates, it indirectly influences plankton production by modulating the mixed layer depth, which affects phytoplankton blooms and zooplankton availability, the major food source of anchovy. In addition, the combination of both the temperature and total mixing effects reveals temperature dominance for the higher trophic level, where the temperature effect is slightly diminished by the total mixing effects. In conclusion, the strong linkage between the climate variability and anchovy production and recruitment numbers implies an important prediction potential for the model for short term anchovy stock estimations. With some modifications the model has a potential to serve for fisheries management purposes.

Keywords: Black Sea anchovy, ecosystem modeling, environmental variability, trophic cascades, anchovy population dynamics

ÖZ

İKLİM DEĞİŞKENLİĞİNİN KARADENİZ HAMSİSİNİN ÜRETİMİ ÜZERİNE ETKİSİ: BİR MODELLEME ÇALIŞMASI

Güraslan, Ceren
Yüksek Lisans, Fiziksel Oşinografi Bölümü
Tez Yöneticisi: Yrd. Doç. Dr. Bettina Fach Salihoğlu
Ortak Tez Yöneticisi: Prof. Dr. Temel Oğuz
Eylül 2010, 101 sayfa

İklim değişkenliğinin hamsi yumurta ve larva üretimi üzerine ve Karadeniz ekosistemindeki trofik etkileşimlere yaptığı etki, tek boyutlu, jelatinli predatör için parametrizasyonlar içeren birleştirilmiş alçak trofik seviye ve hamsi yaşam döngüsü modeli ile çalışılmıştır. İklim aracılığıyla gelen etkilerin farklı trofik seviyeler boyunca nasıl aktarıldığı ve hamsi populasyonunun çevresel düzensizliklere nasıl tepki verdiği, elli senelik, yıl içi deniz suyu sıcaklığı ve toplam karışım hızı formundaki stokastik iklim değişkenliği zaman serisi kullanılarak incelenmiştir. Model sonuçları, sıcaklık değişkenliği ile hamsi yumurta üretiminin ve içgöç başarısının, ayrıca yüksek derecede lineer olmayan alçak trofik seviyedeki etkileşimlerinin yüksek korrelasyon verdiğini göstermiştir. Üstelik sonuçlar sıcaklık değişiminin, hamsi yumurta üretimi ve larva yaşam oranlarını uzun vadeli olarak kontrol ettiğini de göstermektedir. Buna göre, ortalama yaz sıcaklıklarında 2 °C'lik artışın yumurtlama sezonunun başlangıcını 30 gün öne çektiği ve sıcaklıklarda 2 °C'lik düşüşün ise yumurtlama sezonunun başlangıcını 45 gün kadar ertelediği sonucu ortaya çıkmıştır. İleri analizler, yumurta üretim şiddetinin üzerinde, yumurtlama dönemindeki ortalama sıcaklıkların etkisinin, yumurtlayıcı sayısının yaptığı etkiden daha büyük olduğu önermesini yapmıştır. Yapılan analizler, hamsi yumurta ve larva üretiminde sıcaklığın etkisinin, onun mortaliteyle beraber

yumurtlama ve büyüme oranlarını da doğrudan etkilemesi yoluyla ortaya çıktığını, buna karşın, karışmış tabaka derinliklerini modüle etmesi suretiyle de, plankton üretimini ve hamsinin ana besin kaynağı olan zooplanktonun bolluğunu da dolaylı bir şekilde etkilediğini ortaya koymaktadır. Bunlara ilaveten, sıcaklık etkisinin baskın olduğu yüksek trofik seviyede, sıcaklık ve toplam karışım değişkenliğinin kombine etkisi incelendiğinde, toplam karışımın etkisinin sıcaklık etkisini hafifçe bastırdığı ortaya çıkmıştır. Sonuçta, iklim değişkenliği ile hamsi içgöç sayısının kuvvetli bağlantısı, modelin kısa zamanlı hamsi stok tahminleri açısından önemli bir öngörü potensiyeli sunduğunu göstermiştir. Belirli modifikasyonlarla model, balıkçılık yönetimi maksatlarına da hizmet edebilme potansiyeli taşımaktadır.

Anahtar Kelimeler: Karadeniz hamsisi, ekosistem modellemesi, çevresel değişkenlik, trofik aktarımlar, hamsi popülasyon dinamikleri

To my mother Bahar Güraslan, my father Ahmet Güraslan,
my grand parents, Güngör and Metin,my cousins Başak and Begüm

and to the memory of Soner Ali Yılmaz…

ACKNOWLEDGMENTS

I would like to express my deepest appreciation to Asst. Prof. Dr. Bettina Fach Salihoğlu, my supervisor, for her inspiration, invaluable guidance and support throughout the course of my research. Dr. B. Fach Salihoğlu has been an excellent mentor and given me the strength to discover and expand my limits. I would also like to extend my indebtedness to Prof. Dr. Temel Oğuz, whom generously given me the opportunity to work with his model. Without his expertise and criticism, this research would never been completed. Apart from the thesis study, his thoughts have always given me enthusiasm and contributed me in developing a scientific perspective.

I am very grateful to Prof. Dr. Ferit Bingel and Prof. Dr. Zahit Uysal for their contribution through valuable feedback from fisheries perspective.

I am also sending my sincere gratitude to the ecosystem modelers group, especially Asst. Prof. Dr. Barış Salihoğlu and Dr. Heather Anne Cannaby, for their constant interaction and encouraging support.

I would like to extend my kindest regards to my friend and my colleague, Özgür Gürses. His interest in this study and his humanity will always be well-respected.

I am explicitly thankful to Ekin Akoğlu, for his assistance in programming.

It should also worth recognition that I am very grateful to all the people in **METU, Institute of Marine Sciences** and **R/V Bilim2** for providing me the facilities to work with.

TABLE OF CONTENTS

LIST OF TABLES

TABLES

LIST OF FIGURES

FIGURES

1 INTRODUCTION

The Black Sea is the largest anoxic water body in the world. Within the second half of the last century it has gone through several transitions in its physical and biogeochemical characteristics. At the beginning of 1960s it was identified by a healthy and stable environment sheltering high diversity of species in its oligotrophic waters, then its ecosystem destabilized as a response to being subjected to several disturbances operated within the course of few decades. These disturbances include increasing anthropogenic nutrient input in response to increased fertilizer consumption in the former Soviet Union Countries at the Danube catchment basin, excessive fishing, introduction of non-native species (e.g. *Mnemiopsis leidyi*) and climate-induced effects (Oğuz, 2005a,b). The result of these processes was disastrous and the Black Sea lost many of its commercially valuable marine resources irreversibly (including mammals, large pelagics and demersals) at the end of 1960s, followed by the collapse of small pelagic fishes (mainly anchovy, sprat) and medium size pelagic fishes (bonito, mackerel) at the end of 1980s. In addition, the coincidence between the time of anchovy stock decline and the outburst of opportunistic gelatinous carnivores is still not resolved completely and demands for a reasonable explanation in terms of cause and effect (Oğuz et al., 2008a). Only then, more effective marine resource management policies can be developed to release a recently deteriorated ecosystem from a highly eutrophic state, invasion or over-exploitation, or to prevent future fisheries from drastic regime shifts causing a in depletion of commercially valuable fish stocks.

1.1 Physical Characteristics of the Black Sea

The Black Sea is a semi-enclosed basin extending between the latitudes of 41° to 46° N and longitudes of 28° to 41.5° E. It shares boundaries with Europe, Anatolia and the

Caucasus. It is connected to the Mediterranean Sea via the straits of Bosphorus and Dardanelles, called the Turkish Straits System (Oğuz et al., 2005c). In the north, it is connected to the Sea of Azov through Kerch Strait.

It spreads over 432,000 km² approximately, has total volume of 547,000 km³ and extends down to a maximum depth of 2200 m. In terms of water budget, the Black Sea possesses positive water balance, as influx via rainfall (~300 $km^3\ yr^{-1}$) and river discharge (~350 $km^3\ yr^{-1}$) is greater than outflux via evaporation (~350 $km^3\ yr^{-1}$) (Ünlüata et al., 1989; Özsoy and Ünlüata, 1997). The difference represents the net outflow from the Bosphorus Strait.

The Black Sea is very unique for its oceanographic properties. The high degree of density gradient between the surface waters which receive continuous supply from three of Europe's largest rivers (i.e. Danube, Dniepr and Dniestr) and the deeper waters almost blocks vertical mixing (Oğuz et al., 1998). Being nearly isolated from exchanges with the neighboring environments due to landmasses, the lateral oxygen supply to the deep basin is limited (Oğuz et al., 1998). Because of this, persistent anoxic conditions prevail over 87% of the whole basin (Oğuz et al., 1998).

However, the upper layer circulation system exhibits some major formations such as the Rim Current, a cyclonic boundary flow system that is flowing over the steep continental shelf topography, further intensifying in winter. Acoustic Doppler Current Profiler (ADCP) based studies measured the speed of the Rim Current as 50-100 cm/s at the surface and 10-20 cm/s in between depths of 150-300 m. (Oğuz and Beşiktepe, 1999). In addition, there are two cyclonic gyres circling within the peripheral flow with a number of anti-cyclonic eddies located at the coastal side of the Rim Current; namely the Bosphorus, Sakarya, Sinop, Kızılırmak, Batumi, Sukhumi, Caucasus, Kerch, Crimea, Sevastopol, Danube, Constantsa and Kaliakra eddies (Oğuz et al., 1998). Moreover, the Rim Current structure breaks into two branches near the southern Cape of Crimea. They unite to form the Rim Current again at the south of Kaliakra coast. Additionally there is a meso-scale anti-cyclonic formation off the Romanian coast (Oğuz et al., 1998b).

1.2 Ecosystem Characteristics of the Black Sea

From the 1960s to 1990s, the Black Sea ecosystem, contrary to other well-managed inland seas, went through a multi-staged dramatic environmental degradation. The Black Sea ecosystem was profoundly altered under increasing anthropogenic input through River Danube, intense fishing such as removing a total of 75 million tons of marine animals, introduction of alien species, toxic industrial waste release, damming of the major rivers and regional climate changes (Oğuz et al., 2005). Consequently, the commercial fish stocks such as anchovy *Engraulis encrasicolus ponticus* and sprat *Sprat sprattus* rised significantly throughout late1960s to 1980s and later collapsed at the beginning of 1990s (Prodanov et al., 1997; Ivanov and Panayotova 2001; Daskalov, 2003; Oğuz, 2007; Oğuz and Gilbert, 2007). The major elements of its food web structure are briefly reviewed below.

Phytoplankton

The increase in eutrophication altered the phytoplankton structure of the Black Sea concomitantly, such as the diatom to dinoflagellate ratio reported for the north western coast (Bologa, 1986). It was observed to be 76% during the period between 1960 and 1970 and then decreased to 46% during 1972 to 1977. Such qualitative changes signify the appearance of new species in the system (Bat et al., 2007). For example, *Gonyaulax polygramma*, *Raciborshiella salina* and *Eutreptia lanowii* are among the species reported for the first time in the Black Sea waters (Mihnea, 1985). Moreover, quantitative-based studies carried out at the Romanian coast yield a decrease in diatom ratios over the whole phytoplankton taxa from 92.3 % during the period from 1960 to 1970 to 62.2 % within 1983 to 1988, while the dinoflagellate ratio increased from 7.6 % to 30.9 % for the corresponding periods (Bodeanu, 1989). Additionally, at the mouth of the River Danube, a red tidal algae, *Noctiluca scintillans*, was found at a biomass value of 100 g l^{-1}, since then, *Noctiluca* blooms have become a common feature in the Black Sea ecosystem (Caddy and Griffiths, 1990). Since they are small, the phytoplankton groups are very vulnerable to physically- and/or chemically mediated changes in the

system (Bat et al., 2007).

Zooplankton

The zooplankton community was mainly regulated by the gelatinous predator *Aurelia aurita* from the mid-1970s to 1987. In the early 1980s the alien ctenophore *Mnemiopsis leidyi* was introduced into the Black Sea (Shiganova et al., 2001) and took over the control of the system as the top-predator from 1989 to 1991 (Oğuz et al., 2001b). *Mnemiopsis* is the unsatiable consumer of edible zooplankton, which means its feeding potential increases directly as its size increase. Thus, it makes *Mnemiopsis* the competitor of anchovy, competing for anchovy's favorite zooplankton food source copepoda (Tsikhon-Lukanina 1991 and 1993). *Mnemiopsis* has been shown to actively predate on anchovy eggs and larvae (Cowan and Houde, 1993). Accordingly, the clearance of these small copepods by *Mnemiopsis* resulted in a lack of availability of suitable small sized copepods for anchovy larvae. Consequently, this gelatinous predator directly affects zooplankton and fish eggs and larvae through predation (Shiganova, 1998; Shiganova and Bulgakova, 2000) and indirectly affects planktivorous fish (e.g. anchovy) while competing for food sources, which may have one cause of the severe decline of fisheries at the end of 1980s (Kıdeyş, 1994; Kıdeyş et al., 2000).

1.3 Black Sea Anchovy (*Engraulis encrasicolus ponticus*)

The Black Sea anchovy is a short-lived (3 to 4 years) migratory species that spawns in batches. One female anchovy lays between 13.000 to 40.000 eggs during the spawning season (Bat et al., 2007). The spawning occurs when temperatures are above 20°C and the optimum temperature is between 23-25°C (Niermann et al., 1994; Adrianov et al., 1996; Sorokin, 2002), the optimum salinity is 12-18 ‰, the optimum pH 8.3-8.4 (Demir, 1959) and 5-10 m. is the optimum spawning depth in coastal regions (Slastenenko, 1956). The chances for survival of individual eggs spawned by a female anchovy are around % 25-35, larvae and juvenile anchovy survival rates are highly dependent on the abundance and quality of the planktonic food source (Pavloskaya, 1955). Moreover, the

minimum temperature for the growth of the anchovy larvae is 13 °C, maximum spawning intensity is possible only when the temperature is higher than 20 °C (Demir, 1959). Anchovy eggs develop into early larvae, then late larvae and juveniles until reaching sexual maturity in one year. Maturity of a population is defined as the point when 50% of the juveniles become sexually mature.

The North Western Shelf is believed to be the region where the majority of anchovy spawns (Niermann et al., 1994) and forages in the summer. Then in winter, they migrate to the Turkish coasts with warmer conditions for overwintering purposes (Bat et al., 2007), to supply their high metabolic demands (Oğuz et al., 2008a).

Their schooling behavior makes them the primary target species of fisheries at the end of 1970s when the predation pressure imposed by the large pelagics and demersals diminished (Daskalov, 2003; Oğuz et al., 2008a). With the top-predators missing, the system shifted to a simpler food web with anchovy being at top-predator level (Oğuz et al., 2008a,b). Thus, its estimated standing stock size elevated by four-fold from mid-1960s to 1980 (Prodanov, 1997; Ivanov and Panayotova 2001). These high numbers were maintained for a decade with some fluctuations and then an abrupt transition back to the low stock regime took place between 1989-1990 under increasing fishing pressure and the influence of competition for food resources as well as predation by *Mnemiopsis* (Oğuz et al., 2008b).

1.4 Environmental Changes

There are numerous studies indicating close linkage between global scale weather systems and the Black Sea's regional climate conditions (Niermann et al., 1999; Oğuz, 2005b; Oğuz et al., 2006; Oğuz and Gilbert, 2007). Among those climate conditions, the most dominant one is the North Atlantic Oscillation (NAO) index, which is described by the normalized sea level atmospheric pressure difference between the 'Azores high' and 'Iceland low' pressure centers (Marshall et al., 2001). A positive mode of this index indicates a greater degree of pressure difference between both centers. In this case, the Black Sea region is under control of the Azore high pressure system, facing elevated

levels of air pressure at the surface, decreased evaporation and lower sea surface temperatures (SST) and air temperatures (Oğuz et al., 2005). In contrast, when the NAO is in a negative mode, lower pressure gradient exists between Azores and Iceland, which leads to moderate and rather moist winter conditions with temperate sea water and air temperatures (Oğuz et al., 2005).

During 1960s to 1980s a warm period took place in the Black Sea, coinciding with mild mean winter SST's (December to March) (Rayner et al., 2003) and warm mean Cold Intermediate Layer (CIL) temperatures (May to November) (Belokopytov, 1998). This trend preceded a positive index phase from 1980 to 1995 with cool patterns in winter. Especially the years from 1985 to 1987 and 1991 to 1993 exhibited the most severe winter conditions of the last century as winter mean-upper layer temperatures decreasing down to 7.2 °C (Oğuz, 2005b).

1.5 Long-term Changes in Ecosystem Properties

1960s:

The late 1960s were characterized by heavy fishing of large apex predator fishes, dolphins and demersals that led to an order of magnitude increase in the stocks of intermediate trophic level planktivorous pelagic fish. Anchovy became the most abundant species with sprat as second in abundance. Due to the decreasing predation pressure by higher trophic level fish anchovy experienced a marked population increase from estimated low values (~300 kt) to moderately high values (~700 kt) from the end of 1960s to the first half of 1970s. This event has been referred to as the first transition event (TR1) (Oğuz et al, 2008a), by which the trophic cascade was reorganized with anchovy at the apex predator level. Correspondingly, anchovy became the primary target species of the purse seine fleet in the absence of piscivorous fish.

Late 1970s:

During the second half of 1970s a major deviation in the biomass, phylogeny and taxonomy of the plankton community took place due to a strong increase in

eutrophication in response to increasing anthropogenic nutrient load from rivers discharging into the North Wester Shelf. For example, the mean biomass of the phytoplankton that was observed around 1 g m^{-2} in 1960s in the northwestern part of the basin, reached up to 19 g m^{-2} in the 1970s (Zaitsev et al., 1997). In addition, diatoms, the most abundant phytoplankton community prior to 1970s, were replaced by dinoflagellates and coccolithophores (Mikaelyan, 1997; Moncheva et al., 1997; Uysal et al., 1998). Moreover, the early spring and autumn succession of phytoplankton blooms a characteristic feature of the pre-eutrophication phase (before 1970s). But the ecosystem was shifted to more intensive summer peaks during 1970s (Mikaelyan, 1997; Moncheva and Krastev, 1997; Uysal et al., 1998). The reason behind these phenomena lays in the critical role of River Danube. While the inorganic nitrogen and phosphorus input from Danube lead to their enrichment in the northwestern shelf area, dam construction activities on its branches at the beginning of 1970s (Humborg et al., 1997) prevented the release of silicate load into the basin (Moncheva and Krastev, 1997). As a result diatoms which are highly dependent on silicate availability were replaced by smaller sized phytoplankton taxa. For example, populations of the diatoms *Leptocyclindrus danicus* and *Ditylum brightwellii* were reduced in biomass and instead the harmful marine dinoflagellate *Prorocentrum micans* and the coccolithophore *Emiliania huxleyi* increased in biomass (Zaitsev and Aleksandrov, 1997).

As a consequence of increased primary production, mesozooplankton biomass increased after the mid-1970s till early 1980s (Porumb, 1989) and fish stocks reached high stocks (~1500 kt) at 1979 - 1980 (Prodanov et al., 1997). This is called the second transition (TR2) event (Oğuz et al., 2008a) and driven by the bottom-up control operated for over a decade.

1980s:

An abrupt drop in winter temperatures during the 1980s caused more intense winter mixing and with it stronger recycling of nutrients available in the chemocline layer that had accumulated due to the nutrient enrichment process (Oğuz et al., 2005). Higher entrainment rates in this period provided an increased nutrient supply to the biologically

active layer, triggering intense vernal phytoplankton blooms that led to the presence of a high mesozooplankton biomass in the system. By the mid-1980s, mesozooplankton suddenly declined in biomass (more than 80%) under combined predation pressure exerted by *Noctiluca scintillans*, *Aurelia aurita*, *Pleurobrachia rhodopis* and planktivorous fishes (Oğuz et al., 2005). As there was food shortage in the system, jellies was not able to impose serious threat to anchovy which outcompetes the other predators under such conditions (Oğuz et al., 2008a).

The medusae *Aurelia aurita* was the dominant jellyfish in the Black Sea from late 1970s to early 1980s. It was replaced by the alien ctenophore *Mnemiopsis leidyi* soon after its accidental introduction into the Black Sea during the 1980s (Shushkina et al., 1998; Kovalev et al., 1998; Shiganova, 1998; Kıdeyş et al., 2000). The severity of the winters persisting during 1980s suppressed the growth and reproduction characteristics of the *Mnemiopsis*, and postponed *Mnemiopsis* outburst until a warmer period took over from 1988 to 1990 (Oğuz et al., 2008b). The outburst of *Mnemiopsis* incidentally coincided with the collapse of anchovy stocks subjected to fishing pressure. This was the most drastic collapse event (more than 5-fold) reported in the world fisheries (Oğuz and Gilbert, 2007). Accordingly, the anchovy catch at the Turkish coast declined from 295 ktons to 66 ktons between 1988 and 1990 (Anonymous, 2004) while a sudden outburst of *Mnemiopsis* from negligible biomass amounts to more than 1kg m^{-2} was recorded. This regime shift has been called third transition (TR3) (Oğuz et al., 2008a).

Field data revealed that during periods of positive NAO index and cold conditions, prey abundance declines and anchovy outcompetes *Mnemiopsis* when feeding (Oğuz, 2005b). In addition, *Mnemiopsis* is sensitive to turbulence and cold climate conditions, which prevents *Mnemiopsis* from rapid reproduction, such as at the beginning of 1980s. During warm conditions though, such as from 1989 to 1990s, *Mnemiopsis* reproduction increased, seeded from survivors of overwintering, reaching very high biomass numbers (Oğuz et al., 2001). Oğuz et al. (2008a, b) assumed that *Mnemiopsis* has competitive advantage in food exploitation over anchovy and reproductive advantage over the native species *Aurelia*. The complex nonlinear coupling

of increased fishing pressure and competition with *Mnemiopsis* led to the anchovy stock depletion.

1.5.1 Bottom-up control

The 1950s and 1960s represent the oligotrophic state of the Black Sea ecosystem with a human-induced nutrient supply of 150 kilotonnes yr^{-1} from the rivers discharging into the North Western Shelf (NWS) (Oğuz and Gilbert, 2007). The maximum concentrations of the most limiting nutrient, nitrate, in the open waters were around 2-4 μM (Codispodi et al., 1991) while for the shelf region the vertically integrated nitrate concentration of a 40 m deep station located off the coasts of Romania was ~ 4.0 μM. In addition, the maximum phytoplankton biomass and *chl-a* concentration was observed to be ~ 2.0 g m^{-2} and 0.1 mg m^{-3}, respectively, and resembles the characteristics of a typical pristine state ecosystem under weak anthropogenic forcing (Oğuz and Gilbert, 2007). Furthermore, this period corresponds to the warm period in the Black Sea (Oguz, 2005b). During 1970s River Danube continued to accumulate nutrients in the water column and this period referred to as pre-eutrophication state (Oğuz and Gilbert, 2007). The alarming footprints of developing eutrophication include the sudden increase of vertically averaged phosphate load ~ 1.4 μM at the NWS, basinwide pronounced hypoxia-anoxia events, toxic dinoflagellate blooms, decline in sea grass communities and benthic production, enhanced sediment transport (Zaitsev and Mamaev, 1997). Moreover, phytoplankton biomass increased significantly from low values around ~ 3.0 – 4.0 g m^{-2} before 1974 to twice higher values of 7.0 to 8.0 g m^{-2} after 1974 and stayed around the latter range until 1984 (Oğuz and Gilbert, 2007). The intense-eutrophication phase started when the upper chemocline layer (50-75m) nitrate concentration in 1980s experienced a gradual increase (of more than three times) to ~ 6.0 to 8.0 μM at the inner basin (Oğuz and Gilbert, 2007). The climate conditions of the mid-1980s and early 1990s were the most severe of the century. Thus, nutrient pumping from the chemocline to the productive surface waters at the time of winter mixing intensified (Oğuz and Gilbert, 2007). Following, more pronounced phytoplankton blooms responded to

nutrient accumulation at the surface (Oğuz et al., 2008a). Vertically integrated concentrations of phytoplankton were measured around 8.0 to 20.0 g m^{-2} and surface *chl-a* as 0.1 to 0.5 mg m^{-3} in this period (Oğuz and Gilbert, 2007).

1.5.2 Top-down control

During the second half of the previous century the Black Sea was subjected to various types of predator control (Daskalov, 2002). During the pre-eutrophication state (1960s) phytoplankton biomass was low, zooplankton biomass was fairly high, small planktivorous fish were scarce in numbers and the large piscivorous fish was very abundant (Oğuz and Gilbert, 2007). The top-down control changed in the Black Sea during 1970s when the overfishing of medium pelagics, dolphins and demersals caused planktivorous fish stocks (i.e. anchovy) to increase twofold after 1973 to observed stocks of ~ 1100 kilotonnes by the end of decade (Oğuz and Gilbert, 2007). Anchovy became the main consumer of production and this structure of the food web lasted until 1988 (Oğuz et al., 2008b). At this stage, the moon jelly *Aurelia aurita* had a biomass close to 1.0 kg wet weight m^{-2} and *Noctiluca scintillans* became a very common part of the ecosystem structure (Oğuz and Gilbert, 2007). When the predatory fish declined, it is likely that top-down control also set the conditions for increased concentrations of phytoplankton by assigning the small pelagic fish at the top predator level of the ecosystem (Oğuz and Gilbert, 2007). It is hypothesized that the decreased predation pressure by the large pelagics and the intensified bottom-up supply due to severe winters are the possible explanations for the preserved high stock regime in the 1980s (Oğuz, 2005b; Oğuz and Gilbert, 2007). During 1988–1990 the collapse of small pelagic fisheries under coinciding effects of exceedingly high fisheries exploitation and population outburst of ctenophore *Mnemiopsis leidyi* took place. From the fisheries perspective it is believed that the recruitment failure by uncontrolled fisheries led to the abrupt decline (Gücü, 2002; Bilio and Niermann, 2004). Other studies pointed out that *Mnemiopsis* sharing the food source of small pelagics at the same trophic level and its predation on fish larvae further intensified the collapse of the small planktivorous fish

stock and catch down to ~300 and 150 kilotonnes respectively at the end of 1980s (Kıdeyş, 2002; Shiganova et al., 2004). Lacking predation the gelatinous species invaded the system and became the top-predator replacing *Aurelia* biomass of 1.0 kg wet weight m^{-2} in 1988, with a biomass up to 3.0 kg wet weight m^{-2} in 1989 and the system thereafter turned into a gelatinous predator dominated one (Oğuz and Gilbert, 2007).

1.6 Food Web Interactions

According to aquatic biologists studying lake ecosystems, a trophic cascade occurs as a pulse from apex predators and is transmitted down through lower trophic levels (Carpenter et al., 1985) basically acting as a 'top-down' control (e.g. predation, omnivory, diseases etc.). In addition, Hunter et al. (1992), extended this view by cascading-up from primary producers through higher trophic levels of the food web that then regulates biodiversity and fish population dynamics.

In the literature, there are many efforts to understand and differentiate trophic interactions between 'bottom-up' and 'top-down' control in a great variety of food web structures. For instance, Ware and Thompson (2005) analyzed yearly fish catch data and *chlorophyll-a* data obtained from SeaWIFS satellite observations in the western part of North America, found that remarkably high rates of primary production meets zooplankton data and resident fish data at the coasts of British Columbia, evidence for a strong ‘bottom-up’ control over the margin. Ware and Thompson (2005) further state that when fish catch is regressed against *chl-a* concentration, the slope of the regression line is the same in the domains of both intensive upwelling and downwelling. Thus, the primary production energy is directed not only towards the pelagic community but also towards the benthic community, triggering aquatic life there. However, the state at which fishing pressure (i.e. ‘top-down’ control) outcompetes the resource availability control remained uncertain (Ware and Thompson, 2005).

By using worldwide decadal scale time series data, Cury et al. (2000) found that in regions where intense upwelling operates, the middle trophic level is inhabited by small, planktivorous pelagic fish (such as sardine, horse mackerel, anchovy etc. off

California or South Africa) that serves as an essential linkage between high diversity apex and bottom compartments of the food chain. He therefore suggested that heavy fishing fleet may exert a significant influence on these 'wasp-waist' type of ecosystem structure and may even cause pronounced regime shifts (Cury et al., 2000) provided that the ecosystem is in an alternating state (Beddington, 1984). Futhermore, Cury et al. (2000) concluded that attempts to describe 'wasp-waist' type of food webs do not always give satisfactory results when analyzed with 'top-down' or 'bottom-up' type of trophic controls in field studies. Rather it requires a more sophisticated modelling approach to fully comprehend the complex interactions across multiple trophic levels and to address questions about the relative dominance of each mechanism (Rose et al., 1996).

1.7 Modeling Studies

There have been various modeling studies dealing with the abrupt changes that took place in the Black Sea ecosystem during the1960s to 1990s. Since the observed trends alternated between consecutive trophic levels including the small pelagics stocks, they can be evaluated from either bottom-up (resource availability) control or top-down (consumer) control or both (Oğuz et al., 2008a). By implementing different top-down regulations (fishing pressures) with ECOPATH with ECOSYM (EwE) Daskalov (2002) suggested that over-enrichment and over-exploitation both have an effect on the changes in the structure of the Black Sea ecosystem, the role of fishing pressure was however more critical in triggering a trophic cascade. At the same time Gücü (2002) put forward the overfishing hypothesis as main reason for the fisheries collapse with the *Mnemiopsis* outburst coinciding. According to this hypothesis, *Mnemiopsis* stock explosion took place because the ctenophore took over the small planktivorous fish's place as main consumer of zooplankton as a consequence of the strong top-down control of overfishing (Shiganova, 1998; Daskalov et al., 2007). In order to understand the fishing impact on small pelagics fisheries, one should take into account the reduction in the catchment lengths that was observed in 1987 – 1988 with respect to the previous years, thus suggesting an increasing number of immature (recruitment) catches with the

advancements in the fisheries, resulting in a recruitment failure in 1989 (Gücü, 1997). On the other hand, Berdnikov et al. (1999) used a trophodynamic model similar to EwE and found the competition of *Mnemiopsis* and anchovy for food rather than its predation on anchovy larvae as the responsible mechanism for the stock collapse.

In an extensive modeling study Oğuz et al., (2008a,b) tested various mechanisms by using a a coupled model of lower trophic level and anchovy population dynamics and concluded that complex non-linear interactions were responsible for the anchovy-*Mnemiopsis* shift. It was preconditioned by nutrient accumulation in the chemocline as a consequence of intense eutrophication and triggered by strong winter conditions, which by intense mixing made the nutrients available to the productive surface layer. This process increased the carrying capacity of the system. An increased fishing pressure together with competition with and predation by *Mnemiopsis* then caused the anchovy collapse (Oğuz et al., 2008a,b). This multi-trophic-level modelling approach thus elucidated the mechanisms operating behind abrupt transition events that occurred in the Black Sea.

1.8 Objectives of this study

The main focus of this study is to extend the work done by Oğuz et al. (2008a,b) and investigate the role of high frequency (interannual) climatic variations on anchovy population dynamics, and the lower trophic level components of the ecosystem. Climate-induced variability will be limited to the changes in water temperature and vertical mixing rates. This work will put an emphasis on the complex interactions across consecutive trophic levels and focus on possible cascade events generated by climate-induced variations.

The following research questions are going to be answered:

1. What are the different effects of changes in water temperature and mixing rates on the ecosystem and anchovy population? Do these effects change when they

occur at the same time? Are both environmental factors of the same importance?

2. Do such environmental factors cause an observable trophic cascade effect?
3. What does environmental change mean for the Black Sea anchovy population?

2 MATERIAL AND METHODS

The coupled model of lower trophic level and Black Sea anchovy population dynamics is described in this section (for more detail, see the Appendix). Following that, the model input parameters and their values, then, some of the parameter value settings are presented. Lastly, the environmental time series over 65 years used for forcing the model are described.

2.1 Model Description

The model used in this study was developed by Oğuz et al. (2008a) and in its one-dimensional structure keeps track of concentration of all the state variables in mmol N m^{-3} as a function of time. This one- dimensional model resolves the upper water column with three layers and was developed for the south east region of the Black Sea where most purse seine fishing activity and anchovy foraging grounds are located and spawning of anchovies has been observed. The model solves a set of equation representing the ecosystem dynamics, and a detailed description of the equations can be found in Oğuz et al. (2008a).

2.1.1 Lower Trophic Level (LTL) Model Structure

The state variables of the lower trophic level of the model are defined as three phytoplankton groups (diatoms, dinoflagellates and nanoplankton), three zooplankton groups namely micro-, mesozooplankton and gelatinous carnivores (such as *Aurelia* or *Mnemiopsis*). This simplistic representation of both *Aurelia* and *Mnemiopsis* by a single state variable is reasonable for the purpose of present work because growth and

mortality rates of both species are considered as rather similar (Shushkina et al., 1983; Shushkina et al., 1998). It means the differences arising from their life history traits can decide for the relative dominance of one species over the other, thus both can not co-exist together at high biomass values. Since the model was constructed to follow the mechanisms behind the anchovy stock fluctuations and the Black Sea regime shifts from 1960s until the collapse period which took place at the beginning of the 1990s, it assumes no predation effects of *Beroe ovata* on the gelatinous species. The nitrate compartment of the lower trophic level model ignores the complex bacterial dynamics for simplicity and assumes direct remineralization of detritus partly into nitrate while the rest sinks down below the euphotic zone. The nitrate regulating phytoplankton production is supplied via fluxes from nutrient source layer (by vertical mixing and advection processes), through its regeneration from detritus, from unassimilated matter within the euphotic zone when stratification conditions persist, and through diffusive exchanges between layers.

2.1.2 Higher Trophic Level (HTL) Model Structure

The anchovy bioenergetics (life-cycle dynamics) model follows principally the study by Rose et al. (1999), tracking individual spawners' progeny through developmental stages (such as hatching, yolk-sac larvae, early larvae, late larvae, juvenile, young of the year (YoY)) and adult stages. Water temperature is a critical factor for larval stages and determines the initiation of the spawning season. Spawning is limited to the mixed layer in waters above 20^{o}C (Niermann et al., 1994; Kıdeyş et al., 1999; Satılmış et al., 2003). Below this mixed layer the temperature values are always lower than ~7ºC. Consequently, the eggs and non-feeding larvae cannot survive within the thermocline depths, unlike the juveniles, YoY and adults which show voracious and selective feeding on their wide-range of zooplankton prey at different depths. The model starts with the spawning of females on June 1st and the spawning season lasts till the end of August (months are identically represented as 30 day intervals). All eggs spawned on the same day are regarded to belong to the same cohort. Accordingly, the model keeps track of 90

cohorts in one year. As anchovy grow, they are subjected to mortality by either fishing, or natural, or both. The natural mortality comprises the predation, grazing and basal mortality components. In the model formulation, anchovy may also experience losses due to suffering from food shortage that occur when there is not enough food to meet their basal metabolic demands. The individuals in the model are tracked through age-0, age-1, age-2 and age-3 classes. The model uses different predator prey relationships for anchovy and gelatinous carnivores. For further information on the model structure and formulation, parameterization, testing, and validation we refer to Oğuz et al. (2008a).

2.1.3 Vertical Model Structure

In the model the vertical structure extends from the surface to the upper part of the chemocline, comprising the euphotic zone and the nitrate source layer below. The biologically-active part of the water column, the euphotic zone, is assumed to be 50 m deep and is represented by two layers: a daily varying surface mixed layer and a subthermocline layer. This two-layer representation of the euphotic zone is acceptable to represent thermal stratification characteristics in the Black Sea. Below the euphotic zone of the model is the upper part of the chemocline starts that provides nutrients to the euphotic zone by entrainment.

The two layer vertical resolution of the model euphotic zone persists until the mixed layer deepens up to 45 m. Nutrient entrainment from the upper chemocline starts when the mixed layer depth reaches 45 m in winter and nutrients are entrained both into the mixed layer and the sub-thermocline layer. In addition, during the spring shallowing and autumn deepening phases of the mixed layer, the surface mixed layer follows a linear trend of changes between its minimum (15 m) and the maximum (45 m) values (Fig. 2.1a).

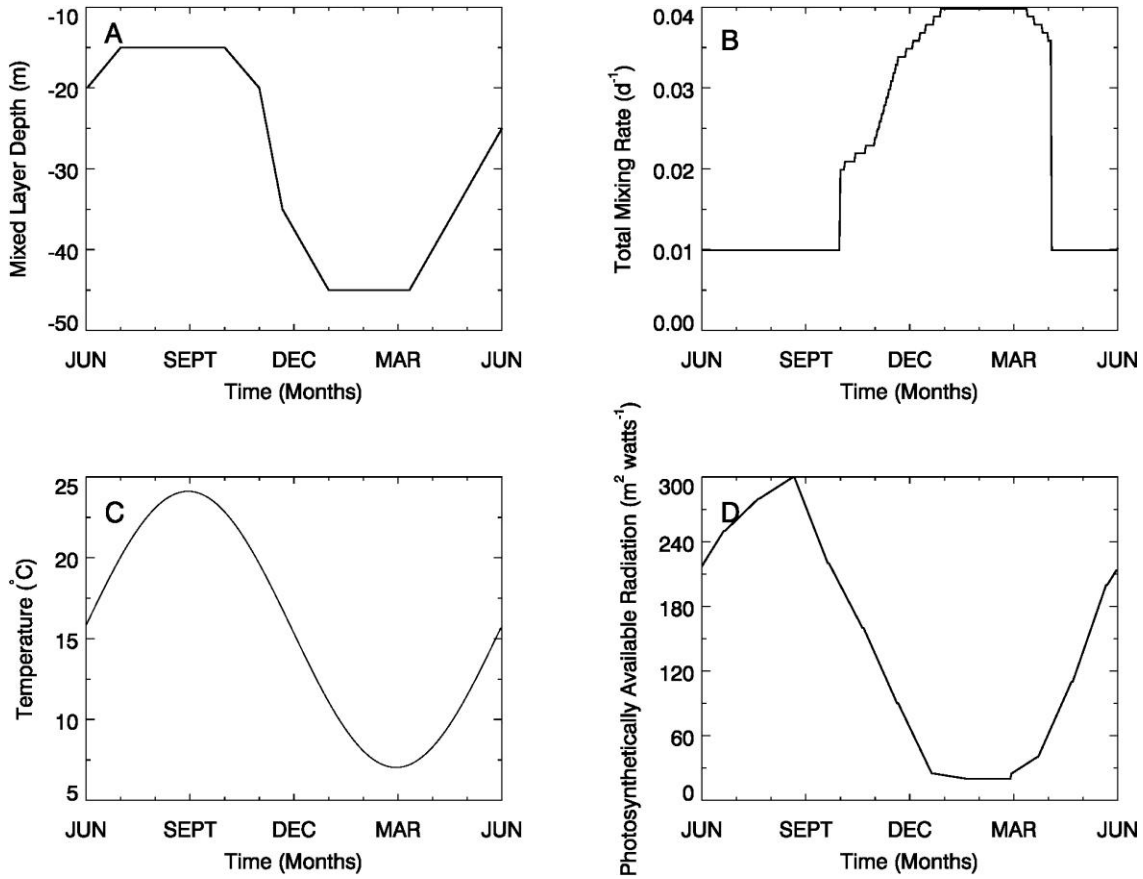

Figure 2.1: Model input derived from mean climatologic conditions for the Black Sea (Oğuz et al., 2008a). Annual cycle for daily a) mixed layer depths (m), b) total mixing rates (d^{-1}), c) mixed layer temperatures (ºC), and d) photosynthetically available radiation (PAR) (m^2 $watts^{-1}$).

2.2 Model Input

Daily variations of mixed layer depth, total mixing rate, temperature and photosynthetically available radiation (PAR) reaching the successive model layers over a year are input to the model (Fig. 2.1a-e). The model starts in June 1st and the corresponding mixed layer depth assigns the value of 20 m (Fig. 2.1a). But as the water gets warmer, the mixed layer continues to shallow up to 15 m. During summer the water remains stratified and the mixed layer depth stays intact at 15 m until October. As the severe winter conditions approach, intense winter mixing destabilizes the water column

and the surface mixed layer deepens until January when it reaches the maximum depth of 45 m. No more deepening of the mixed layer is allowed afterwards. This structure always retains the two layer structure of the euphotic zone which has a fixed depth of 50 m. in the model. Thus the 45 m. deep mixed layer and 5 m. thick sub-thermocline structure prevails until mid-March (Fig. 2.1.a).

When the mixed layer depth reaches 45 m., then the source layer is allowed to entrain nutrients both with the upper layer and the lower layer, as a result of wind-induced intense mixing. Only during the period of the intense mixing, which lasts from January till mid-March, efficient nutrient supply from the source layer (upper chemocline) to the upper layer is possible, otherwise the upper layer exchange nutrients with the lower layer.

The mixed layer starts shallowing after mid-March as the warming of the air and water temperatures take place. It follows a linear trend shallowing to 20 m in until June and completes its annual cycle.

The total mixing rate is the sum of daily diffusive flux which is assumed to be constant throughout the year at 0.01 m^{-1} and temporally varying entrainment flux (Fig. 2.1b). Therefore, during the summer when entrainment is inactive, total mixing is 0.01 m^{-1}. Towards the end of October, as vertical mixing gets activated, total mixing rate reaches ~0.02 m^{-1}. In the subsequent time period the total mixing rate keeps increasing to the maximum value of 0.04 m^{-1} in January. From January until mid-March maximum mixing conditions preserve and active nutrient transport from the source layer to the upper layer takes place. Following this intense mixing period the total mixing rate starts to decline and it reaches 0.035 m^{-1} at the end of March and then the entrainment diminishes as the mixed layer starts shallowing. Accordingly, total mixing rate attains the diffusion rate constant of 0.01 m^{-1} from April to June due to warming conditions. This reference (baseline) mixing cycle represents the mean climate conditions and is used in the long-term simulations as spin up for the first 15 years of the 65-year input timeseries.

The mixed layer temperature cycle follows a sinusoidal pattern in order represent the warming and cooling periods in a realistic manner (Fig. 2.1c) whereas the

subthermocline temperature is set to a constant value of 7 °C throughout the year. On the first day of the model year, June 1st, the water temperature is ~16 °C, increasing to the maximum temperature of 24.11 °C on August 29th. After that temperatures decrease until the coolest temperature of 7.03 °C occurs at the end of February. Following that time the temperature keeps increasing while reaching ~16 °C on the 1st of June and completes the annual cycle. This reference (baseline) temperature cycle represents the mean climate conditions and is used in the long-term simulations as spin up for the first 15 years of the 65-year input timeseries.

Photosynthetically available radiation (PAR) is also given as an input to the model (Fig. 2.1d). Its value is around 220 m^2 $watts^{-1}$ at the beginning of the model year (June 1st) and rises up to 300 m^2 $watts^{-1}$ until the 15 of August. During the following four-months the PAR values decline linearly and reach around 20 m^2 $watts^{-1}$ by the 15th of December. Then it remains around ~20 m^2 $watts^{-1}$ until March and in the upcoming spring season radiance starts increasing leading to more efficient illumination of the water column. Thus, at the end of May PAR value is around 210 m^2 $watts^{-1}$.

2.3 Parameter Setting

In this study, the model is run with the scenario setting representing the late 1970s ecosystem conditions, the time when nutrient supply to the system was elevated in comparison to the pristine state. This implies that the average nitrate concentration in the subsurface source layer is taken as 3.0 mmol m^{-3}. The late 1970s resemble the post-transition stage, when anchovy are able to develop from moderate (8 t km^{-2} or 1200 kt) to high (10 t km^{-2} or 1500 kt) stocks. Nutrient induced production is effectively utilized by anchovy in the vacancy of gelatinous biomass and during relatively low gelatinous transport from the shelf (0.0005 d^{-1}), medium predation pressure by higher order predator fishes (0.00003 m^3 d^{-1}), medium fishing mortality (0.3 f yr^{-1}) obtained by multiplying daily fishing rate with the duration of fishing season (Table 2.1). Fishing season lasts from the 1st of October to 15th of March (165 days) every year, basically corresponds to more than 80% of the total annual catchment (Prodanov et al. 1997).

Further, necessary parameter adjustments were done to the anchovy model as it is described in Oğuz et al. (2008a, Table 3, 5 and 6). Food preferences for anchovy grazing, coefficients of the length-weight relationship of anchovy, spawning efficiency and weight loss due to spawning were readjusted (Table 2.2), as well as basal mortality rates for hatching, yolk-sac and late larva, and consumption and respiration parameters (Table 2.3).

Table 2.1: Input parameter values for the late 1970s ecosystem conditions.

Input Parameters	Value
Source layer nitrate concentration	3.0 mmol m^{-3}
Predation mortality	2.0 x 10^{-4} m^3 d^{-1}
Gelatinous import rate	0.5 x 10^{-3} d^{-1}
Fishing mortality	0.3 fyr^{-1}

Table 2.2: Higher trophic level (HTL) parameter setting.

Description	Value
Food preference coefficient of anchovy for mesozooplankton	0.5
Food preference coefficient of anchovy for microzooplankton	0.5
Weight-length conversion factor b_1	0.0040 cm
Exponent of weight-length conversion b_2	3.16
Spawning efficiency S	0.3
Weight loss due to spawning E_g	0.15 d^{-1}

Table 2.3: Anchovy weight growth model parameters for different development stages. Var indicates parameters changing with time.

Description	Unit	Early larva	Late larva	Juvenile	YoY	Adult
Basal mortality rate*, m_b	d^{-1}	0.3	0.07	0.02	0.006	0.002
Max. consumption rate, c_1	mgC d^{-1}	1.23	0.78	0.88	0.69	0.417
Weight parameter of consumption, c_2		0.27	0.27	0.27	0.35	0.35
Max. respiration rate, r_1	mgC d^{-1}	0.022	0.022	0.25	var	0.0299
Weight parameter of respiration, r_2		0.34	0.34	0.34	0.34	0.34
Half saturation const. of zooplankton feeding, K_{Z4}	mgC m^{-3}	2.7	2.7	2.7	2.7	2.7
Activity factor of respiration, A_F		1.5	1.5	1.5	1.5	1.5
* for hatching and yolk-sac larvae 0.9, 0.8 d^{-1}						

2.4 Simulation Characteristics

Stochastic time series of temperature and mixing rate are generated in order to mimic their climatic variations (Fig. 2.2). A regression equation was fit to the climatological temperature cycle of the Black Sea described in section 2.2 that produces a yearly temperature cycle as seen in Fig. 2.1.c:

$$T = \alpha_0 - \alpha_1 \cos(0.01745\ day) - \alpha_2 \sin(0.01745\ day) \qquad (1)$$

where *day* is day of the year and α_0, α_1, α_2 are constant parameters having values of 15.5, 0.1, and 8.5, respectively. This temperature cycle was repeated for the first 15 years of the 65 year time series to allow for spin-up of the model. For the following 50 years stochastically created white noise was added to the values of the three coefficients (α_0, α_1, α_2) (Eqn. 1) to create varying yearly cycles representing changes in temperature.

$$\begin{bmatrix} \beta_0 = noise \bullet \alpha_0 \\ \beta_1 = noise \bullet \alpha_1 \\ \beta_2 = noise \bullet \alpha_2 \end{bmatrix}$$

The white noise was created in form of normally-distributed, pseudo-random numbers with a mean of zero and a standard deviation of using the Box-Muller method for generating normally-distributed (Gaussian) random numbers. Assuming A & B are independent, random variables uniformly distributed in the interval (0, 1], then;

$$Z_0 = \sqrt{-2\ln A}\cos(2\pi B)$$
$$Z_1 = \sqrt{-2\ln A}\sin(2\pi B) \qquad (2)$$

with Z_0 and Z_1 being the independent random variables with normal distribution, a mean of zero and standard deviation of one (Eqn. 2).

This randomly generated noise is an anomaly that translates to different temperature and mixing rates during each respective year but summed up over the total of 50 years gives no deviation from the climatological conditions. Similarly it was done for the total mixing rate cycle given in the section 2.2 (Fig. 2.1b), however the noise was applied with reversed sign so that colder temperatures correspond to higher mixing rates and vice versa. The response of the higher trophic level population (spawners, recruitment and eggs), as well as anchovy-gelatinous interactions and the lower trophic level (phytoplankton and zooplankton) were studied:

To investigate the influence of changing temperature and mixing on the Black Sea ecosystem as defined in the model, three different simulations are performed:

1) Simulation A (Temperature (*T*) only case): in this simulation the model is forced with stochastically changing temperature input only. The rest of the parameters are as given by their default settings. The 65 year time series of temperature input

described above is read into the model (Fig. 2.2a), while the total mixing cycle is kept fixed for all of the 65 years as in the baseline simulation (Fig. 2.1b). This simulation is used to explore the impact of long-term variability in temperature as may be induced by climate change on higher and lower trophic levels.

2) Simulation B (Mixing (κ) only case): in this simulation the model is forced with stochastically changing mixing input only. The above described 65 year time series of total mixing rate is read into the model (Figure 2.2b), while the temperature cycle is kept fixed for all 65 years as the baseline simulation described above (Fig. 2.1.a).). This simulation is used to explore the impact of changes in the total mixing rate as may be induced by climatic changes on higher and lower trophic levels.

3) Simulation C (T & κ): in this simulation the model is forced with both 65 year time series of stochastically changing temperature and mixing rate (Fig. 2.2a & b). The overall ecosystem response to the combination of these forcing is investigated. In addition, seasonal changes of the lower and higher trophic level compartments are investigated by looking at model input over the course of one year using low temperature (year 12), maximum (year 16) and average (year 14) environmental conditions.

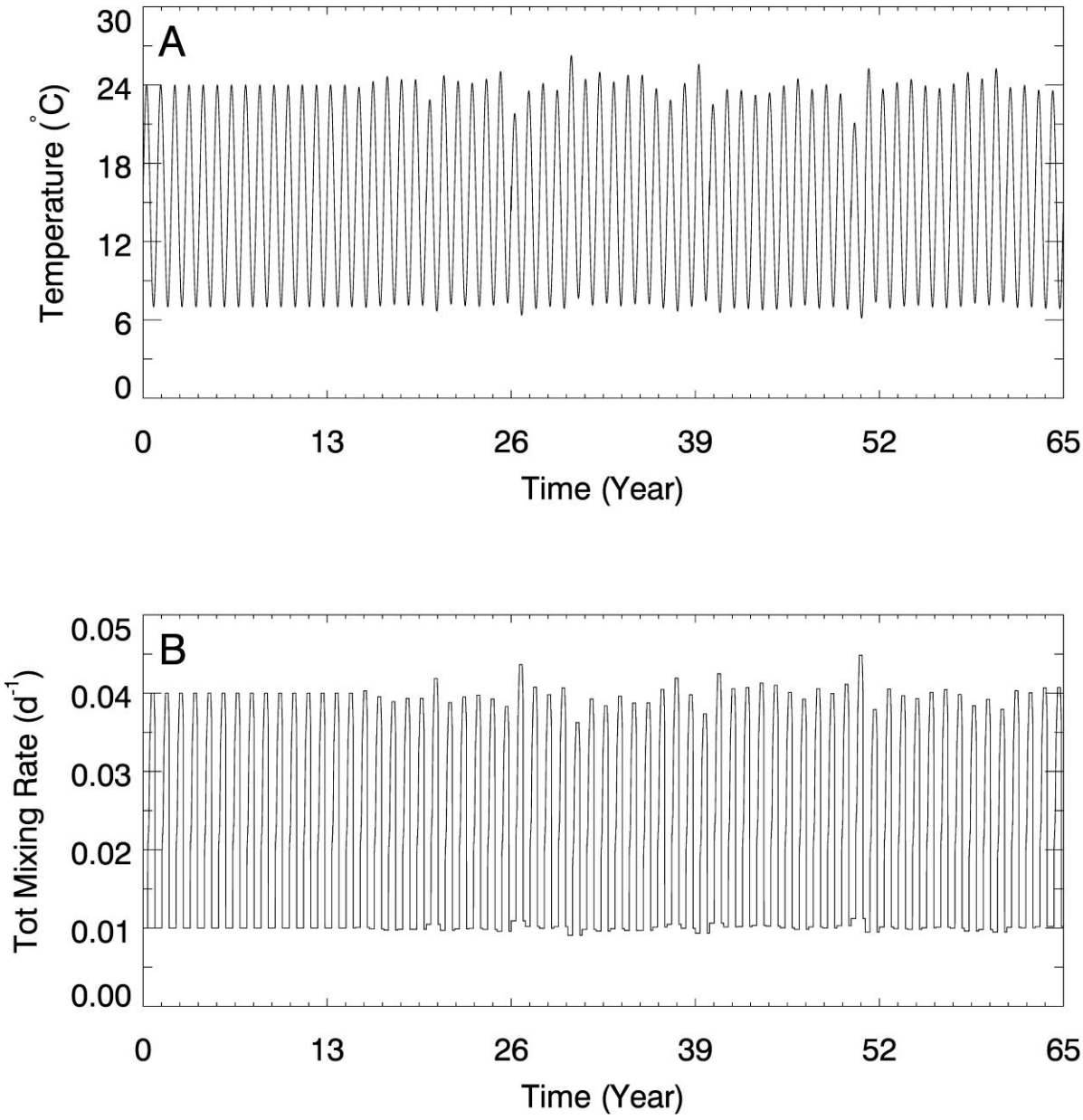

Figure 2.2: Stochastically generated 65-year time series data serving as model input. a) Temperature (°C) and b) total mixing rate (d^{-1}) derived from the mean climatologic data for the Black Sea (Fig. 2.1b,c) (Oğuz et. al., 2008a).

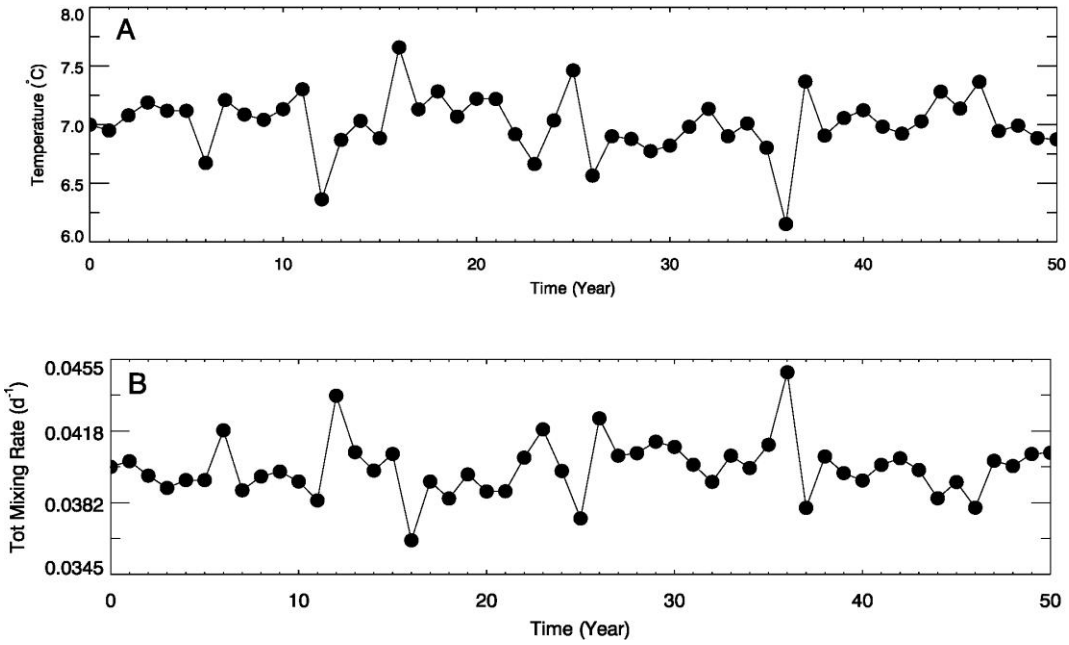

Figure 2.3: Fifty year-long time series data of coldest day of the year (on 28 February) showing the a) temperature (°C) and b) total mixing rate (d^{-1}) differences between consecutive years of the basic model input (Fig. 2.2).

The date (February 28) at which the minimum temperature occurs in each year, as well as the corresponding maximum total mixing rate at the same day are plotted as a representative of long-term inter-annual variability (Fig 2.3).

3 RESULTS

The model described above in combination with different time series are used to evaluate the impact of environmental changes on the lower and higher trophic levels of the Black Sea. Therefore, first the reference (baseline) simulation to which the subsequent model results will be compared is presented. Following this, the development of lower and higher trophic level compartments over one specific year and its reaction to long-term (65 years) climatic variability are presented. After that the influence of environmental change on the higher trophic level is described while considering the interactions between the different trophic levels.

3.1 Reference Simulation

In the reference simulation temperature and total mixing rate representing mean climatologic conditions of the Black Sea corresponding to the baseline year (Fig. 2.2) was read into the model.

In considering the lower trophic level (LTL) components, the nitrate is unique for being the only abiotic compartment of this group. Therefore, being directly controlled by primary forcing data (such as mixing, heat flux and etc.) it plays an important role in carrying the physical information to the rest of the biotic compartments at the LTL. Hence, annual variability of the subsurface nitrate concentration is expected to get influenced by daily variations in the entrainment rate. The source layer actively supplies nutrients to the upper layer at times of intense mixing which takes place during the period from January to February. Therefore, the nutrient concentrations in the euphotic layer stay at the range between background values of ~0.6 and 1.5 mmolN m^{-2} during the first half of the year (Fig. 3.1a). Then, the nutrient concentration that is built up via mixing induced accumulations, reaches peak values of 2.75 mmolN m^{-2} at the beginning of April. At the surface, while the mixed layer gets shallower in the early spring, the

nutrients are made available for uptake in the primary production. The fifteenth of April corresponds to the time of initiation of vernal bloom of the phytoplankton groups that is triggered by radiation and nutrient availability. Towards May, the phytoplankton severely depletes the nitrate and reaches biomass amounts around ~10. gC m^{-2} (Fig. 3.1b). Phytoplankton blooms again during early autumn with somewhat lower intensity of ~5. gC m^{-2} but this time over a longer period. Correspondingly, microzooplankton responds to phytoplankton variability with a bloom biomass around 1.15 gC m^{-2} at the beginning of June and with ~0.4 gC m^{-2} in the middle of November (Fig. 3.1c). Then mesozooplankton which constitutes the primary food source for anchovy reaches a peak biomass value of more than 1.8 gC m^{-2} in the middle of May and ~1. gC m^{-2} at the beginning of December (Fig. 3.1d). The timing of the mesozooplankton bloom takes place with a fifteen day shift with respect to microzooplankton.

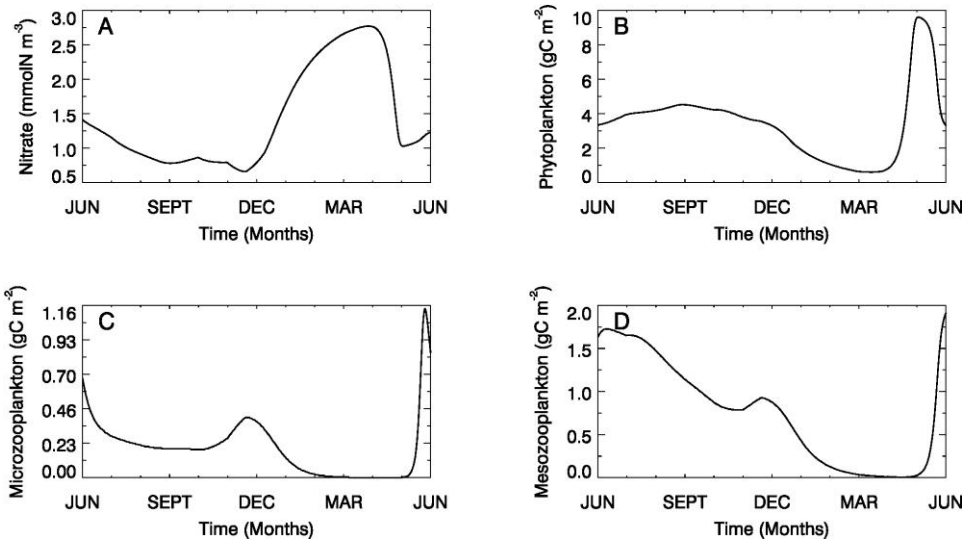

Fig. 3.1: Model lower trophic level state variables. Daily variations of water column integrated (a) nitrate concentrations (mmolN m^{-3}) and biomass of (b) phytoplankton (gC m^{-2}), (c) microzooplankton (gC m^{-2}) and (d) mesozooplankton (gC m^{-2}).

Table 3.1: The corresponding output values for egg production, standing stock, total catch and gelatinous biomass, under 1970s input parameter setting.

Model Output	Value
Total number of eggs produced	558 $m^3 d^{-1}$
Exploitable anchovy stock	6.19 t $km^{-2} d^{-1}$
Anchovy catch	2.52 t $km^{-2} yr^{-1}$
Gelatinous biomass	0.285 gC m^{-2}

Given the late 1970s parameter setting, the corresponding output for total egg production during the spawning season is 558 $m^3 d^{-1}$, standing stock at the first day of fishing season (October 1st) is 6.19 t km^{-2}, total landing during the fishing season (October 1st to 15 March) is 2.52 t km^{-2} and the annual mean gelatinous biomass is 0.285 gC m^{-2} (Table 2.1). With the new parameter setting for anchovy vital rates, the calculated model output (Table 3.1) deviated from that in the original model (Oğuz et al, 2008a).

Anchovy spawning season is assumed to start at the first day of June in the model. However, anchovy starts spawning only when the water temperature exceeds 20 °C. Until then, egg production is delayed and daily egg number is assigned to a constant small number (500 no. $m^{-3} d^{-1}$) beginning from the 1st of June. Keeping this in mind, in the reference run the actual production starts at the 20th of June with an amplitude around 6000 no. $m^{-3} d^{-1}$ (Fig. 3.2a). Egg numbers increase gradually from this time on to ~ 9600 no. m^{-3} at the end of August. Recruitment in the model is defined as all anchovy that survive larval and juvenile stages and manage to grow up to 6.0 cm. This length is assumed to correspond to anchovy that are able to reproduce. Towards the end of August, the mean length of all cohorts reaches 6.0 cm (Fig. 3.2b). Recruitment population increases steeply until December and peaks at 10.5 no. $m^{-3} d^{-1}$ in the middle of December. Their population starts to decrease, as they are being subjected to severe winter conditions and food shortage. In summer, when the conditions improve, by the end of May anchovy stock rise again but being assigned to age-1 then.

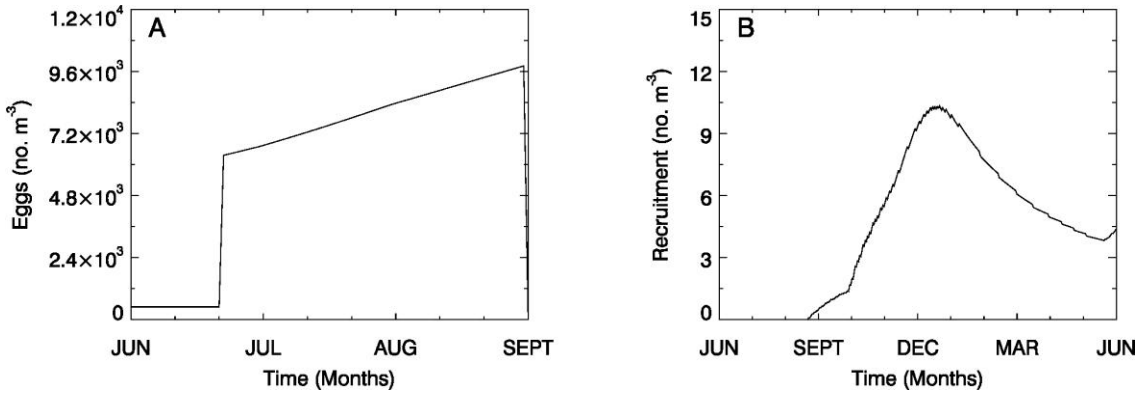

Fig. 3.2: Model higher trophic level compartments. Daily numbers of (a) egg production during the spawning season and, (b) recruitment population over the course of one year.

Daily mean weight and length values of anchovy age group 0+, 1+, 2+ (Fig. 3.3) are in close agreement with the data collected in Turkish coasts during the fishing seasons of mid-80s to 2005 (Uçkun et al., 2005; Samsun et al., 2006). It can be seen that the maximum growth, in both weight and length, takes place within the first 6 months where larvae growing up to 2 ±1 gww and 7 ±1 cm. For the adult groups, weight growth was 3 gww yr^{-1} and 6 gww yr^{-1} for the age-1 and age-2 classes, respectively. The corresponding length growth was 2.5 cm yr^{-1} for considered adult ages.

The results of weight and length growth reveal very critical features on anchovy early life history traits (Fig. 3.3). From the beginning of summer to winter (from June to January) the individuals belonging to each age class (age 0+, 1+ and 2+) experience positive weight growth as a result of availability of zooplankton food resource, which is triggered by increased primary production (Fig. 3.3a). As the winter conditions take over, scarcity in the food sources limits the weight growth. As a result, weight growth slows down and finally leads to weight loss (negative weight growth) during the period from January to the end of May. Besides, as the individuals grow older, they divert increasingly more amount of energy to building up body tissues for reproduction.

The results of stock and catch numbers analyzed for varied nutrient input (N) reveal that anchovy numbers increase most when nitrate content in the source layer is increased from 2.0 mmol m^{-3} to 3.0 mmol m^{-3} (Fig. 3.4). For N of 2.0 mmol m^{-3} the

anchovy stock and catch is around ~ 3.0 t km^{-2} (450 kt) and 1.0 t km^{-2} (150 kt), respectively (Fig. 3.4a,b). When the nitrate content is increased to 3.0 mmol m^{-3} , the corresponding stock and catch reach up to around 6.0 t km^{-2} (900 kt) and ~2.5 t km^{-2} (375 kt), respectively.

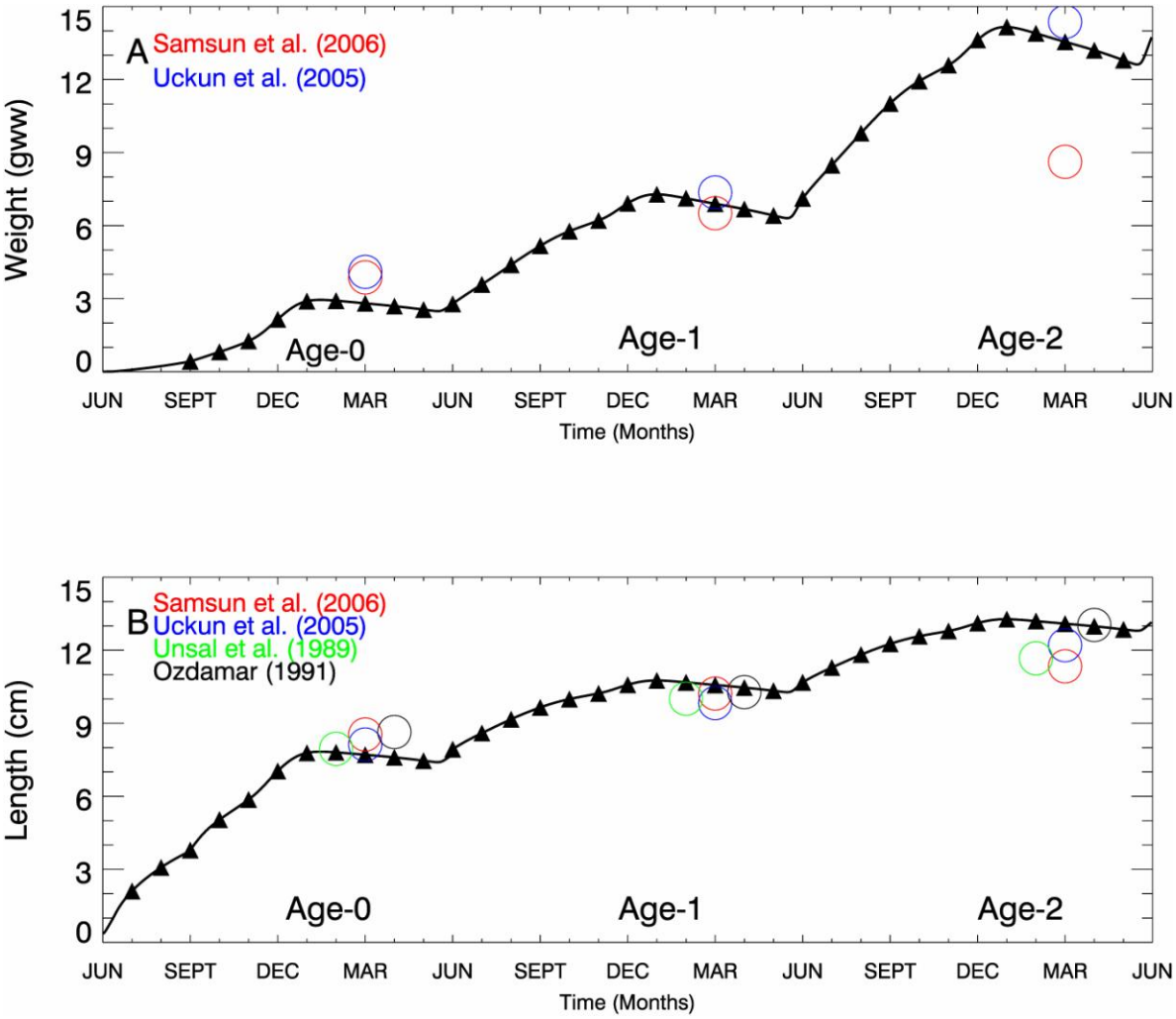

Fig. 3.3: Model higher trophic level compartments. Daily a) weight (gww), and (b) length (cm) growth of age-0 (mean of all 90 cohorts), age-1 and age-2 populations of anchovy. Data collected within the fishing season of the Black Sea and Izmir Bay is documented in open circles (Uçkun et al. 2005, Samsun et al. 2006).

The changes in N content from 2.0 to 3.0 mmol m^{-3} are accompanied with a gelatinous biomass of 0.2 gC m^{-2} and 0.6 gC m^{-2}, thus indicating that the available resources are more efficiently diverted to anchovy within this range (Fig. 3.4c). In

contrast, for N concentrations beyond 4 mmol m^{-3}, the gelatinous group consumes more efficiently and outcompetes anchovy in food competition at the same trophic level. Correspondingly, the anchovy stocks and catch start to decline, whereas gelatinous biomass reaches the critical concentration which enables more adventageous consumption of fodder zooplankton prey beyond this nitrate limit.

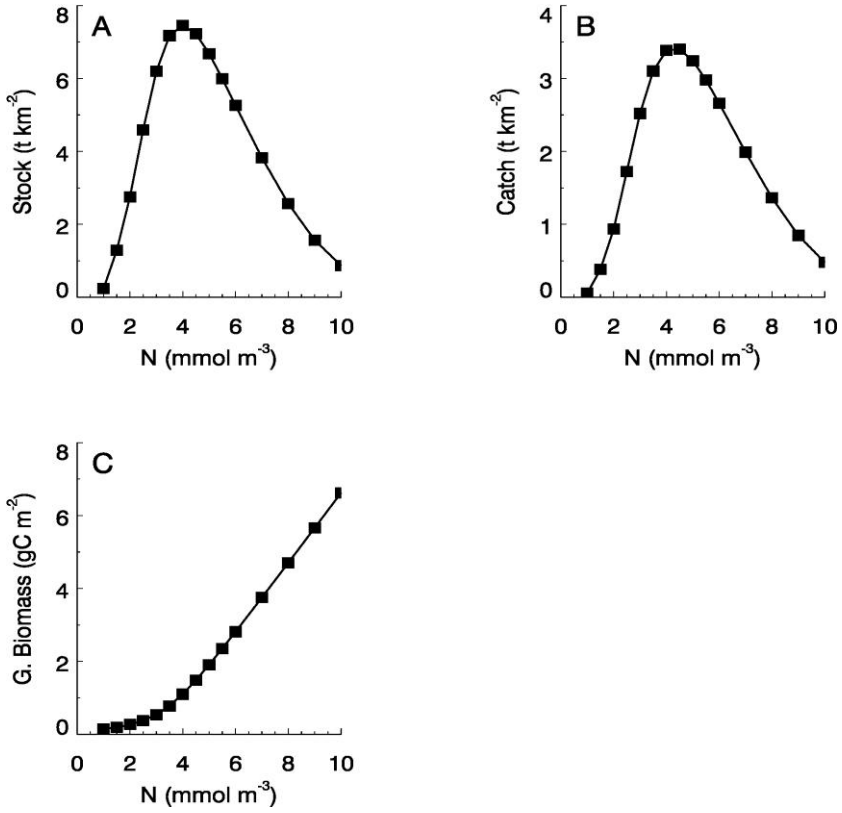

Fig. 3.4: Nitrate concentration of the source layer, Nc, versus variability of (a) anchovy stocks at the beginning of fishing season (October 1st), (b) total landings within the fishing season (from October to mid March) and (c) gelatinous biomass at the euphotic zone in yearly average values.

3.2 Environmental Effects on Ecosystem

In the following two sections, the effect of environmental variability introduced to the model, in the form of temperature and total mixing variations, is analyzed. In the first part, the influence of extreme cases, such as the years with maximum/minimum

temperatures and/or minimum/maximum total mixing, on the seasonal variations of both lower and higher trophic level compartments is described. In the second section, the long-term interannual variability of ecosystem compartments in response to changing environmental conditions (temperature and/or total mixing) and also their interactions with each other are studied.

3.2.1 Seasonal Variations

3.2.1.1 Lower Trophic Level

Simulation A: Seasonal variations in the lower trophic level compartments in response to changing temperature and fixed total mixing rates are studied in this section. The years of lower (no.12) and higher (no.16) temperature extremes and fixed baseline year (no.14) total mixing rates are inputs (Fig. 3.5a,b).

Nitrate

The nitrate concentrations over one year between years of temperature extremes does not introduce changes in the annual cycle of nitrate concentration (Fig. 3.5c). At the beginning of the model year, euphotic layer nitrate concentration is around 1.4 mmol N m^{-3} and linearly decreases to around 0.85 mmol N m^{-3} in September. Then between September and October the concentration slightly increases above 0.85 mmol N m^{-3} and the nitrate values during the temperature minima are slightly exceeding the nitrate values during maximum temperature effects. From October on, nitrate concentration decreases down to the lowest limit (~0.6 mmol N m^{-3}) in November. Then, by December, the nitrate concentration in the euphotic layer rises from its lowest value in the water column via strong winter mixing effects and reaches peak values of 2.75 mmol N m^{-3} by mid-March. These accumulated nutrients are readily taken up in primary production in April and fall steeply down to ~1.1 mmol N m^{-3} and stay around this value during May.

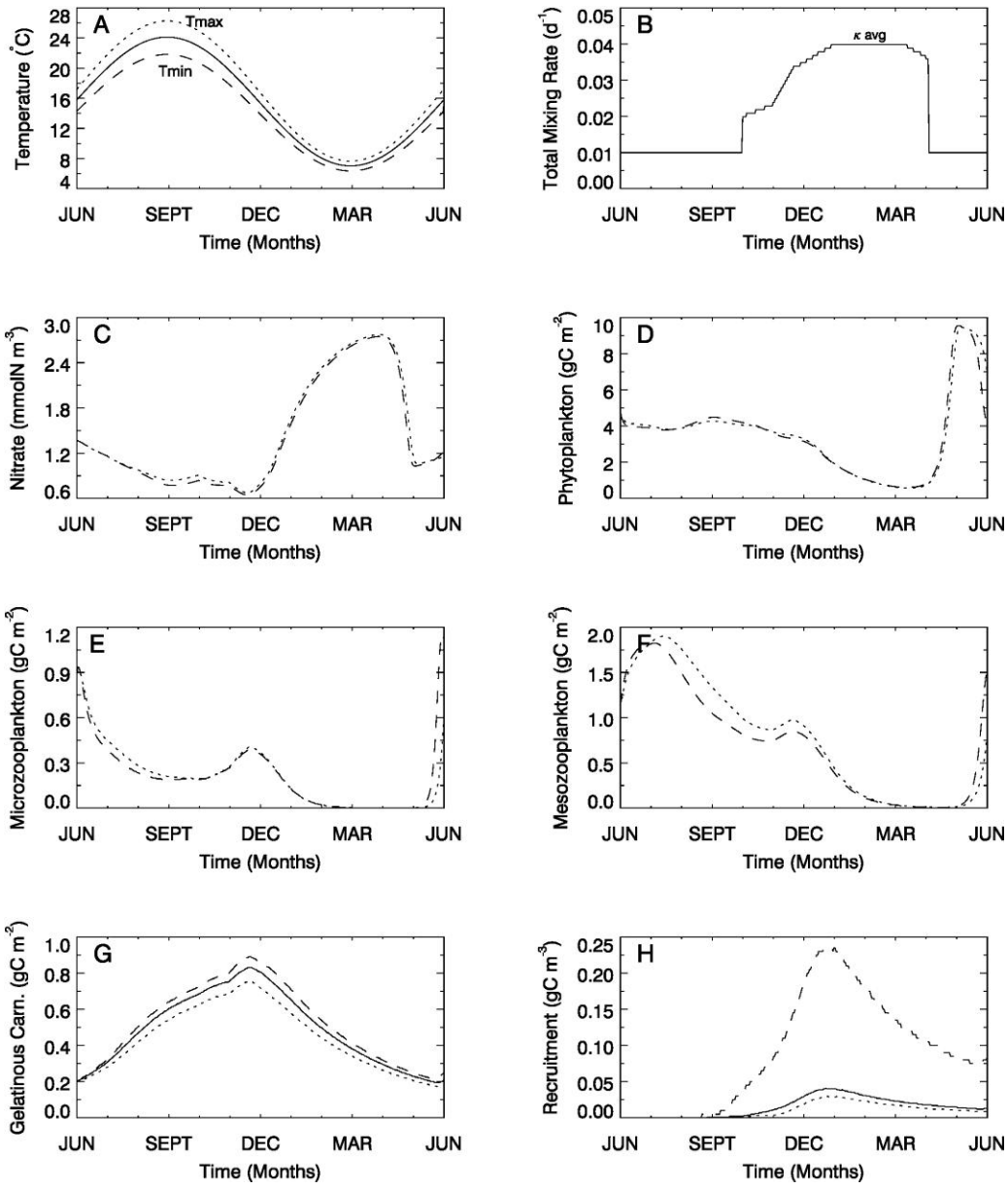

Figure 3.5: Simulation A. Model input in the form of a) temperature (^{o}C) for minimum, maximum and baseline years, and b) total mixing rate (d^{-1}) of the baseline year which is kept constant for each different temperature cycle. Model output: c) euphotic layer nitrate concentrations (mmol N m^{-3}), euphotic zone integrated d) phytoplankton (gC m^{-2}), e) microzooplankton (gC m^{-2}), f) mesozooplankton (gC m^{-2}), g) gelatinous predator (gC m^{-2}) biomass variations and single layer h) anchovy recruitment biomass (gC m^{-3}) variations.

Phytoplankton

The phytoplankton biomass for the years of different temperature extremes stays almost the same in the 3.0 to 5.0 gC m^{-2} range between the period from June to December (Fig. 3.5d). During the severe conditions of winter the biomass further decreases reaching around 0.5 gC m^{-2} in March. In April, following the shallowing phase of the mixed layer which contributes to nutrient availability in the surface layer, the phytoplankton biomass rises to a peak biomass value of 9.5 gC m^{-2} at the beginning of May. Although, the timing of bloom in the year with maximum temperature character is delayed by one day or two with respect to the bloom that took place in the minimum temperature year, and is accompanied with a slightly lower magnitude this time, the duration of the bloom in the maximum temperature period is longer than the duration in the minimum temperature period.

Microzooplankton

Model results for microzooplankton reveal almost identical biomasses for each temperature cycle except for the periods between mid-November to mid-December and at the end of May (Fig. 3.5e). For instance, at the beginning of June the microzooplankton biomass in both cases is around 0.9 gC m^{-2} and they are consumed rapidly during the second half of June and their biomass continues to decrease rather slowly reaching around 0.2 gC m^{-2} in October. In the period between October to mid-November, the biomass increases and makes a secondary peak around 0.4 gC m^{-2} followed by a decline that lasts between December to March. Thus, at the beginning of March, the microzooplankton biomass is around zero biomass value and remains depleted until mid-May before it starts developing again. In the second half of May, the microzooplankton biomass of the minimum temperature cycle shows a rapid growth and reaches bloom biomass of ~1.15 gC m^{-2} at the end of May. On the other hand, the microzooplankton of the higher temperature period shows a rather slow development and increases up to ~0.55 gC m^{-2} at the end of May, less than half the biomass of the colder temperature cycle.

Mesozooplankton

At the beginning of June, the mesozooplankton biomass is ~1.2 gC m^{-2} (Fig. 3.5f). Then the mesozooplankton biomass in the minimum temperature year rise in June and reach bloom concentrations around 1.75 gC m^{-2} at the beginning of July. Likewise, mesozooplankton bloom in the maximum temperature year develops rather slowly and reaches peak concentrations of values around 1.9 gC m^{-2} in mid July, yet the magnitude of this bloom is relatively more intense than the bloom in the minimum temperature year. In the period between July to the end of October, the mesozooplankton values of the maximum and minimum temperature years decrease continuously down to biomass around 0.9 gC m^{-2} and 0.75 gC m^{-2}, respectively. Within the first two weeks of November, a secondary biomass peak in both mesozooplankton with amounts of 1.0 gC m^{-2} and 0.8 gC m^{-2} is observed for the maximum and minimum temperature years, respectively. In the severe winter season from mid-November to mid-February, the mesozooplankton biomass gradually decreases to zero and stays at negligible biomass values until May for both temperature cycles. In May, mesozooplakton of the minimum temperature cycle experiences a steep growth and reaches up to 1.5 gC m^{-2} at the beginning of June, whereas, the mesozooplankton which developes in maximum temperature period grows rather slowly and reaches 0.75 gC m^{-2} at the beginning of June.

Gelatinous predator

Gelatinous predator biomasses indicate major differences between the temperature extremes (Fig. 3.5g). Gelatinous predator biomass for the minimum temperature cycle rises continuously from biomass value of 0.2 gC m^{-2} in June to 0.9 gC m^{-2} in the second half of November. In contrast, gelatinous biomass in the maximum temperature period increases from 0.2 gC m^{-2} in June to ~0.75 gC m^{-2} in the second half of November. Gelatinous biomass starts declining from peak biomass values at the beginning of December through the second half of the year when food sources become scarce and winter conditions dominate. At the end of May the biomass values are around 0.18 gC

m^{-2} and 0.2 gC m^{-2} for the years of maximum and minimum temperature cycles, respectively. Furthermore, gelatinous predator biomass values in the average temperature period stay close to the mean of maximum and minimum temperature years.

Anchovy Recruitment

Within the age group 0+ anchovies, it takes some time before all cohorts can satisfy maturity length criteria of 6.0 cm (Fig. 3.5h). A significant departure exists between the recruitment biomass under minimum and maximum temperature conditions. When the recruitment is exposed to minimum temperature cycle, the mean length of all cohorts satisfies recruitment criteria after mid-August. In the following four months the recruitment experiences a rapid increase and reaches biomass values above 0.225 gC m^{-3} at the end of December. In the period from January to next June, their biomass keeps decreasing from peak values down to 0.075 gC m^{-3} at the end of May due to high mortality of the age-0 groups and adverse conditions in winter time. On the maximum temperature cycle side, recruitment does satisfy the length criteria with a 10 days time delay than the minimum temperature case and yet their increase is very low until November. In November recruitment biomass starts increasing until the end of December and peaks at around 0.025 gC m^{-3} after which slowly declines down to 0.01 gC m^{-3} until the end of May.

Simulation B: Seasonal variations in the lower trophic level compartments in response to fixed temperature and varying total mixing rates are studied in this section (Fig. 3.5a,b). The years of upper (no.12) and lower (no.16) mixing extremes and fixed baseline year (no.14) temperatures are input.

Nitrate

In simulation B, the nitrate compartment experiences more remarkable differences between maximum and minimum mixing conditions as compared to the response it gave in simulation A (Fig. 3.6c). During the first half of the year, when nutrient supply from source layer to the euphotic zone is inactive, nutrient concentration decreases from the

value of ~1.3 mmol N m^{-3} in June to 0.6 mmol N m^{-3} in mid-November as a result of being heavily utilized by primary producers. When mixing intensifies in December nutrient levels increase and reach ~2.8 mmol N m^{-3} and 2.7 mmol N m^{-3} by March for the minimum and maximum mixing cycles, respectively. In mid-April, when the mixed layer shallows, the accumulated nutrients are used up by primary production, thus the nitrate concentration decreases steeply below 1.1 mmol N m^{-3} at the end of April and stays around this value until the end of May.

Phytoplankton

The phytoplankton biomasses for the years of total mixing extremes are almost identical within 4.5 and 3.0 gC m^{-2} range between the period from June to December (Fig. 3.6d). During winter conditions the biomass further decreases to ~0.5 gC m^{-2} in mid March. Following the shallowing phase of the mixed layer at the beginning of April, which contributes to nutrient availability in the surface mixed layer, phytoplankton biomass increases with a peak biomass value of 9.1 and 9.6 gC m^{-2} at the beginning of May for the years with minimum and maximum mixing rate extremes, respectively. Each bloom stays around three weeks and decrease to ~5.0 gC m^{-2} at the end of May.

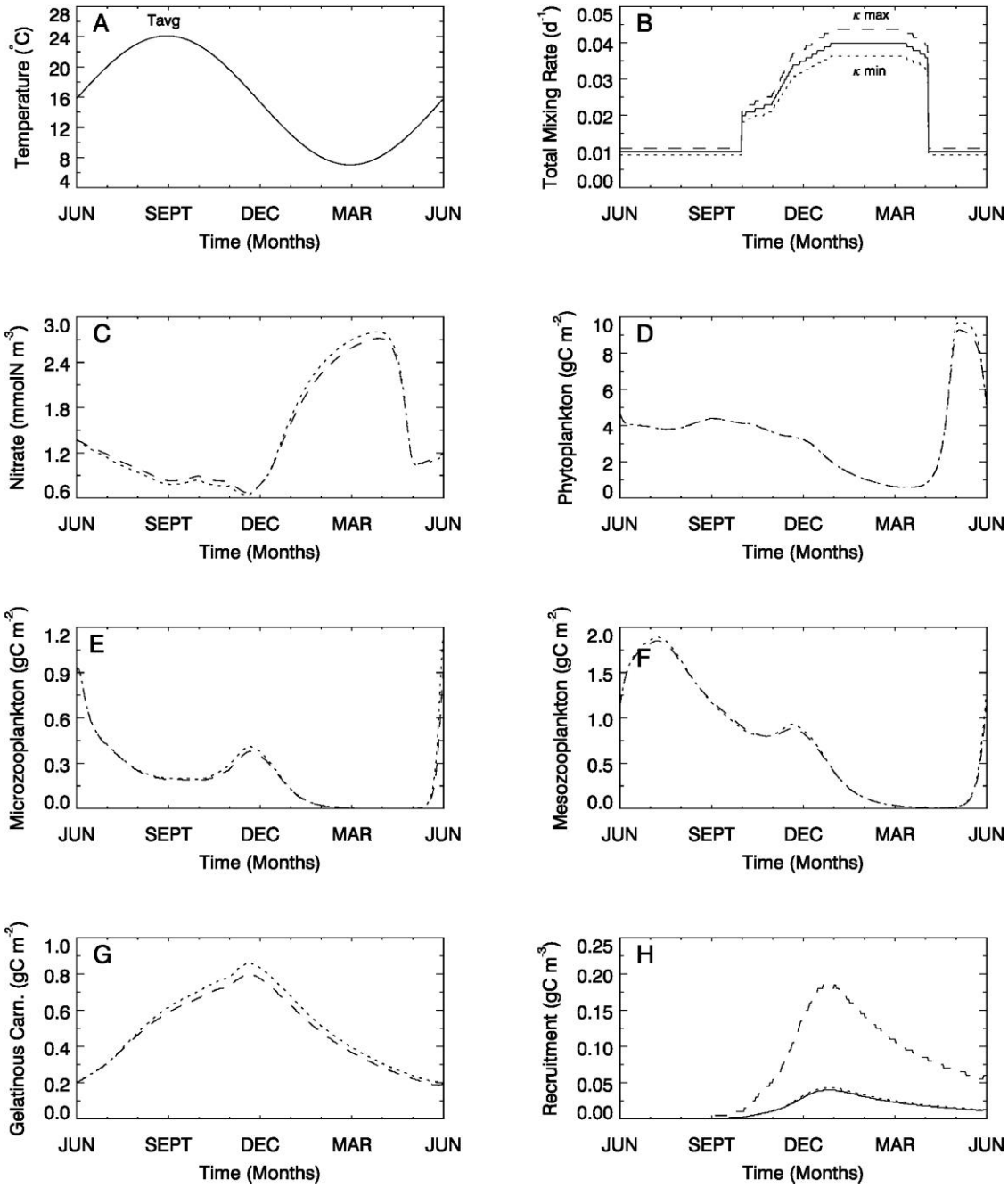

Figure 3.6: Simulation B. Model input in the form of a) temperature (^{o}C) of the baseline year which is kept constant for each different mixing cycle, and b) total mixing rate (d^{-1}) for minimum, maximum and baseline years. Model output: c) euphotic layer nitrate concentration (mmol N m^{-3}), euphotic zone integrated d) phytoplankton (gC m^{-2}), e) microzooplankton (gC m^{-2}), f) mesozooplankton (gC m^{-2}), g) gelatinous predator (gC m^{-2}) and single layer h) anchovy recruitment biomass (gC m^{-3}) variations.

Microzooplankton

Model results for annual microzooplankton concentrations are almost identical for mixing periods in the two extremes (Fig. 3.6e). For example, at the beginning of the model year (June 1st) the microzooplankton biomass is around 0.9 gC m^{-2} and is consumed rapidly during the second half of June and later decline more slowly reaching 0.2 gC m^{-2} in mid September. In the period between mid-October to mid-November, the biomass increases and makes an additional peak around 0.4 gC m^{-2} which is followed by a decline during December to mid-February when it reaches zero. Thus, at the beginning of March, the microzooplankton biomass is around zero and remains depleted until mid-May before it starts developing again. In the second half of May, the microzooplankton biomass that is influenced by minimum and maximum mixing cycle, experiences a rapid growth and reaches bloom biomass amounts of ~1.15 and ~0.80 gC m^{-2} at the end of May, respectively.

Mesozooplankton

During the years of total mixing extremes the mesozooplankton biomasses are nearly identical (Fig. 3.6f). At the beginning of June, the mesozooplankton biomass is around 1.2 gC m^{-2} and it further develops throughout June and reaches ~1.8 gC m^{-2} in the middle of July. Between July to mid-October, the mesozooplankton values decrease continuously, and the biomass is slightly above 0.8 gC m^{-2} in mid-October. From mid-October to the end of November, a secondary peak develops with a biomass around 0.9 gC m^{-2}. During winter conditions from mid-November to mid-March, the mesozooplankton biomass gradually decreases down to zero and stays at negligible biomass values until May. During May, mesozooplakton experiences a steep growth and reaches up to 1.25 gC m^{-2} at the end of May.

Gelatinous predator

Gelatinous predator biomasses reveal significant differences between the extreme mixing cycles especially in the winter season (Fig. 3.6g). Gelatinous predator biomass for the minimum mixing cycle rises continuously from biomass value of 0.2 gC m^{-2} in

June to 0.86 gC m^{-2} in the second half of November. On the other hand, gelatinous biomass in the maximum mixing period increases from 0.2 gC m^{-2} in June to ~0.8 gC m^{-2} in the second half of November. After the bloom period (at the end of November), the gelatinous biomass keeps declining during the second half of the year when scarcity in the food sources arises and winter conditions dominate. At the end of May the biomass values are still around ~0.2 gC m^{-2} for extreme mixing cycles which indicates their existance throughout the year.

Anchovy Recruitment

As in simulation A, significant differences exist between the recruitment biomass under minimum and maximum mixing conditions (Fig. 3.6h). When the recruitment is exposed to maximum mixing cycle, the mean length of all cohorts satisfy recruitment criteria at the beginning of September. In the following four months the recruitment experience a rapid increase and reach biomass values above 0.18 gC m^{-3} towards the end of December. In the period from January to next June, their biomass keeps decreasing from peak values down to ~0.05 gC m^{-3} at the end of May due to high mortality and adverse conditions in winter time. When exposed to minimum mixing, recruits satisfy the length criteria at the same time with the maximum mixing case, however their biomass increase is slower. Finally, at the end of December they reach their maximum biomass (below 0.05 gC m^{-3}). The biomass then slowly declines until the end of May down to ~0.01 gC m^{-3}. Moreover, the effects of minimum total mixing period are similar to the average mixing period.

Simulation C: In the last simulation, the lower trophic level (LTL) ecosystem response to both changing temperature and total mixing rate is studied for the years of lower and higher extremes (model input: Fig. 3.7a,b).

Nitrate

The nutrient concentrations available in the euphotic zone are identical in the maximum and minimum extreme conditions between June and December (Fig. 3.7c). At the

beginning of June, nitrate concentration is around 1.3 mmol N m^{-3} and it linearly decreases to 0.8 mmol N m^{-3} in September. Then between September and October the concentration slightly exceeds 0.85 mmol N m^{-3}. From October on, nitrate concentration decreases, and reaches to the lowest limit (~0.6 mmol N m^{-3}) by mid-November. Following that, the nitrate concentrations in the euphotic layer rise from their lowest values from December on and nutrient accumulation enhances via strong winter mixing effects. The peak concentrations reached by the end of March are above 2.75 mmol N m^{-3} for maximum temperature/minimum total mixing cycle and below 2.75 mmol N m^{-3} for minimum temperature/maximum total mixing conditions. These nutrients are used up during primary production in April and both fall down to 1.1 mmol N m^{-3} remaining like this until May.

Phytoplankton

The phytoplankton biomass in May, when it is under different environmental conditions, behaves differently than those simulations A and B, specifically with the duration and intensity of blooms (Fig. 3.7d). The magnitude of the bloom under maximum temperature/minimum mixing conditions is around ~9.75 gC m^{-2} which is slightly more than the intensity under temperature maximum conditions and its duration is longer than the bloom in simulation A. Under minimum temperature/maximum mixing conditions, the bloom intensity (~9.25 gC m^{-2}) is lower and is also slightly lower than the bloom under minimum temperature conditions in simulation A.

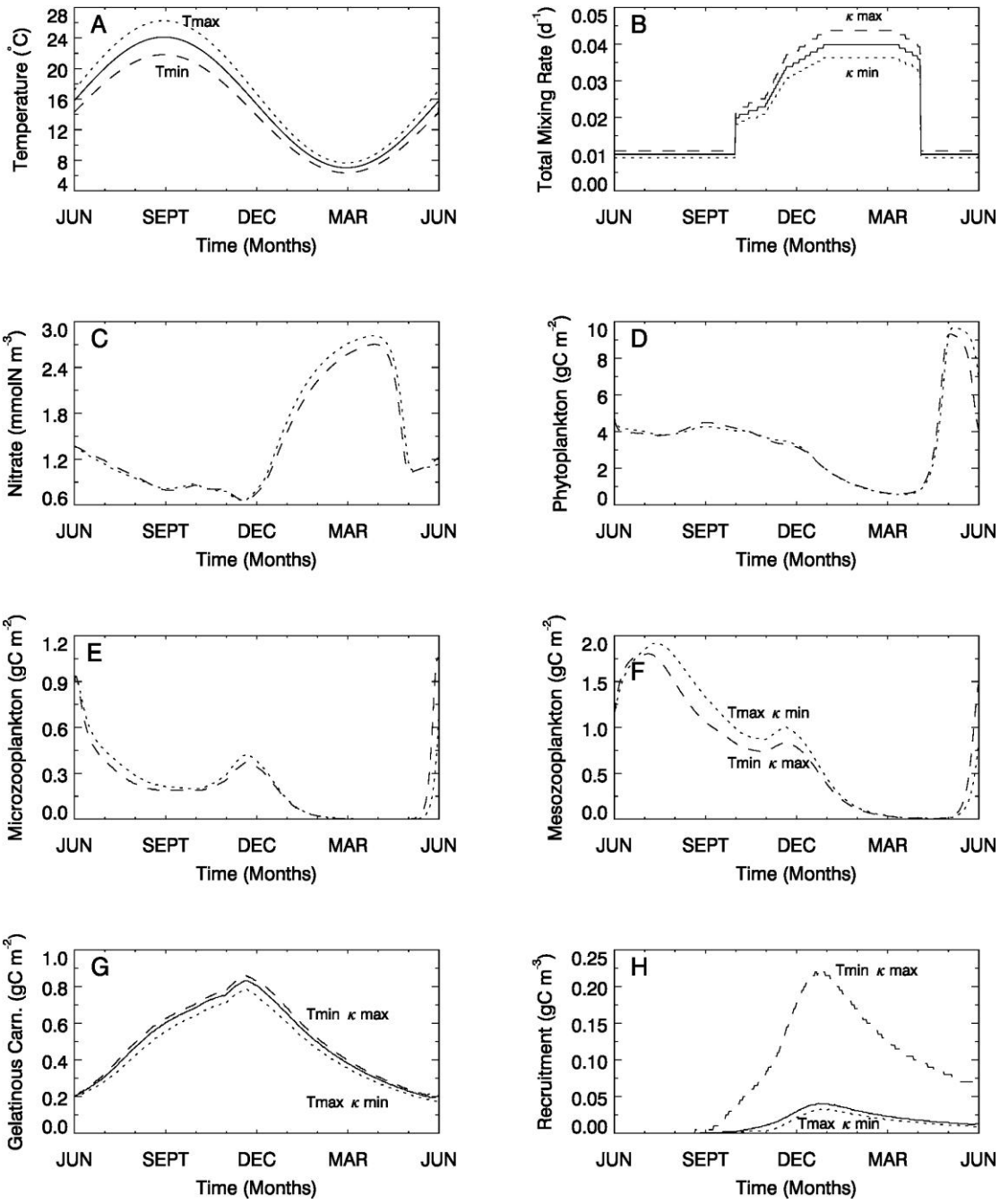

Figure 3.7: Simulation C. Model input in the form of a) temperature (^{o}C), and b) total mixing rate (d^{-1}) for the minimum, maximum and baseline years. Model output: c) nitrate concentration (mmol N m^{-3}) in the water column, euphotic zone integrated d) phytoplankton (gC m^{-2}), e) microzooplankton (gC m^{-2}), f) mesozooplankton (gC m^{-2}), g) gelatinous predator (gC m^{-2}), and single layer h) recruitment biomass (gC m^{-3}) variations.

Microzooplankton

Microzooplankton biomass preserves the characteristics of both previous simulations A and B (Fig. 3.7e). For example, it shows the similar characteristics to simulation A from June to September and from May to June, whereas it shows the information from case B at the time of active winter mixing that takes place during November to mid-January. At the beginning of the model year (June 1st), the microzooplankton biomass is around 0.9 gC m^{-2} and they are consumed rapidly during the second half of June and their biomass continues to decrease rather slowly until October and reach around ~0.2 gC m^{-2} at the beginning of October. In the period between mid-October to mid-November, the biomass increases and makes an additional peak around 0.4 gC m^{-2} and 0.45 gC m^{-2} for minimum temperature & maximum mixing and maximum temperature & minimum mixing periods, respectively. Following that, microzooplankton declines until mid-February. Thus, at the beginning of March, the microzooplankton biomass is around zero and remains depleted until mid-May before it starts growing steeply again. In the second half of May, the microzooplankton biomass that is influenced by minimum temperature & maximum mixing, experiences a rapid growth and reaches bloom biomass values around ~1.05 gC m^{-2} at the end of May. In contrast, the microzooplankton which is exposed to maximum temperature & minimum mixing experiences a rather slow development and increases up to ~0.65 gC m^{-2} at the end of May.

Mesozooplankton

Mesozooplankton biomass in simulation C is almost identical with the outcome of simulation A with a slightly higher biomass in maximum temperature/minimum mixing cycle in respect to the maximum temperature cycle in simulation A. The minimum temperature/maximum mixing biomass is also similar to the minimum temperature solution in case A except for a minor deviation in minimum biomass values (Fig. 3.7f).

Gelatinous predator

Both gelatinous predator biomass show that changes in mixing forcing contributes for a slightly suppressed peak concentration around ~0.85 gC m^{-2} for minimum

temperature/maximum mixing and a slightly pronounced concentration 0.77 gC m^{-2} for the maximum temperature/minimum mixing at the end of November (Fig. 3.7g). Thus, the seasonal variation is similar to the one that is obtained in case A (Fig. 3.5g), except that the mixing effects counteract temperature effects.

Anchovy Recruitment

In the recruitment group, there is a significant difference between the biomass in the extreme years (Fig. 3.7h) which is similar to the seasonal pattern observed in simulation A (Fig. 3.5h). The addition of maximum mixing cycle effect slightly diminishes the minimum temperature effect and peak biomass value so it is 0.22 gC m^{-3} at the end of December. Moreover, the contribution of minimum mixing slightly adds to the maximum temperature cycle effect, thus the peak biomass is increased to above 0.035 gC m^{-3} in December.

3.2.1.2 Higher Trophic Level

In this section the timing of egg production, spawning intensity and the recruitment success of the different simulation (A, B and C) is studied.

Simulation A:

Throughout the spawning season each day there is a 2 °C difference between the minimum, maximum temperature years and the baseline year (Fig. 3.8a). Knowing that egg production is only possible when temperature exceed 20 °C, the differences between the three specific temperature cycles is the key factor affecting spawning intensity and recruitment success. The temperature difference between the years of extreme values and the baseline directly influence the start date of egg production (Fig. 8e). Until the water temperature reaches 20°C the model assigns a constant value of 500 individual eggs in order to provide a stable egg influx and different years show a delay in reaching 20°C and with it spawning time. The start of egg production is delayed by 45 days for a

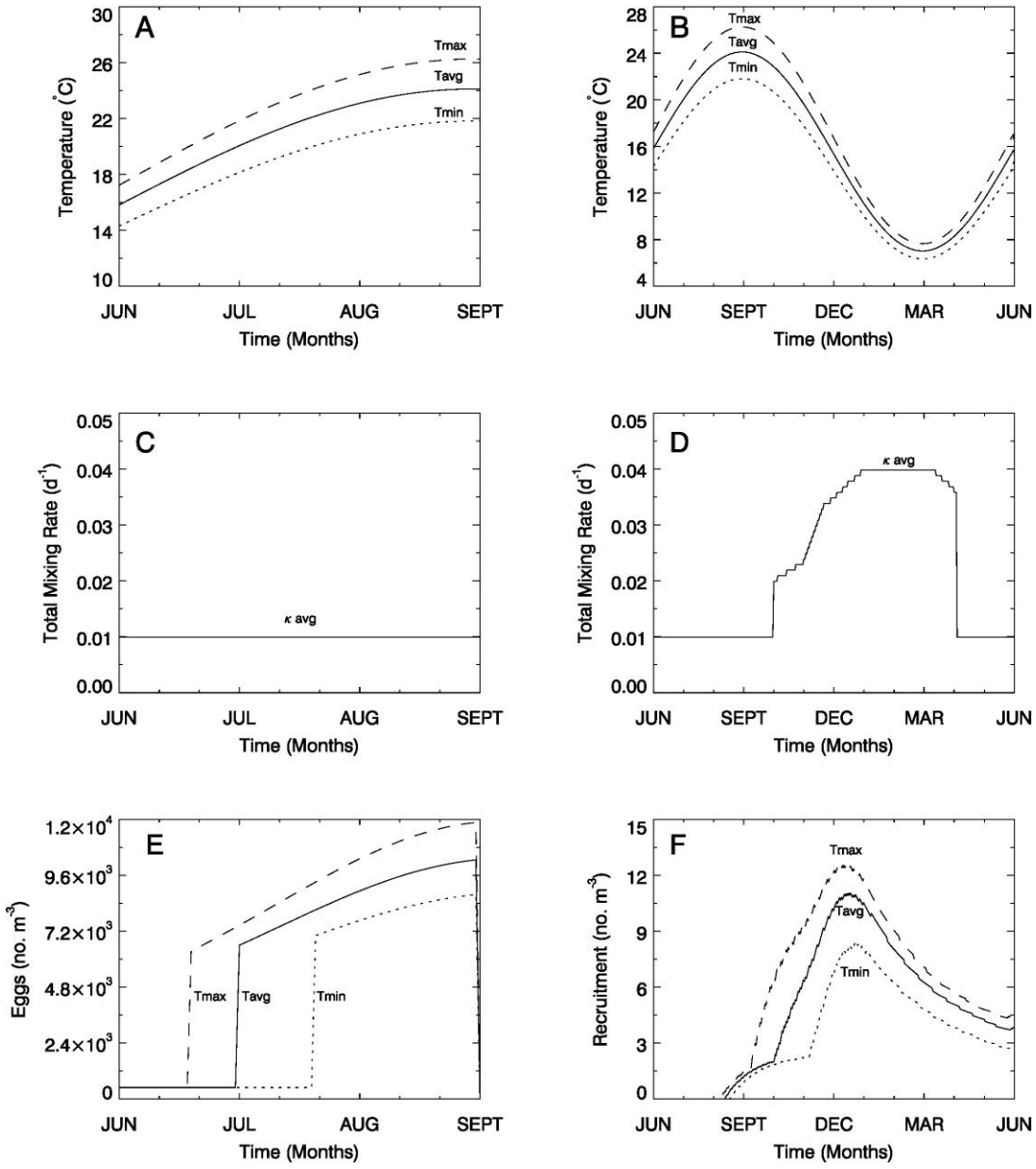

Figure 3.8: Simulation A. Model input: Seasonal variations of temperature (°C) a) during the spawning season (June to September), b) during the course of one year for minimum, maximum and baseline years. Seasonal variation of total mixing rate (d^{-1}) c) during the spawning season, and d) during the course of the baseline year which is repeated with different temperature cycles. Model output: variations of e) eggs (no. m^{-3}) during the spawning season and f) recruits (no. m^{-3}) over the course of one year, for minimum, maximum and baseline years.

2°C drop in mean summer temperatures from the mean (Fig. 8e). At the end of the spawning season it can be seen that there are significant differences between the number of egg survivors for the years of maximum, minimum and baseline temperature years as, ~12x10³, <8.4x10³ and ~10.2x10³, respectively.

In the model larvae hatched from eggs develop into recruits when they satisfy the recruitment criteria of reaching 6.0 cm length. It takes until September for the individuals in the maximum temperature year to reach maturity and at that time their population is slightly exceeding 1.5 no. m^{-3} (Fig. 8f). The individuals coming from the average and minimum temperature cycles satisfy the maturity criteria with a somewhat higher population numbers but with one and two months delay timing, respectively. The recruitment population grows gradually during autumn season due to availability of mesozooplankton food source. Consequently, at the beginning December recruitment population in the maximum, average and minimum temperature cases reach ~13.0, ~11.0 and 8.0 no. m^{-3}, respectively. Then, due to food limitation and of the start of winter their population decreases down to 4.50, 3.75 and 3.00 no. m^{-3} in maximum, average and minimum year cycles, respectively.

Simulation B:

Because the total mixing rate is high in winter only, changes in total mixing has no influence on egg production (Fig. 3.9e), which takes place from June to September. As in the result of baseline year temperature input, the active spawning starts at the end of August with an intensity of ~6.6 no. m^{-3} and the number of survivors at the last day of spawning season is measured as 10.2 no. m^{-3}.

As the total mixing is active during winter, it plays a role in nutrient cycling which slightly promotes recruitment in the early winter before scarcity of food conditions cause a decline (to ~3.75 no. m^{-3}) in recruited stocks (Fig. 3.9f). Hence, the peak biomass values by the recruitment of maximum, average and minimum total mixing year are around 10.5, 11.0 and 11.5 no. m^{-3}, respectively.

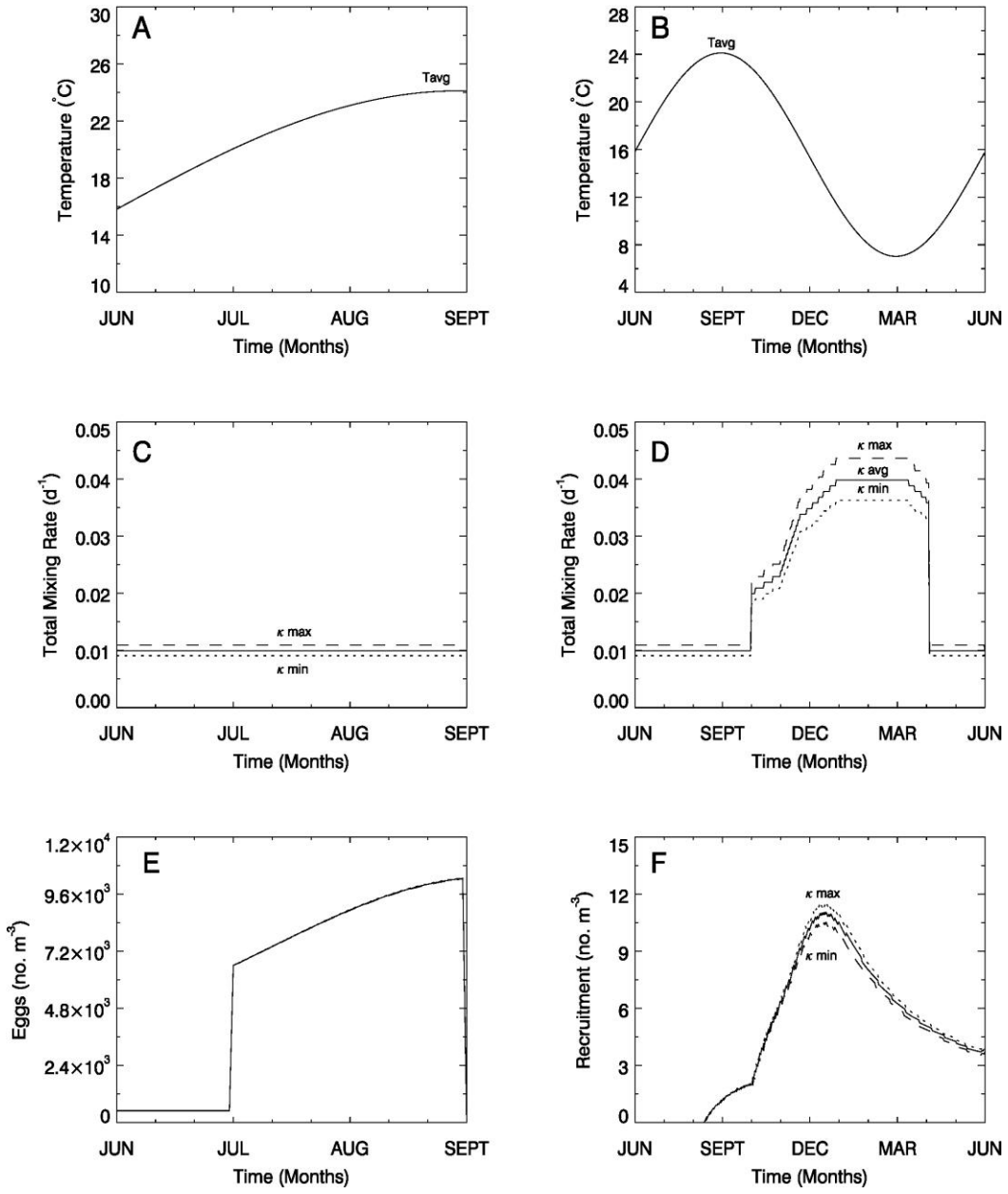

Figure 3.9: Simulation B. Model input: Seasonal variations of temperature (°C) a) during the spawning season (June to September) and b) during the course of the baseline year which is repeated with the different mixing cycles. Seasonal variation of total mixing rate (d^{-1}) c) during the spawning season and d) during the course a year during minimum, maximum and baseline years. Model output: variation of e) eggs (no. m^{-3}) during the spawning season and f) recruits (no. m^{-3}) over the course of one year, for the minimum, maximum and baseline years.

Simulation C:

When both temperature and total mixing are varying the egg production in this case is identical with the results for simulation A (Fig. 3.10e) since total mixing is inactive during the summer period. However, the recruitment variability is responding to both temperature and total mixing effects as they are operating simultaneously. As a result of combination of two effects, the population numbers for maximum temperature and minimum total mixing year in this simulation (12 no. m^{-3}) are lower than the population numbers for simulation A (Fig. 8f). This may be a consequence of counter effect introduced by low mixing that supply fewer resources for larvae feeding. The result of the baseline year (~11.0 no. m^{-3}) is almost identical with the results of 'average temperature' in case A. In the maximum temperature and minimum total mixing simulation the recruitment population in December is ~9.0 no. m^{-3}, the maximum total mixing effects contributes to lowest temperature effects, and increasing them above 'minimum temperature' population in simulation A.

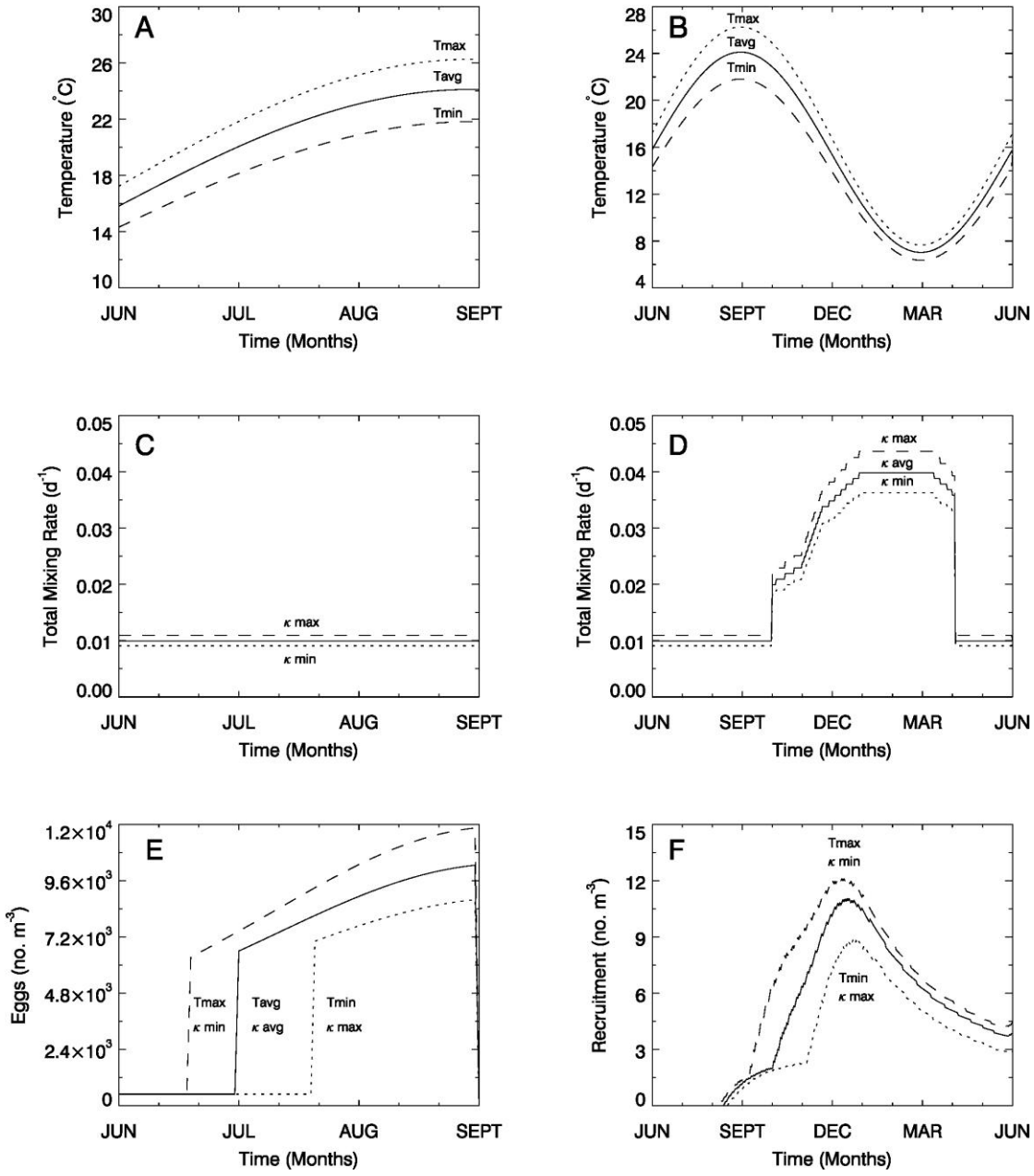

Figure 3.10: Simulation C. Model input: Seasonal variations temperature (°C) a) during the spawning season (June to September) of minimum, maximum and baseline years and b) during the course of one year during minimum, maximum and baseline years. Seasonal variation of total mixing rate (d^{-1}), c) during the spawning season of different years and d) over the course of one year during minimum, maximum and baseline years. Model output: variation of e) eggs (no. m^{-3}) during the spawning season and f) recruits (no. m^{-3}) over the course of one year, for minimum, maximum and baseline years.

3.2.2 Interannual Variations

3.2.2.1 Lower Trophic Level

Simulation A:

In this section, the individual long-term response given by each lower trophic layer compartment to climate variability observed in the three simulations A, B, and C is presented.

Nitrate

The model results reveal that the effect of temperature on nitrate group is indirect, as there is a negative relationship between lowest winter temperatures (Fig. 2.3a,b) and euphotic zone nitrate concentrations (Fig. 3.11b). When considering two different periods, a period of temperature increase from the year 12 to 16 and a period of abrupt temperature decrease between 25 and 36 (Fig. 2.3a), the temperature increase from ~6.35 °C to 7.65 °C is accompanied by a decrease in column integrated nutrient concentrations from 525 mmol N m^{-3} to below 510 mmol N m^{-3}, while the temperature decrease from 7.5 °C to 6.3 °C corresponds to an increase in nitrate concentrations is from ~ 511 mmol N m^{-3} to 527 mmol N m^{-3}.

Phytoplankton

Total phytoplankton biomass varies directly proportionally to varying nutrient concentrations. In the period of temperature increase, phytoplankton biomass slightly decreases from 1245 gC m^{-2} to 1240 gC m^{-2} (Fig. 3.11c). During the temperature decrease the corresponding phytoplankton biomass rises from 1240 to 1246 gC m^{-2}. However, in the years following major temperature increase (such as year no. 6, 12, 26, 36, 37 and 25) the phytoplankton biomass develops additional peaks via indirect effects of temperature.

Microzooplankton

Microzooplankton biomass is closely correlated with phytoplankton long-term variations

and it is best explained by closely examining the variability in two specific periods. During the temperature increase period microzooplankton rises from a biomass value of 72 gC m^{-2} to 76.5 gC m^{-2} within this period (Fig. 3.11d). More interestingly, in the abrupt temperature decrease period the microzooplankton value stays at constant biomass around ~75 gC m^{-2}. At this point, understanding the indirect temperature effects is of crucial importance because at least the output without any significant deviation between the years of 25 and 36 is by itself a major sign of nonlinearity, which carries the information from the previous periods. The indirect influence of temperature phenomena, which actually acts like an additional entrainment forcing, is seen with a delay of one year. Consequently, for the time interval in which the temperature is increasing from year 12 to 16, we need to look for the microzooplankton biomass amounts for the years 13 and 17 to track outcome of nonlinear effects. Then microzooplankton gives a response around ~77 gC m^{-2} (yr. 13) and ~71 gC m^{-2} (yr. 17) within the respective year range. Moreover, when the period of abrupt temperature change is considered (between years 25 and 36), the biomass of the shifted years (26 and 37) is given as ~77.5 gC m^{-2} and it decreases down to ~71.5 gC m^{-2}.

Mesozooplankton

Mesozooplankton biomass is inversely proportional to the coldest winter temperature data as coldest winter temperature plays an indirect mixing mechanism (Fig. 3.11e). On the closer scale, during the period of temperature increase (between year 12 to 16) mesozooplankton concentration decreases from 275 gC m^{-2} to 257 gC m^{-2}, respectively. Within the period from year 25 to 36 the corresponding biomass varies from 257 gC m^{-2} to ~285 gC m^{-2}.

Gelatinous predator

Interannual variations in the gelatinous predator biomass reveal that temperature directly controls gelatinous biomass. When the annual biomass is studied in more detail, the growth advantage of gelatinous predator can be resolved more easily. In the first decade of timeseries, there is no major decrease in temperature range except for the 6^{th} year. In

general, the total biomass produced each year varies between ~175 gC m^{-2} and 185 gC m^{-2} during the first ten years, except for a sharp decrease in biomass in year 6. Then, during the temperature increase trend that takes place between years 12 to 16, the gelatinous biomass develops gradually from 165 gC m^{-2} to 187 gC m^{-2} (Fig. 3.11f). Moreover, between years 16 and 23, annual temperatures are in a decreasing trend. Then, while gelatinous biomass is 187 gC m^{-2} at the beginning of the period, they decrease to 170 gC m^{-2} at the end of it. Finally, within the period of abrupt temperature change, between the 25^{th} and 36^{th} years and are accompanied with an almost constant temperature cycle in between, the corresponding gelatinous biomass values are declined from 185 gC m^{-2} at the beginning to 150 gC m^{-2} at the end, and vary between 170 gC m^{-2} and 180 gC m^{-2} within the rest of the period.

Simulation B:

Nitrate

In 'total mixing only' simulation (Fig. 3.12), euphotic layer nitrate concentrations are in direct proportion to total mixing rates (Fig. 3.12a) but they are not as sensitive to variations of total mixing as they were to variations in temperature (simulation A). Thus, the concentrations are around baseline value of 516 mmol N m^{-3} (Fig. 3.12b). Only the strong variations in total mixing that occurred in years no. 6, 12, 16, 25, 26, 36 and 37 are shown to influence nitrate concentrations slightly, which indicates the contribution of total mixing on nutrient pumping to be a minor.

Phytoplankton

Phytoplankton biomass varies directly proportionally with the changes in 50 years total mixing rate data without any nonlinear effects carried over from the previous periods as observed in simulation A. Moreover, in the period of decreasing total mixing rates (from year 12 to 16) (Fig. 2.3b), the phytoplankton biomass decreases from 1250 gC m^{-2} to 1238 gC m^{-2} (Fig. 3.12c). In addition, when total mixing rates change abruptly between years 25 and 36, the phytoplankton biomass rises from 1240 gC m^{-2} to 1253 gC m^{-2}.

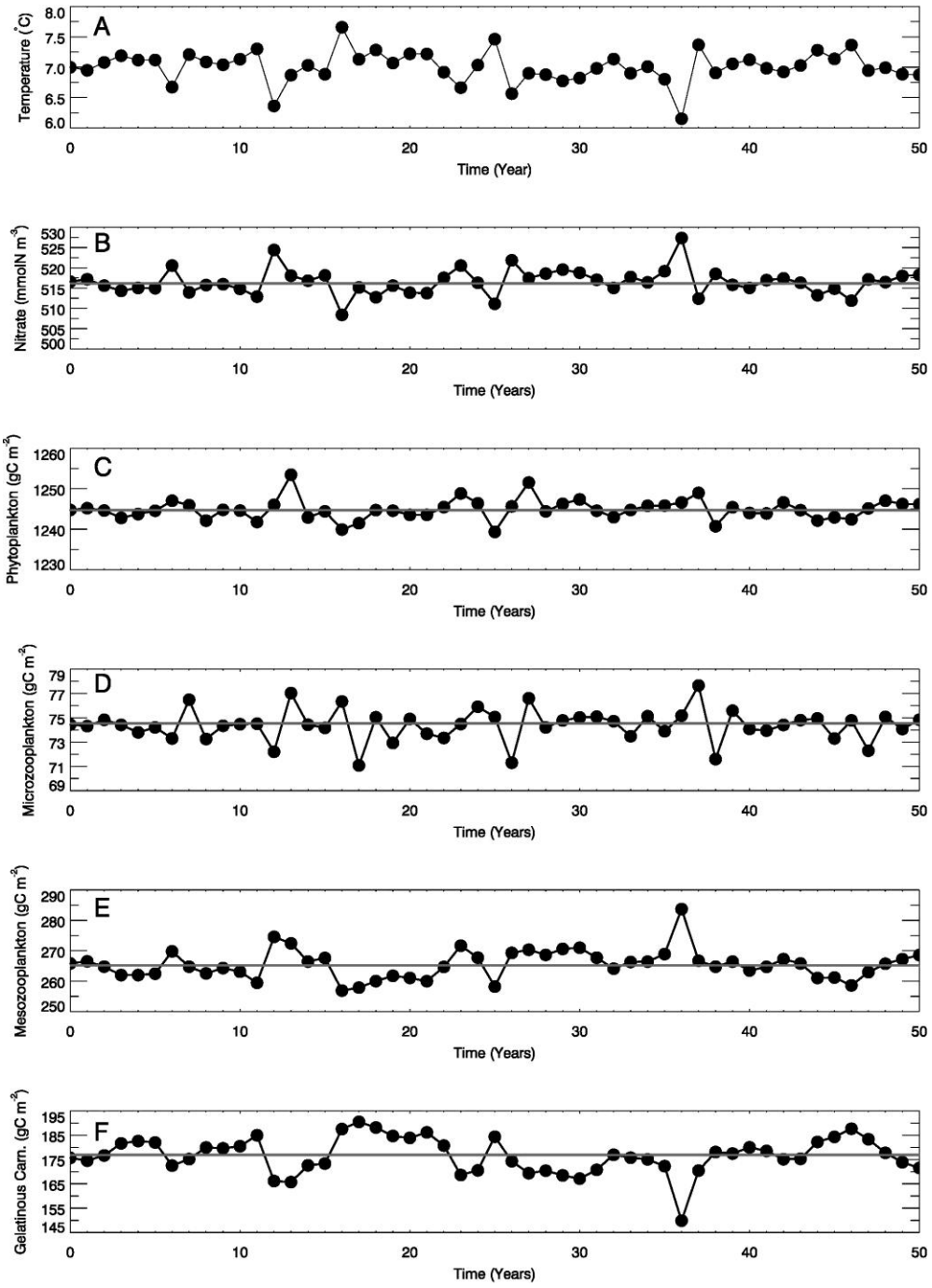

Figure 3.11: Simulation A. Model input in the form of a) temperature (^{o}C). Model output: interannual variability of euphotic layer annual total b) nitrate concentration (mmol N m^{-3}), euphotic zone integrated total annual c) phytoplankton (gC m^{-2}), d) microzooplankton (gC m^{-2}), e) mesozooplankton (gC m^{-2}) and f) gelatinous carnivore biomass (gC m^{-2}) variations. Straight line represents the baseline simulation.

Microzooplankton

Microzooplankton biomass variations are elevated (/depressed) corresponding to higher (/lower) rates of total mixing (Fig. 3.12d). During the period in which mixing decrease from ~0.04375 d^{-1} (yr. 12) to 0.03625 d^{-1} (yr. 16), the corresponding biomass decreases from ~76 gC m^{-2} to ~72 gC m^{-2}, respectively. Similarly, during the period of abrupt mixing change which takes place in between the years 25 to 36, the microzooplankton biomass response to increasing total mixing rates is from 72.5 gC m^{-2} and 77.5 gC m^{-2}, respectively.

Mesozooplankton

Mesozooplankton gives a much weaker response to total mixing forcing in comparison to the mesozooplankton biomass response in simulation A (Fig. 3.11,12e). Such that, most of the concentrations stay close to baseline value of 265 gC m^{-2} (Fig. 3.12e). Only when the mixing values exceed threshold of 0.04125 d^{-1} or fall below 0.0375 d^{-1} a slight deviation from baseline occurs.

Gelatinous predator

Gelatinous predator biomass variation is controlled directly by the intensity of the total mixing rate (Fig. 3.12a-f). However in this case, the gelatinous biomass is not so responsive to changes in the mixing cycle as it is to temperature in simulation A (Fig. 3.12f). That is why, the gelatinous biomass does not deviate much from the baseline which corresponds to ~177 gC m^{-2} (Fig. 3.12f). To be more specific, in the period from year 12 to year 16, where total mixing rate are decreasing, gelatinous biomass decreases from 180 gC m^{-2} to ~175 gC m^{-2}. And in the following period when total mixing rate changes abruptly between the years 25 to 36, gelatinous predator biomass rises from 175 gC m^{-2} to 188 gC m^{-2}.

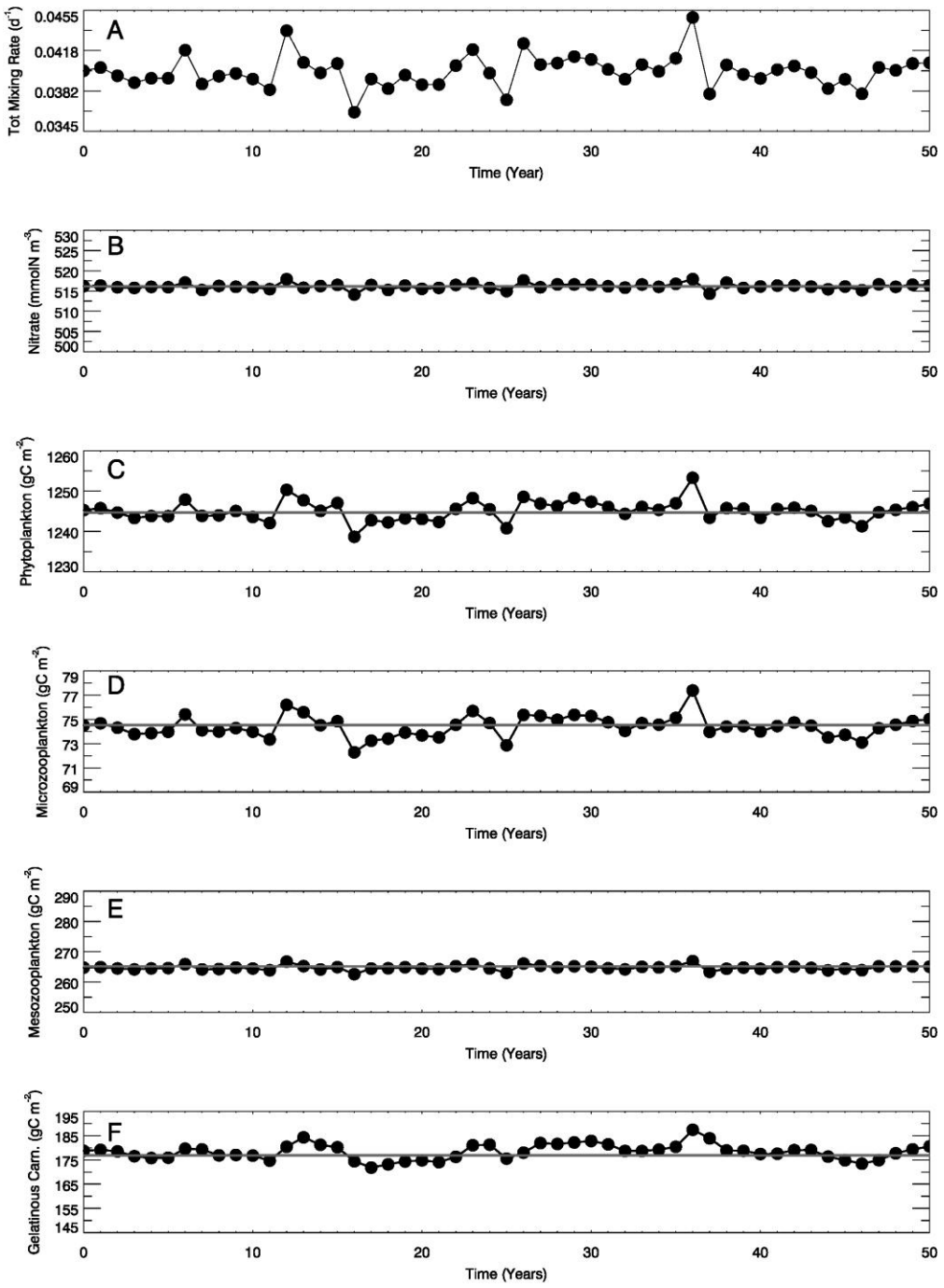

Figure 3.12: Simulaton B. Model input in the form of a) total mixing rate (d^{-1}). Model output: interannual variability of euphotic layer annual total b) nitrate concentration (mmol N m^{-3}), euphotic zone integrated total annual c) phytoplankton (gC m^{-2}), d) microzooplankton (gC m^{-2}), e) mesozooplankton (gC m^{-2}) and f) gelatinous carnivore biomass (gC m^{-2}) variations. Straight line represents the baseline simulation.

Simulation C:

Nitrate

In simulations A and B it was seen that nutrient supply is regulated directly by colder winter temperatures and higher rates in total mixing. When both environmental forcings are considered simultaneously (Fig. 3.13a,b), it is seen that nutrients decrease from ~ 526 mmol N m^{-3} to 506 mmol N m^{-3} (Fig. 3.13c) during the period of temperature increase accompanied by total mixing decrease (between years 12 and 16 respectively). For the period of abrupt temperature and total mixing rate change, the nitrate concentrations rise from 510 mmol N m^{-3} up to ~ 530 mmol N m^{-3} (between years 25 and 36).

Phytoplankton

In simulation C, the response of primary producer is more intensified and complicated than in simulations A and B.

Such that, in the period between year 12 to 16 where temperature is increasing and corresponding mixing rates are decreasing, phytoplankton is decreasing from 1252 gC m^{-2} to 1234 gC m^{-2} (Fig. 3.13d). Then, during years from 25 to 36 which is referred to as the period of abrupt temperature and total mixing rate change phytoplankton biomass varies from 1234 gC m^{-2} to 1256 gC m^{-2}. In addition, there is an influence from nitrate concentrations that is delayed by one year (yr. 7, 13, 24, 26, 27, 37 and 38).

Microzooplankton

In period from year 12 to 16 which is accompanied by temperature increase and total mixing decrease, microzooplankton biomass increases slightly from 73.75 gC m^{-2} to 74 gC m^{-2} (Fig. 3.13e). Then, during the period in which the temperature (and mixing) changes abruptly between years 25 and 36 the corresponding biomass value rises from 73.75 gC m^{-2} to 77.5 gC m^{-2}, respectively. Secondly, the one year delayed temperature influence can be seen in the microzooplankton biomass. Accordingly, the biomass

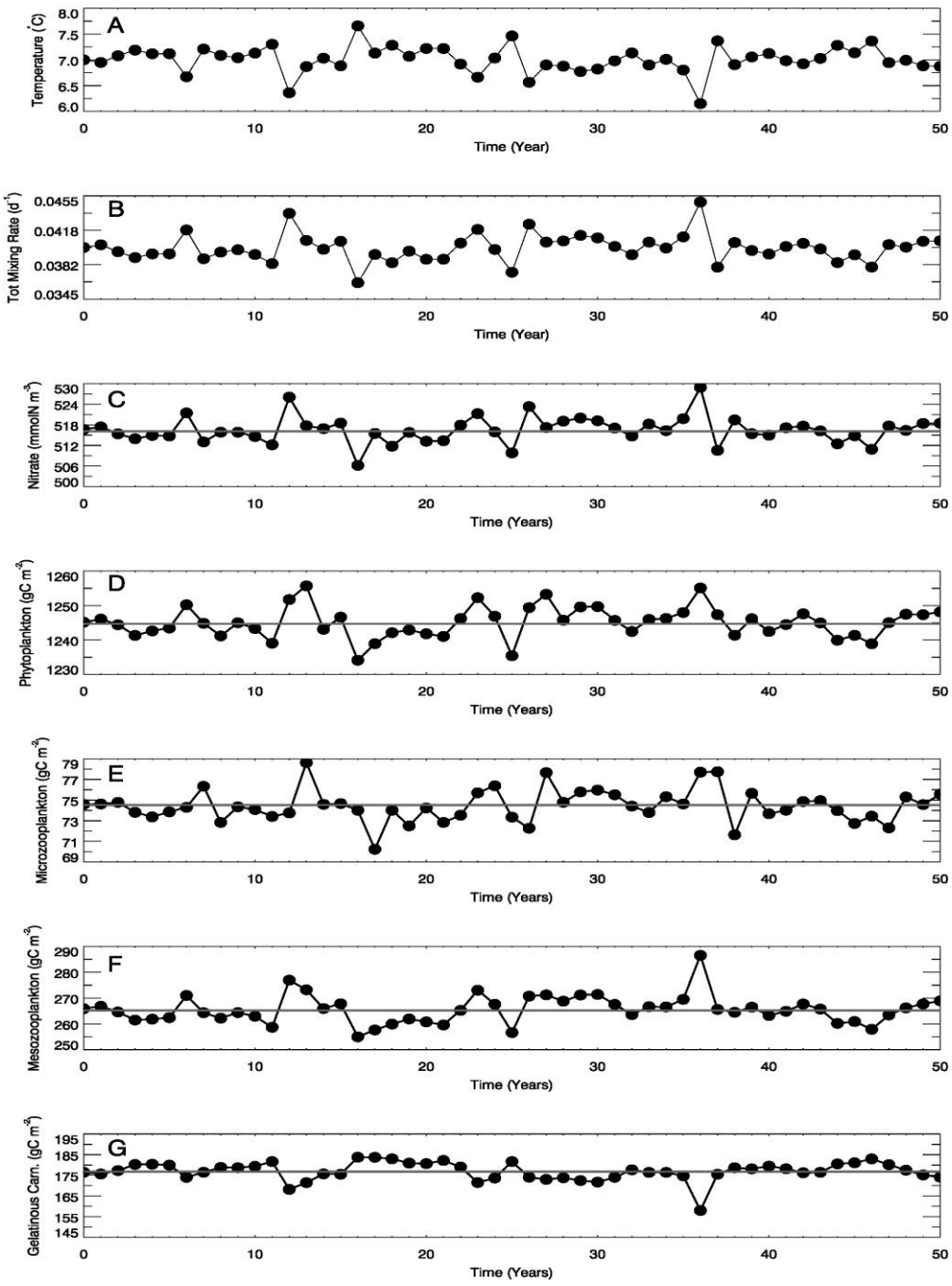

Figure 3.13: Simulation C. Model input in the form of a) temperature (^{o}C) and b) total mixing rate (d^{-1}). Model output: interannual variability of euphotic layer c) total annual nitrate concentration (mmol N m^{-3}), euphotic zone integrated total annual d) phytoplankton (gC m^{-2}), e) microzooplankton (gC m^{-2}), f) mesozooplankton (gC m^{-2}) and g) gelatinous carnivore biomass (gC m^{-2}) variations. Straight line represents the baseline simulation.

variations in the first period, within years 13 and 17, vary between 78.5 gC m^{-2} and 70.5 gC m^{-2}, respectively. In the second period, the biomass values between years 26 and 37 years are 72.5 gC m^{-2} and 77.5 gC m^{-2}, respectively.

Mesozooplankton

The combined effects of temperature increase accompanied by total mixing decrease reduce mesozooplankton biomass from 277 gC m^{-2} to 255 gC m^{-2} between the years from 12 to 16 (Fig. 3.13f). Likewise, within the period of abrupt temperature and total mixing change, mesozooplankton is elevated from 257.5 to 287.5 gC m^{-2} during the period between 25 to 36. Consequently, the combined effects of temperature and total mixing amplify mesozooplankton biomass by an amount of (+/-) 2.5 gC m^{-2} with respect to temperature effects only.

Gelatinous predator

The influence of temperature and total mixing rate together seem to cancel out each other's influence on gelatinous. Since the gelatinous biomass varies in directly proportionally with individual forcings, the combination of the two is expected to override each other. Hence, owing to the fact that the effect of temperature is more dominant, the results for case C (combining A and B) are shown to deviate towards simulation A, but this time with a less pronounced response.

In order to understand the counter effect phenomena, understanding of the particular two periods is necessary. Thus, between the years 12 and 16 in which the temperature follows an increasing trend and total mixing follows a decreasing trend, gelatinous carnivore biomass values increase from 167.5 gC m^{-2} to 185 gC m^{-2} (Fig. 3.13g). Correspondingly, during the period from year 25 to 36, the temperature (total mixing rate) variations present abrupt changes, gelatinous biomass decreased from 181 gC m^{-2} to 158 gC m^{-2}.

3.2.2.2Higher Trophic Level

Simulation A:

Anchovy production is directly correlated to temperature variation as it follows the same variability pattern as the temperature (Fig. 3.14a, b). For example, during the period in which temperature increases from 6.35 (year 12) to 7.65 °C (year 16) the egg population increases from 350 to ~700 no. m^{-3}. Thus, for a 1.30 °C increase in temperature in half a decade the egg numbers experienced a total of 100% increase. In the period of abrupt temperature change (years 25 to 36) egg numbers decrease from ~650 to below 300 no. m^{-3}. Hence, a 1.2 °C temperature decrease within a decade results in a ~54 % decrease in egg numbers.

Anchovy recruits are also highly correlated with temperature (Fig. 3.14c). For period of temperature recruitment numbers increase from 1.125 (yr. 12) to 2.125 (yr. 16) no. m^{-3} which amounts to ~88.9% increase for a temperature increase of 1.3°C. On the other hand, during the period of abrupt temperature change, a 1.2 °C decrease in temperature (between yrs. 25 and 36) causes the recruitment numbers to decline from around 2.0 to 1.0 no. m^{-3}, a decrease of ~50%.

Spawner numbers vary directly proportional to the temperature variations as well (Fig. 3.14d). During the temperature increase period, spawners rise from 1.7 (yr. 12) to 2.2 no. m^{-3} (yr. 16). Thus, an increase in temperature by 1.3°C, results in ~30% of increase in spawners. On the other hand, during abrupt temperature change the number of spawners decrease from 2.12 (yr. 25) to 1.60 no. m^{-3} (yr. 36) which is a 24.5% decrease.

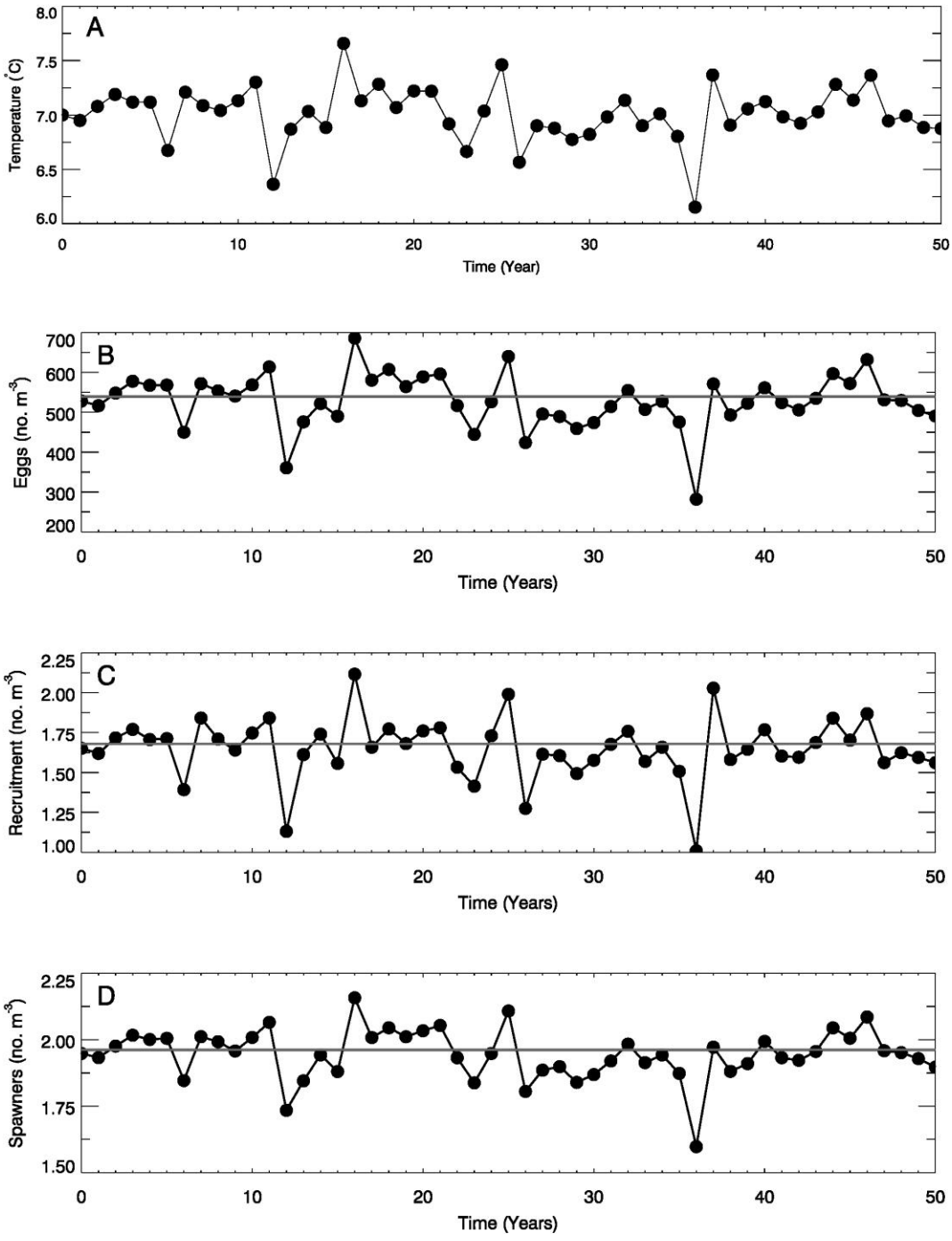

Figure 3.14: Simulation A. Model input: Interannual variation of a) lowest winter temperatures (°C) (at the end of Feb.). Model output: interannual variability of total annual anchovy b) eggs, c) recruits and d) spawner population (no. m^{-3}). Solid line represents the baseline simulation. Spawner numbers represent female adults that constitute 50% of total population.

Simulation B:

Although egg numbers do not commonly deviate from the baseline (~550 no. m^{-3}) (Fig 3.15b), minor deviations from the baseline can occur when intensity of mixing is either very high or considerably low, such as in years 7, 13, 17, 26, 37 and 47 (Fig 3.15a). It can be seen that it takes one year for the egg numbers to respond to total mixing forcing since the model year starts with spawning season in summer and the number of eggs produced is influenced by the mixing effects that operated on the previous year. Thus, the influence of total mixing on eggs variations is indirect.

Recruitment numbers are sensitive to total mixing variations (Fig 3.15c), owing to the fact that they reach peak population numbers in December which corresponds to the start time of the intense winter mixing. For instance, during the time interval in which total mixing rate decreases (from year 12 to 16), the recruitment population decreases from 1.75 (year 12) to 1.625 no. m^{-3} (year 16) (Fig. 3.15c). Thus, the recruitment decreases by ~7% when total mixing rates decrease by ~17%. In the period of abrupt total mixing change (from yr. 25 to 36), the recruitment biomass increases from 1.625 to 1.75 no. m^{-3}, respectively. As a result, 20% increase in the total mixing rate is accompanied with a 7% increase in total recruitment population.

Model results indicate that, the spawners are subjected to total mixing mediated influences at the time when they are foraging for food. Similar to the recruitment case, they are positively correlated with the total mixing rate variations which means when total mixing is intensified, spawners increase in the same year without any delay in timing (Fig. 3.15d). In the mixing decrease period (from year 12 to 16), the spawner population decreases from 2.0 (yr. 12) to 1.94 no. m^{-3} (yr. 16), resulting in a total of ~5% decrease in population numbers, for a 17% decrease in total mixing rates (Fig. 3.15d). Futhermore, during the period of abrupt total mixing change (from year 25 to 36), the total spawner numbers increase from 1.95 to 2.05 no. m^{-3}. That means a 20% increase in total mixing rate produces ~5% increase in spawner numbers.

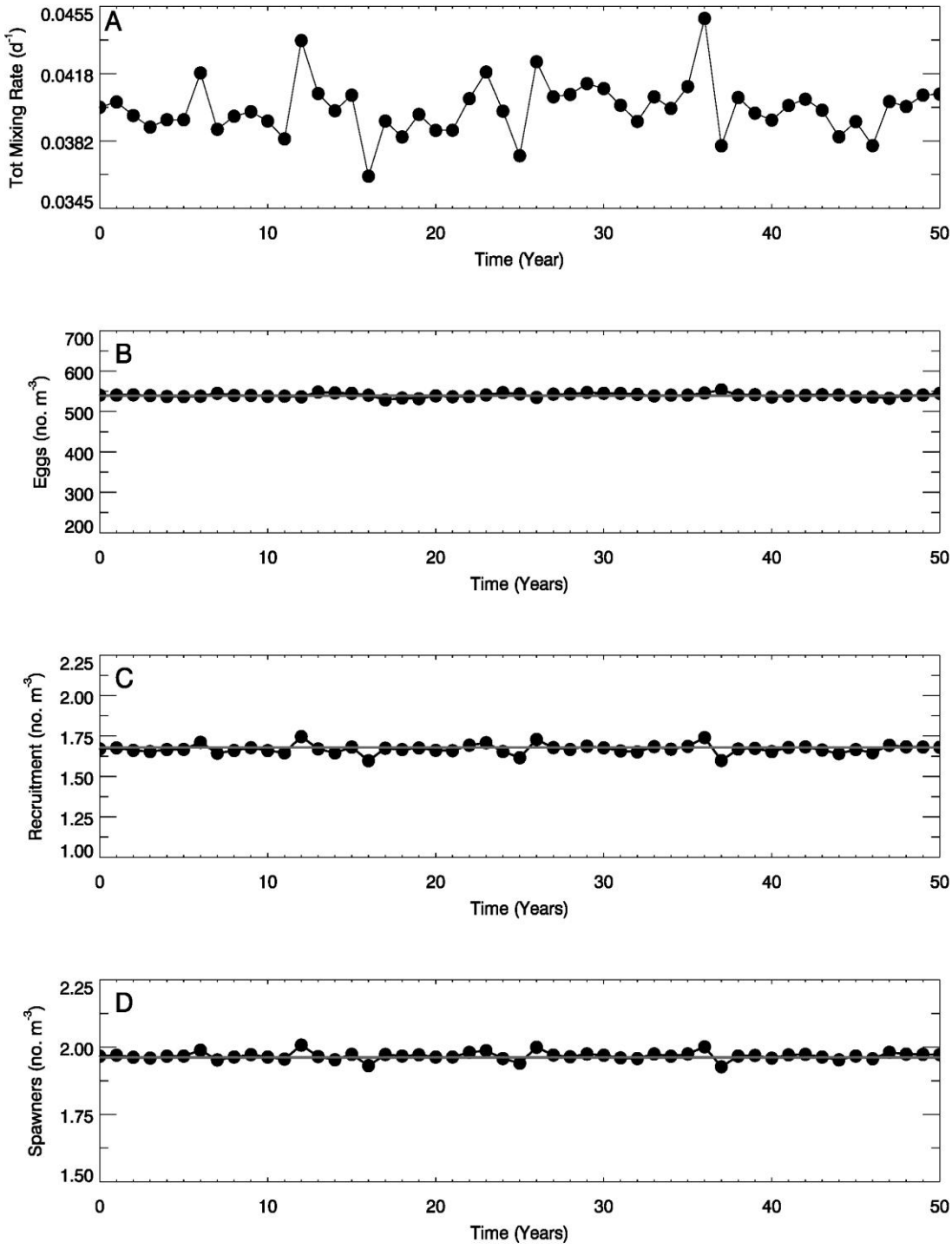

Figure 3.15: Simulation B. Model input: interannual variation of a) total mixing rates (d^{-1}) (at the end of Feb.). Model output: interannual variability of total annual anchovy b) eggs, c) recruits and d) spawners population (no. m^{-3}). Solid line represents the baseline simulation. Spawner numbers represent female adults that constitute 50% of total population.

Simulation C:

Although temperature effects are dominating the egg population development, results are slightly deviating from the egg population values in simulation A when both temperature and mixing are taken into account (Fig. 3.16a,b). The reason behind these slight differences is the indirect effect of total mixing rates, which acts with opposite dynamics to temperature influence and is the information propagating from the previous years. For instance, in the period of temperature (total mixing) increase (decrease) from year 12 to 16, eggs increased from 350 to 700 no. m^{-3}, respectively (Fig. 3.16c). While, within the period of abrupt temperature (total mixing) change from year 25 to 36, the egg numbers decrease from 650 to 300 no. m^{-3}, respectively.

The recruitment population is mainly affected by temperature and the indirect effect of total mixing acts as a counter effect, which is why the recruitment population numbers are more suppressed compared to simulation A (Fig. 3.16d). Hence, in the period between years 12 and 16, the recruitment increases from 1.19 to 2.06 no. m^{-3} (Fig. 3.16d), whereas in the period from 25 to 36, the recruitment decreases from 1.94 to 1.06 no. m^{-3}. As a result, in the former period recruitment population increases by 73%, and in the latter period it decreases by 45%.

Spawners' interannual variations respond directly to the effects of both temperature and total mixing in the same year. And since the years of high temperature domination correspond to the years of low total mixing rates in the stochastic timeseries data, when both forcing are input to the model their simultaneous effects cancel out each other (Fig. 3.16e). In more detail, the results for the period of temperature (total mixing) increase (decrease), between years 12 and 16, show a population increase in the spawners from 1.77 to 2.125 no. m^{-3} during this period. Moreover, within the period of abrupt temperature (total mixing) change (from year 25 to 36), the spawner numbers decrease abruptly from 2.06 to 1.63 no. m^{-3}. Hence, the corresponding percent changes for the former and latter periods are ~20% increase and 21% decrease, respectively.

Anchovy Reproduction and Recruitment

So far, it is seen that temperature has a more dominant influence on the development of interannual variation of eggs, recruits and spawners. In order to understand the egg production and recruitment success in relation to climate variability in more detail a correlation analysis was carried out.

It can be seen that there is a linear relationship between the egg production numbers and the total number of spawners when considering temperature variation only (Fig. 3.17a) and a very high correlation is found to be 99%. The same correlation amounts to 94% when both temperature and total mixing is combined (Fig. 3.18a). This indicates that gonadal development is limited when subjected to stochastic mixing effects in the winter months.

The relationship between the total number of eggs produced and the total number of recruits that survive under different environmental effects reveals that correlation of recruitment versus eggs is 86% when only temperature forcing is used (Fig. 3.17b), but 91% when both temperature and total mixing is included (Fig. 3.18b). Thus the results show that, the eggs that are subjected to combined effects of temperature and total mixing together do more successfully grow up to become recruits than the eggs subjected to temperature forcing only.

The correlation between spawners and recruits shows that when temperature influence alone is considered the correlation coefficient is 82% (Fig. 3.17c), but when both mixing and temperature are considered it is 76% (Fig. 3.18c), indicating that under constant nutrient supply the recruits more successfully develop into spawners than under varying nutrient supply. To further investigate whether there is a relationship between this year's spawners and next years egg production a correlation between the spawners that are subjected to climate of this year and eggs they produce the following year is calculated for simulation A and C (Fig. 3.19). Both analyses show no correlation. An additional correlation analysis of the mean length of recruits in relation to total number of recruits is performed for simulation A and B to investigate if the recruits in different simulations have different length distribution. The results show a weak correlation in

simulation A (temperature variation only) (Fig. 3.20a) and in no correlation in simulation C (temperature and total mixing variation) (Fig. 3.20b).

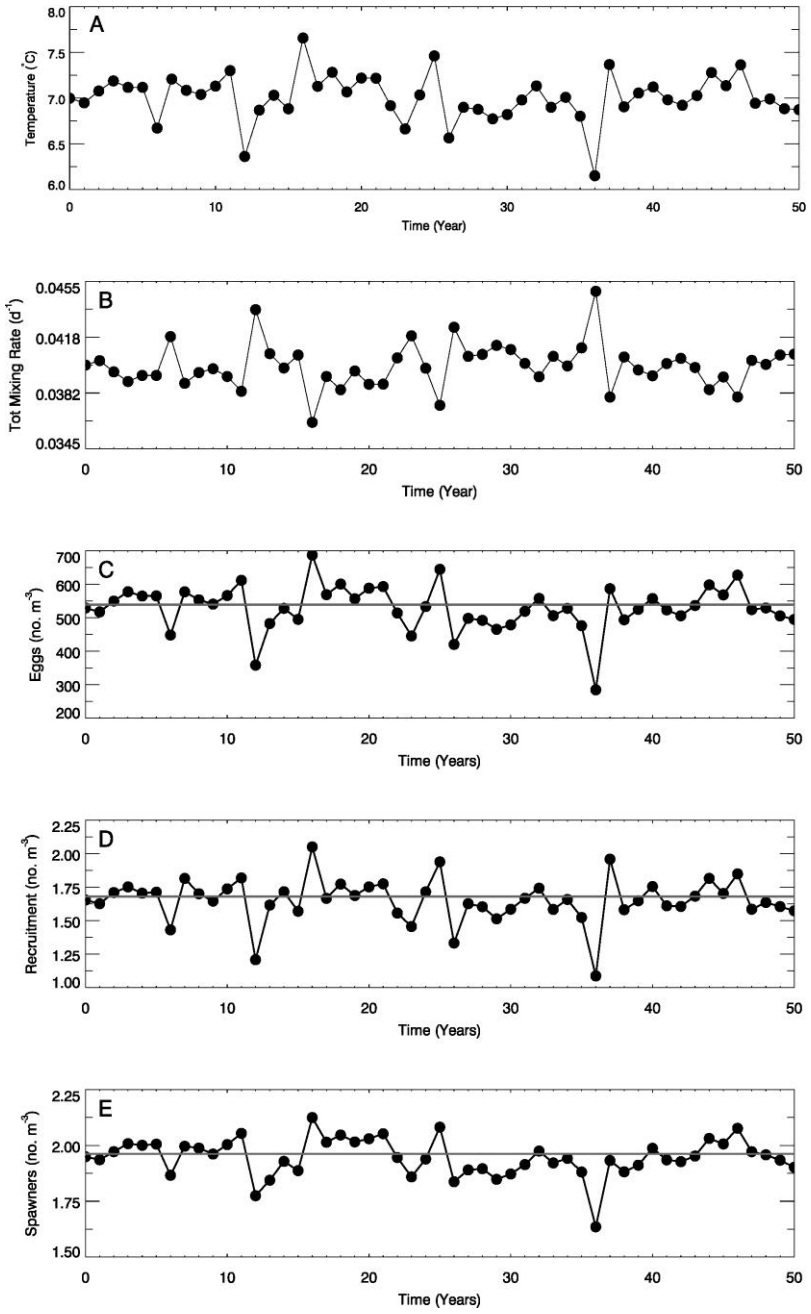

Figure 3.16: Simulation C. Model input: Interannual variation of a) lowest winter temperatures (°C) and b) total mixing rates (d^{-1}) (at the end of Feb.). Model output: interannual variability of total annual anchovy c) eggs, d) recruits and e) spawners population (no. m^{-3}). Solid line represents the baseline simulation. Spawner numbers represent female adults that constitute 50% of total population.

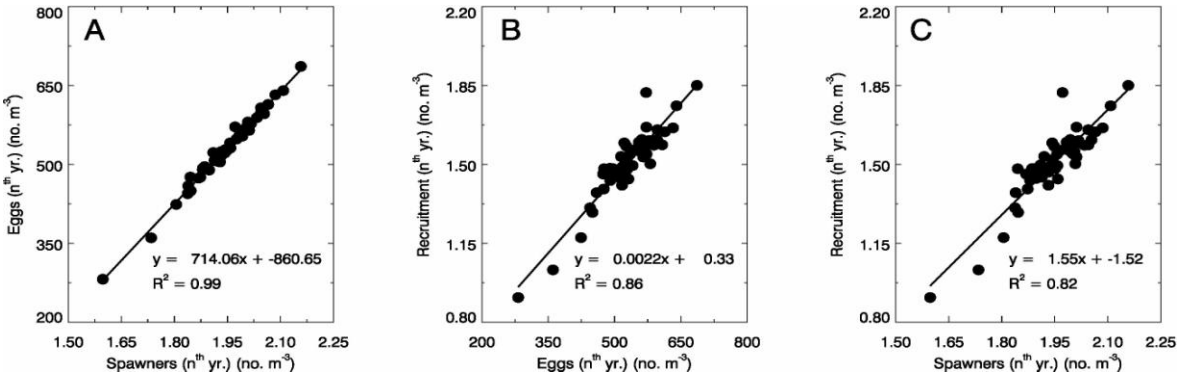

Figure 3.17: Simulation A. Correlation analysis of total annual a) spawners versus eggs, b) eggs versus recruitment and c) spawners versus recruits (no. m^{-3}) for 50 years of varying temperature input (Fig. 2.3a). Spawner numbers represent female adults that constitute 50 % of total population.

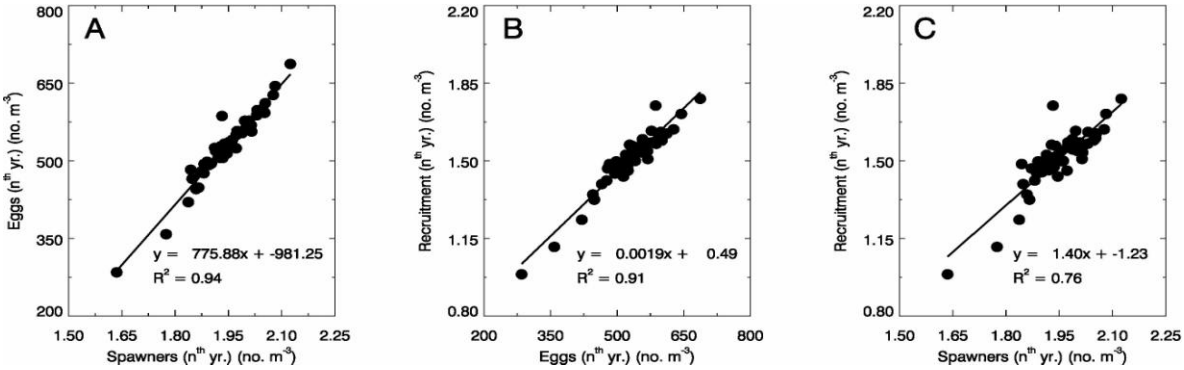

Figure 3.18: Simulation C. Correlation analysis of total annual a) spawners versus eggs, b) eggs versus recruits and c) spawners versus recruits (no. m^{-3}) for 50 years of varying temperature and total mixing input (Fig. 2.3). Spawner numbers represent female adults that constitute 50 % of total population.

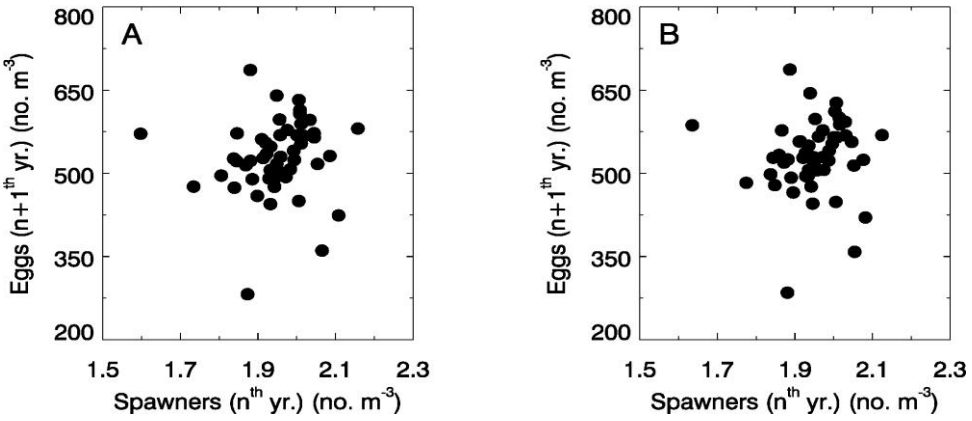

Figure 3.19: Simulation A and C. Correlation analysis of (nth year) total annual spawners versus (n+1th year) eggs for 50 years of a) varying temperature input (Fig. 2.3a) and b) varying temperature and total mixing input (Fig. 2.3). Spawner numbers represent female adults that constitute 50 % of total population.

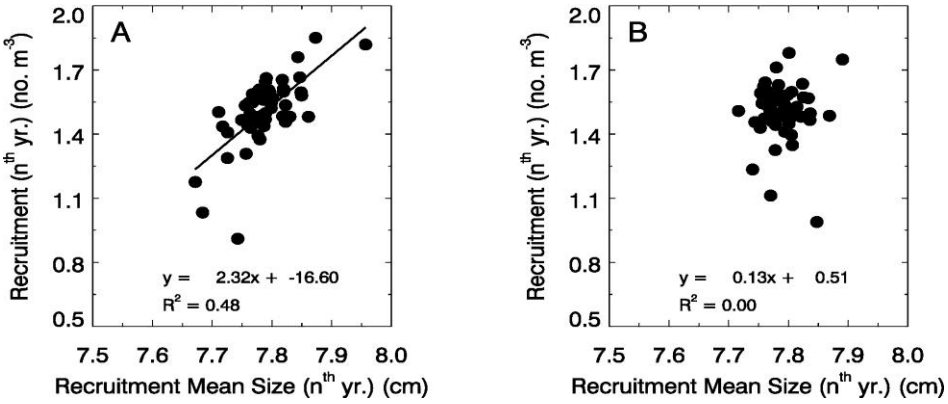

Figure 3.20: Simulation A and C. Correlation analysis of mean size of recruits (cm) versus total annual number of recruits (no. m^{-3}) for 50 years of a) varying temperature input (Fig. 2.3a) and b) varying temperature and total mixing input (Fig. 2.3).

4 DISCUSSION

The modeling approach used in this study provides a framework for investigating the response of the Black Sea ecosystem and more specific the anchovy recruitment, to changes in environmental perturbations triggered by climate variability. In this chapter the individual response of the lower trophic level components of the ecosystem and the higher trophic level in form of anchovy population dynamics will be discussed.

4.1 Lower Trophic Level

To begin with, the response given by successive lower trophic levels has a non-linear nature, which means reaction patterns deviate across state variables under the applied forcing. The most significant finding of the model with regard to lower trophic level is that, when all three simulations (A, B and C) are compared, the influence of temperature while promoting 'bottom-up' type of control, has a more prominent regulatory power on the ecosystem components and their trophic interactions alone which agrees with Oğuz, (2005b) and Oğuz et al. (2006). Apparently, temperature forcing derives a two way control mechanism on the lower trophic level. One is, by contributing to biotic compartments' metabolic rates and the other is via generating a wind-induced vertical mixing effect with a strong structuring potential. On the other hand, total mixing forcing is seen to be inducing only a minor response in the lower trophic levels of the model. In the last simulation (C) where the two environmental variables are used together as model forcing, the response by the LTL groups is in either a boosted or a diminished manner, decided by how the indirect temperature effect is received by the individual group. To be more precise, in the nitrate compartment, the indirect effect of temperature is instantaneous, which means that cold winter conditions cause wind-mixing effects at the same time. Thus, when the model is forced with the overlapping effects of (indirect) temperature and total mixing, in simulation C, the resultant 50-year nitrate

concentrations reveal more elevated patterns than the results with single environmental forcing, ‘temperature_only (A)’ or ‘mixing_only (B)’ simulation. The response given by the rest of the LTL (biota) is more of a complex one. For instance, it takes one year until the bottom-up control by temperature to reaches the phytoplankton level. Then, this indirect influence is added to this year’s direct effects of temperature and total mixing whether to promote or suppress the resultant effect. Thus the model results for phytoplankton reveal promoted concentrations in ‘both temperature and mixing included’ simulation (C) (Fig. 3.13d). The same indirect and direct mechanisms also apply for the microzooplankton level by boosting the annually integrated biomasses in simulation C (Fig. 3.13e). In mesozooplankton, the bottom-up effect diminishes and the cascade effects slightly diminish owing to the on-going prey-predator interactions between mesozooplankton with gelatinous carnivore and anchovy. Yet, the predation by the gelatinous carnivore is evident (Figs. 3.13f,g). Thus, mesozooplankton grows more when gelatinous biomass is less and mesozooplankton grows less when gelatinous species concentration increases. One interesting implication of gelatinous predator is that it grows increasingly more when the temperature conditions are favorable because, since it is not limited by predation by the higher order trophics, it survives in the system throughout the year. Correspondingly, during adverse climate conditions, its biomass severely declines. Moreover, in simulation C, the total mixing forcing act as to diminish direct temperature effects on gelatinous predator (Fig.3.13g) because both counteract each other (Fig.3.11-12g).

4.2 Higher Trophic Level

Houde (1987) suggested that in early life-history of marine fishes cohort specific survival rates are closely related to the 'transition length', the length at which weight growth outreaches the instant mortality rate and after which the biomass growth starts increasing progressively. Thus our model results reveal a transition length of 6.0 cm after which body energy is allocated more to weight growth (Fig. 3.3).

4.2.1 Timing of Anchovy Spawning and Recruitment Success

When the model is run with temperature forcing only (simulation A), the start of actual fish production is shown to be highly dependent on temperature effects. Such as, for a 2 °C drop in mean summer temperature the start date of egg production delays by 45 days with respect to baseline year. Similarly, as a result of 2 °C increase in mean summer temperature, the start of egg production is 30 days earlier with respect to the baseline year (Fig. 3.8e). Moreover, not only the start of spawning season but also the daily and seasonal egg production amounts reveal distinct differences in the years of maximum and minimum temperatures with respect to average temperature year.

Furthermore, the larval survival rates are influenced significantly by temperature effects, such as, recruitment experiences the highest population growth under maximum temperatures and the lowest population numbers under minimum temperatures when compared to case C (Fig. 3.8-10f).

Another implication of the analysis is that, under ‘both temperature and mixing included (C)’ forcing, during the summer season, the contribution of total mixing has no influence on egg production amounts. Thus, the start of egg production and spawning intensity is essentially controlled by temperature effects. However, when recruitment is considered, it can be seen that the recruitment numbers under maximum temperature effect are decreased by the additional minimum total mixing cycle, whereas, the contribution of maximum total mixing cycle promotes the recruitment population response given under minimum temperature effect. Here, the addition of total mixing effects acts as to diminish temperature effects (Fig. 3.8-10f).

4.2.2 Interannual Variability of Anchovy Biomass

Eggs

When the model is forced with ‘temperature_only (simulation C)’ forcing, egg production varies most sensitively over fifty years (Fig. 3.14b). Temperature's direct effect is responsible for the variation in egg production whereas the indirect effect of

temperature (due to wind-induced mixing) remains negligible in regulating the egg production levels.

The effect of total mixing variations (simulation B) on egg production is very limited due to weaker diffusion rates during the spawning season (Fig. 3.15b). However, the bottom-up supply of resources via peak total mixing rate can be tracked with the available model output as small jumps. Those small jumps indicate that it takes one year for the bottom-up resource supply to reach ichthyoplankton.

When the simulation A and B forcing is combined under simulation C, the additional total mixing forcing slightly diminishes the effects of temperature forcing on egg production.

Climate variability may seriously affect anchovy egg production and larval survival rates by promoting the prey-predator interactions between gelatinous carnivores and the ichthyoplankton under high carrying capacity conditions (Fig. 3.16c). Similar prey-predator relationships as a result of climate-induced changes are also defined for the sprat-cod interactions which constitute the majority of the fish species in the Baltic Sea (Köster et al., 2001).

Recruitment

The results of the current model output show a close relationship between climate variability and anchovy production in the Black Sea (Fig. 3.14c). A similar relationship also has been observed during field studies for the Baltic Sea sprat recruitment variability and 45-years climate variations (MacKenzie and Köster, 2004). Low temperatures affect recruitment numbers while regulating the production intensity of spawners (Grauman and Yula, 1989) and survival probabilities (Grauman and Yula, 1989; Ojaveer, 1998; Nissling, 2004) of eggs and larvae for sprat.

Anchovy recruitment is the second most sensitive compartment to temperature changes in the higher trophic level in the model used here. When the model is run with case B forcing, only limited changes in recruitment variations are observed (Fig. 3.15c), indicating that the instantaneous bottom-up resource supply has little effect compared to the temperature effects.

While, the single effects of increasing temperature and total mixing, increase recruitment variability, the combination of these two under simulation C act as to weaken each other effects (Fig. 3.14-16d). As the temperature effect on recruitment is more dominant, the variability similar to simulation A, but the response is slightly less strong.

Spawners

With temperature only forcing, the variations of annual total spawners is tracked for fifty-years (Fig. 3.14d). The results reveal that spawner numbers alter notably in response to the changes in the temperature cycle. The resultant spawner response arises via direct effects of temperature and indirect effects seem to be trivial in this case.

Under simulation B conditions, spawner population varies in direct relation to total mixing rate changes but this time the response is even weaker as compared to the response given in simulation A (Fig. 3.15d).

In simulation C (combined effects of temperature and total mixing) forcing, the contribution of total mixing forcing introduces counter effects to the spawner population variations under simulation A, so that in simulation C, the spawner variations are similar those in simulation A but in a slightly diminished magnitude (Fig. 3.14,16e).

Regression Analysis

When the temperature only effects (simulation A) on egg production of anchovy spawners are analyzed, spawners versus egg numbers reveal a 99 % correlation (Fig. 3.17a). This implies that the temperature increase effectively promotes egg production levels of anchovy adults. On the other hand, addition of total mixing effects to temperature forcing in simulation C, decreases the resultant correlation to 94 % (Fig. 3.18a). Thus, the total mixing forcing weakened slightly the fish production response with respect to simulation A by 5 %, that could be a result of the grazing effect imposed by the gelatinous predator on the eggs and larvae. Similarly, when the survival possibility of produced eggs is analyzed by regressing egg numbers against recruitment numbers, the egg population gives survival response with a correlation of 86 % under

temperature only forcing (Fig. 3.17b), whereas the chances for survival of larvae increases more when the total mixing effects are added (in simulation C), then the correlation is elevated to 91 % (Fig. 3.18b). Recruitment versus spawner population relationship gives a 82% correlation in simulation A (Fig. 3.17c), further adding mixing forcing in simulation C adds more scatter to the results which gives reduced (76%) correlation (Fig. 3.18c).

Wang et al. (1997) introduced an IBM (Individual-Based Model) to investigate bay anchovy population dynamics in the Chesapeake Bay. The aim was to resolve the operating density-dependent processes on spawner - recruitment populations and recruitment length variability via implicit suppressors for multi life-history species (Rothschild, 1986). They found that there is a linear relationship between egg production and spawner population, and between the recruitment-spawner population numbers, which agree with our findings (Fig. 3.18). In the study of Chesapeake Bay anchovy simulated mean size of recruitment versus recruitment population simulations revealed an inverse relationship due to density dependent growth (Wang et al., 1997; Rose et al., 1999). However, in this study such a relationship gives no correlation (Fig. 3.20b).

4.2.3 Fish Production and Climate Indices

Regime shifts happen in marine ecosystems when a nonlinear system loses its internal buffering capacity (Scheffer et al., 2001; Mayer and Rietkerk, 2004). It happens when a strong disturbance is imposed onto the system, which can be in the form of anthropogenic input, fishing pressure, introduction of non-native species and decadal scale climate variations, in the Black Sea and in other parts in the world oceans as well.

4.2.3.1 Black Sea

The Black Sea was pre-conditioned by strong top-down and bottom-up type of trophic control became increasingly vulnerable to interannual-to-decadal scale perturbations. As a result, it responded to the external forcing at all ecosystem levels. Therefore, the

regime shifts between 1960s' pre-eutrophication state and 1990s' post-eutrophication state led to reorganization of the Black Sea ecosystem and has many implications for understanding the likely responses of top-down, bottom-up or wasp-waist type controlled non-linear marine ecosystems (Oğuz and Gilbert, 2007).

When evaluating these Black Sea regime transitions, the role of climate-induced forcing is undeniable (Bilio and Niermann, 2004; Oğuz et al., 2003, 2006; Oğuz, 2005b).

1960's – 1980's

During the second half of the last century, Black Sea was influenced by the North Atlantic Oscillation (NAO) (Oğuz, 2005b). During the time from 1960 to 1980, negative NAO index was active which causes mild winters and warmer sea surface temperature (SST) readings for the Black Sea region (Oğuz, 2005b). At the same time, the Black Sea ecosystem was in the pre-eutrophication state in early 1960s and it was regulated by top-down type of control mechanism (Oğuz et al. 2008a). Hence, low stocks (~300 ktons) of *Engraulis encrasicolus ponticus* existed due to high predation pressure exerted by large piscivores (Oğuz and Gilbert, 2007). The depletion of large pelagics and demersals during 1960s led to tremendous stock increase in anchovy to ~700 ktons at the beginning of 1970s (Oğuz and Gilbert, 2007). After 1973, the standing stock of small pelagic fish kept increasing. Moreover, as a consequence of built-up enrichment in the water column, estimated anchovy stock was able to double to ~1500 ktons by the end of 1970s (Oğuz et al., 2008a).

1980's -1990's:

By the beginning of 1980s, NAO index changed into the positive mode (Oğuz, 2005b) leading to more severe winter conditions with a 1.5 – 2.0 ° C decrease for observed winter mean monthly SST until 1993 (Oğuz and Gilbert, 2007). Moreover, the period from 1985 to 1993 is among the coldest winters of the last century in Black Sea basin (Oğuz, 2005b). Despite of the fact that small pelagics were heavily exploitated at the time, the coinciding positive NAO index caused for an enhanced fish production through introducing strong bottom-up nutrient supply and that prevented a fisheries collapse over

a decade (Oğuz, 2005a,b). Actually, the period between 1980 and 1988 was defined by an annual landing of ~700 ktons of small planktivorous fish which corresponds to more than 70 % of total standing stock and also corresponds to ~100 % in 1982 to 1984 (Oğuz and Gilbert, 2007). It was evident that, the fish stock was almost about to collapse during 1982-1984, but this event did not happen until 1988, due to continuous bottom-up resource supply through the lowest trophic level (Oğuz, 2005a,b). Between years 1988 to 1990 then the abrupt stock decline (of more than 5-fold) in anchovy fisheries took place in the Black Sea, such that estimated standing stock was ~300 ktons at the time of collapse (Oğuz et al., 2008a).

1990's – 2000:

The anchovy stocks which were estimated as ~600 ktons in 1992, started to rise again as the sign of NAO index turned to negative after 1993 and returned to warm SST (Oğuz, 2005b). Consequently, in the period between 1993 and 2000, basin averaged winter mean SST rose from 7.2 ºC to 9.0 ºC (Oğuz, 2005b).

Therefore, observation data suggest that the Black Sea anchovy stocks are controlled by large-scale climate phenomena through promoted bottom-up supply and through influencing their survival via contributing to overall growth and gonadal development. And this explains why eggs and recruits of the anchovy population in the model are the two most vulnerable compartments to direct/indirect effects of the externally introduced stochastic temperature forcing in this model. Moreover, according to the model results, the effects of bottom-up control is shown to be diminishing at the mesozooplankton level and a pronounced response to temperature driven bottom-up forcing is given at the phytoplankton and microzooplankton levels. These findings are also comparable with the observations during the climate-driven Black Sea regime transitions, that the effect of bottom-up control is restricted to the lowest trophic level (Oğuz and Gilbert, 2007).

4.2.3.2. Global Scale

One of the commonly accepted theories on recruitment relates the recruitment variability to the available spawner stock (Cushing, 1996). In order to understand whether the spawner abundance plays a significant role on the egg production variability, the 50-year long model output of total annual spawner numbers are correlated with total number of egg produced over a certain time each year (Fig. 4.1). In each analysis, the numbers of females are summed up over different periods to better resolve the possible combinations, such as at the beginning of spawning season (June 1st) (Fig. 4.1a), during the spawning season (June to September) (Fig. 4.1b) and winter period (December to March) (Fig. 4.1c) are correlated with egg production. However, the analysis provided no correlation between number of spawners in these time frames and total egg production. This indicates the existence of more dominant factors to determine egg production variations, such as temperature effects. When the 50-year mean summer (Fig. 4.2a) and mean winter temperatures (Fig. 4.2b) are regressed against the total number of eggs produced, a very high correlation (98%) is provided for the summer temperatures, which are incidentally the temperatures anchovy encounter during spawning season. The analysis indicates a strong linkage between spawning season temperature conditions and egg production. The analysis further suggests that the spawner availability is a secondary contributor to egg production which is in agreement with MacKenzie and Köster (2004).

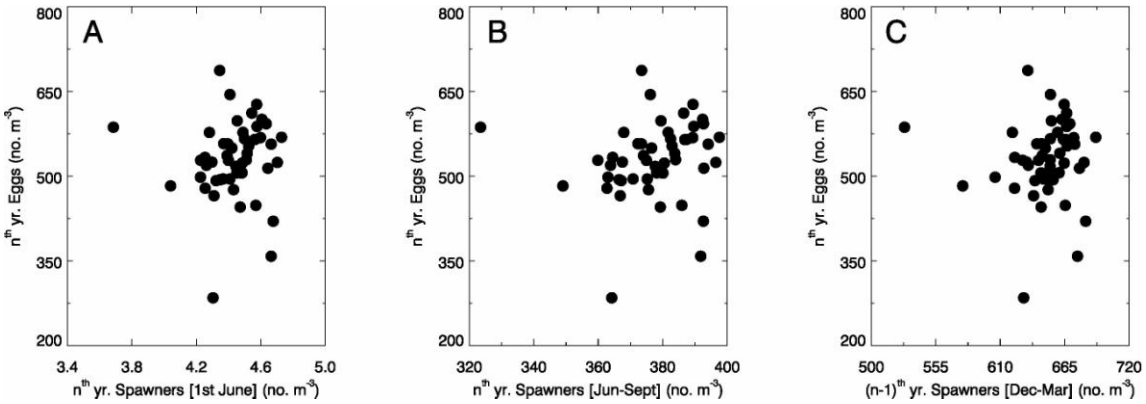

Fig. 4.1: Simulation C: Number of total (age 0+, 1+, 2+ and age 3+) (no. m^{-3}) a) spawners (n^{th} year) at the beginning of the spawning season (June 1^{st}), b) spawners (n^{th} year) during the spawning season (June to September) and c) spawners ($n+1^{th}$ year) during winter time (December to March) versus total egg production (n^{th} year) (no. m^{-3}) in the spawning season. Spawner numbers represent female adults that constitute 50 % of total population.

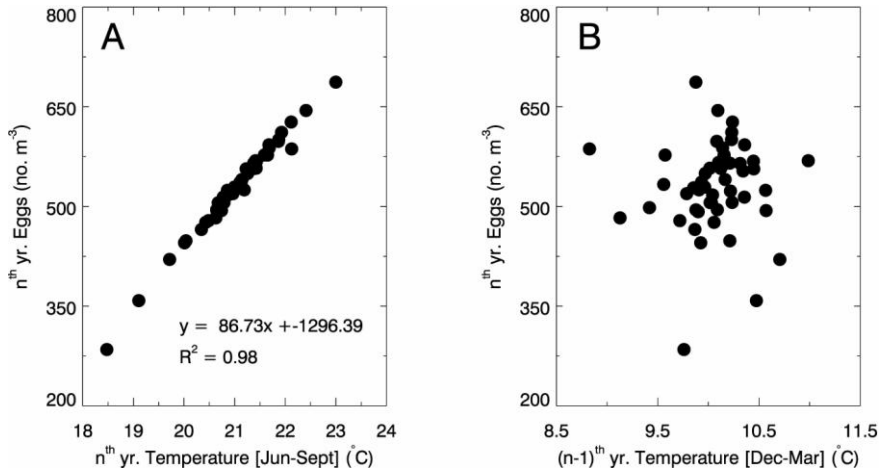

Fig. 4.2: Simulation C: Mean temperatures (ºC) a) from June to September and b) from December to March in relation to egg production potentials (no. m^{-3}) in the spawning season.

However, the model results also show the critical importance of temperature in deciding long-term recruitment variability. The results of this study indicate that cooler years (with cold winters and cool spawning seasons) result in lower anchovy recruitment. On the contrary, in warmer years (with mild winters and warm spawning seasons) the recruitment success is higher. This is in agreement with a study on Baltic Sea sprat by MacKenzie and Köster (2004) who found a similar relationship. Furthermore, analysis of the 45 years long data from the Baltic Sea implies a high consistency between sprat recruitment and large scale climatic variations (i.e., NAO) that even makes estimation of the potential recruitment and landing abundance possible for the following years (MacKenzie and Köster, 2004). Meanwhile, the impact of environmental variability in the form of long-term climate-induced changes would have serious implications in terms of prey-predator relationships. In the Baltic Sea example, sprat are the major predators of cod ichthyoplankton and therefore warm atmospheric indices can cause a regime transition towards high sprat abundance while leading to a decreased population growth of cod (Köster et al., 2001; MacKenzie and Köster, 2004).

As the structure and functionality of ecosystems deviate during regime shifts (Beamish et al., 2000), it is important to determine the extent of the variability of fish populations in terms of fishery regulations (MacKenzie and Köster, 2004). In the North Pacific Ocean, switchbacks in the polarity of climatic indices that occured in 1925, 1947 and 1977 are found to be closely related with the shifts in Alaskan salmon production (Mantua et al., 1997). Among the climate systems, the lower frequency Pacific Decadal Oscillation provides the best fit to the slowly varying salmon catch timeseries compared to the tropical El Niño/La Niña-Southern Oscillation (ENSO) systems (Mantua et al., 1997).

Recent studies turned their attention to the compelling evidence that links climate impacts with the development of fish, recruitment and also population dynamics and therefore point to the need for models as a useful tool to assess climate-induced effects on fish production (Megrey et al., 2007). At this point, bioenergetics modeling is appreciated as a powerful approach for its capability of simulating the fish life history dynamics under environmental variations (Megrey et al., 2007). In the lack of

availability of the coupled fish and plankton models, NEMURO.FISH offers a rarely established higher trophic level (HTL) and lower trophic level (LTL) model to simulate 30 year realistic variations of age and weight of Pacific herring which constitute a link between predators and plankton levels and therefore contributing to the on-going affords to predict how the large marine ecosystems would react against global warming (Megrey et al., 2007).

Another example of multi-trophic level modeling was developed to analyze the impact of regional environmental variations over plankton level and tuna fish production in the Pacific (Lehodey et al., 2003). The simulations indicate that the production of tropical tuna such as, skipjack (*Katsuwonus pelamis*) and yellowfin (*Thunnus albacares*) and subtropical tuna, albacore (*Thunnus albacares*) are regulated remarkably under control of climate indices such as ENSO and Pacific Decadal Oscillation (Lehodey et al., 2003).

5 CONCLUSIONS

The attempts to understand the role of climate variability on fish growth, production, recruitment success/failure and population dynamics is getting increasingly more attention due to the recognition that climate-induced effects can introduce strong perturbations to highly non-linear marine ecosystems. Modeling offers an innovative approach to explore such questions and resolve the impact of environmental stresses on disturbed marine ecosystems. Keeping in mind that fish stocks have already undergone heavy exploitation in the Black Sea as well as in the world oceans, the external causes for observed trends in fish productivity of the exploited stock need to be explored extensively.

The aim of this study was to investigate whether environmental influences in the form of temperature and nutrient entrainment variability play a role on the trophodynamics of the Black Sea ecosystem and if it does, then to determine the extent of direct or indirect impacts across the trophic levels, especially those which have an affect on anchovy production and recruitment.

In order to achieve this goal, a 1D ecosystem model was used. It is a multi-trophic-level model which successively couples a plankton model with a fish life-cycle (bioenergetics) model (Oğuz et al., 2008a). The model was run with a fifty year long, stochastically generated, daily climate forcing time series of temperature and mixing rates.

The results reveal that, for a given 2°C increase in the summer mean temperature, the start of egg production shifts to 30 days earlier than the baseline year. Similarly, a 2°C drop in the mean summer temperatures result in a 45 day delay in the start of egg production with respect to the baseline year. The temperature variability has a significant regulatory power on the intensity of egg production. Moreover, a 1.3°C increase in temperature increased the total egg production in the spawning season by 100%, total annual recruitment numbers by ~73%, and annual total number of spawners

by 20%. Thus, eggs and larvae were found to be the most sensitive compartments in the higher trophic level to temperature, and adult anchovy were found to be the less sensitive. Adults are shown to be tolerating temperature variations more, owing to the fact that they have higher body volume per unit area which makes their response to temperature changes less vulnerable compared to young anchovy. In addition, dependency of recruitment on temperature is critical, such that, high temperatures promoted recruitment whereas low temperatures caused a decrease in their numbers.

Further results indicated that changes of total mixing effect higher trophics little. However, the total mixing effects counteracted temperature effects to slightly diminish the higher trophic level reaction to temperature. Additionally, in the model, the mixing is only limited to the nutrient supply. Turbulence effect is not incorporated due to complexity, although it has a significant characteristic in determining the anchovy population growth in weight. Anchovy are visual feeders, thus, the turbulence level is either expected to promote or suppress the feeding behavior of anchovy that may also have serious consequences for the resulting prey-predator dynamics (Megrey and Hinckley, 2001).

Ultimately, this study may contribute to the efforts that try to answer climate-related questions about the way that marine ecosystems function. Moreover, the model used in this study is one of the very few that successively links lower trophic level to anchovy bioenergetics. The bioenergetics modeling is a promising tool that enables projections of fish growth under changing environmental conditions (Megrey et al., 2007). Thus, with slight modification to the model, such as to allow additional inputs in form of fishing and predation mortality, gelatinous transport from the shelf and sub-surface nitrate concentration, model results may be usable for effective fisheries assessment and management. The connections between anchovy population (esp. recruitment) and climate variability provided here may allow for short-term anchovy yield estimations in the future. This kind of modeling approach that enables feedbacks between higher and lower trophic levels has a high prediction potential. And it can be used in determining timing and direction of ecosystem shifts that are likely to occur in enclosed basins under strong climatic perturbations.

REFERENCES

Adrianov, D.P., Lisovenko, L.A., Bulgakova, Yu.V. and Oven, L.S., 1996. Reproductive ecology of the Black Sea anchovy (*Engraulis encrasicholus ponticus*): 1. Circadian rhythms of oogenesis and spawning. J. Ichthyology, 36(7), 515–526.

Anonymns, 2004. (DİE) Devlet İstatistik Enstitüsü, Su ürünleri 2003 verileri, Ankara.

Bat, L., Şahin, F., Satılmış, H.H., Üstün, F., Özdemir, Z.B., Kıdeyş, A.E., Shulman, G. E., 2007. The changed ecosystem of the Black Sea and its impact on the anchovy fisheries. J. Fish. Sci. 1(4), 191-227.

Beamish, R.J., Noakes, D.J., McFarlane, Pinnix, W., Sweeting, R., and King, J., 2000. Trends in cohort marine survival in relation to regime concept. Fisheries Oceanography, 9, 14-19.

Beddington, J.R., 1984. The response of multispecies systems to perturbations. In: Exploitation of marine communities (May, R.M., ed.), Dah. Konf. Life Sci. Res. Rep., Springer, 32, 209–226.

Belokopytov, B., 1998. Long-term variability of Cold Intermediate Layer renewal conditions in the Black Sea. In: Ecosystem Modeling as a Management Tool for the Black Sea (Ivanov, L.I., Oguz, T., eds.), NATO ASI Series 2: Environment-Vol. 47. Kluwer Academic Publishers. Dordrecht, The Netherlands, 47-52.

Berdnikov, S.V., Selyutin, V.V., Vasilchenko, V.V., Caddy, J.F., 1999. Trophodynamic model of the Black and Azov Sea pelagic ecosystem: consequences of the comb jelly, *Mnemiopsis leidyi*, invasion. Fish. Res., 42, 261-289.

Bilio, M., Niermann, U., 2004. Is the comb jelly really to blame for it all? *Mnemiopsis leidyi* and the ecological concerns about the Caspian Sea. Mar. Ecol. Prog. Ser., 269, 173-183.

Bodeanu, N., 1989. Algal blooms and development of the main planktonic species at the Romanian Black Sea littoral under eutrophication conditions. Cercet. Mar. I. R. C. M., 22, 107-125.

Bologa, A.S., 1986. Planktonic primary productivity of the Black Sea: review. J. Thallassia Jugoslavica, 21-22 (1-2), 1-22.

Caddy, J., Griffiths, R., 1999. A perspective on recent fishery related events in the Black Sea, studies and review. General Fisheries Council for the Mediterranean, 63, 43-71.

Carpenter, S.R., Kitchell, J.F., Hodgson, J.R., 1985. Cascading trophic interactions and lake productivity. BioScience, 35, 634-639.

Codispoti, L.A., Friederich, G.E., Murray, J.W., Sakamoto, C.M., 1991. Chemical variability in the Black Sea: implications of continuous vertical profiles that penetrated the oxic/anoxic interface. Deep-Sea Res. I, 38(Suppl. 2), 691-710.

Cowan, V.G., Houde, E.D., 1993. Relative predation potentials of scyphomedusae, ctenophores and planktivorous fish on ichthyoplankton in Chesapeake Bay. Mar. Ecol. Prog. Ser., 95, 55-65.

Cury, P., Bakun, A., Crawford, R.J.M., Jarre, A., Quinones, R.A., Shannon, L.J., Verheye, H.M., 2000. Small pelagics in upwelling systems: patterns of interaction and structural changes in "wasp-waist" ecosystems. ICES J. Mar. Sci., 57, 603- 618.

Cushing, D.H., 1996. Towards a science of recruitment in fish populations. Ecology Institute, D-21385, Oldendorf /Luhe, Germany.

Daskalov, G.M., 2002. Overfishing drives a trophic cascade in the Black Sea. Mar. Ecol. Prog. Ser., 225, 53-63.

Daskalov, G.M., 2003. Long-term changes in fish abundance and environmental indices in the Black Sea. Mar. Ecol. Prog. Ser., 255, 259–270.

Daskalov, G.M., Grishin, A.N., Rodionov, S., Mihneva, V., 2007. Trophic cascades triggered by overfishing reveal possible mechanisms of ecosystem regime shifts. Proc. Natl. Acad. Sci. USA, 104, 10 518-10 523.

Demir, N., 1959. N. Notes on variations of the eggs of anchovy *Engraulis encrasicolus* Cuv. from the Black, Marmara, Aegean and Mediterranean Seas. *Hidrobiol. Istanbul* B4, pp. 180–187.

Fulton, E.A., Smith, A.D,M., Johnson, C.R., 2003. Mortality and predation in ecosystem models: Is it important how these are expressed? Ecol Model, 169, 157–178.

Grauman, G.B. and Yula, E., 1989. The importance of abiotic and biotic factors in the early ontogenesis of cod and sprat. Rapports et Process-verbaux des Réunions Conseil international pour l'Exploration de la Mer, 190, 207-210.

Gücü, A.C., 1997. Role of fishing in the Black Sea ecosystem. In: Sensitivity to Change: Black Sea, Baltic Sea and North Sea (Ozsoy, E., Mikaelyan, A., eds.), Kluwer Academic Publishers, The Netherlands, 149-162.

Gücü, A.C., 2002. Can overfishing be responsible for the successful establisment of

Mneiopsis leidyi in the Black Sea? Estuarine, Coastal and Shelf Science, 54, 439-451.

Houde, E.D., 1987. Fish early life history dynamics and recruitment variability. Am. Fish. Soc. Symp.2,17-29.

Humborg, C., Ittekkot, V., Cociasu, A., Bodungen, B., 1997. Effect of Danube River dam on Black Sea biogeochemistry and ecosystem structure. Nature, 386, 385-388.

Hunter, H.D., Price, P.W., 1992. Playing chutes and ladders: Heterogeneity and the relative roles of bottom-up and top-down forces in natural communities. Ecology, 73(3), 724-732.

Ivanov, L., Panayotova, M., 2001. Determination of the Black Sea anchovy stocks during the period 1968-1993 by Ivanov's combined method. Proc. Inst. Oceanol., Bulg. Acad. Sci., 3, 128-154.

Kıdeyş, A.E., 1994. Recent dramatic changes in the Black Sea ecosystem: The reason for the sharp decrease in Turkish anchovy fisheries. J. Mar. Sys., 5, 171-181.

Kıdeyş, A.E., 2002. Fall and rise of the Black Sea ecosystem. Science, 297, 1482-1483.

Kıdeyş, A.E., Gordina, A.D., Bingel, F., Niermann, U., 1999. The effect of environmental conditions on the distribution of eggs and larvae of anchovy (*Engraulis encrasicolus* L.) in the Black Sea. ICES J. Mar. Sci., 56(Suppl.), 58-64.

Kıdeyş, A.E., Kovalev, A.V., Shulman, G., Gordina, A., Bingel, F., 2000. A review of zooplankton investigations of the Black Sea over the last decade. J. Mar. Sys.,

24, 355-371.

Kovalev, A. V., Neirman, U., Melnikov, V. V., Belokopytov, V., Uysal, Z., Kideys, A. E., Unsal, M., Altukov, D., 1998. Long-term changes in the Black Sea zooplankton: the role of natural and anthropogenic factors. In: Ecosystem Modeling as a Management Tool for the Black Sea (Ivanov, L.I., Oguz, T., eds.), NATO ASI Series 2: Environment-Vol. 47. Kluwer Academic Publishers. Dordrecht, The Netherlands, 221-234.

Köster, F.W., Hinrichsen, H.H., St.John, M.A., Schnack, D., MacKenzie, B.R., Tomkiewicz, J., and Plikshs, M., 2001. Developing Baltic cod recruitment models. II. Incorporation of environmental variability and species interaction. Canadian Journal of Fisheries and Aquatic Sciences, 58:1534-1556.

Lehodey, P., Chai, F. and Hampton, J., 2003. Modelling climate-related variability of tuna populations from a coupled ocean-biogeochemical-populations dynamics model. Fish. Oceanogr., 12, 483-494.

Lisovenko, L.A., Andrianov, D.P., 1996. Reproductive biology of anchovy (*Engraulis encrasicolus ponticus* Alexandrov 1927) in the Black Sea. Sci Mar, 60(Suppl), 209–218.

Luo, J., Brandt, S.B., 1993. Bay anchovy *Anchoa mitchilli* production and consumption in mid-Chesapeake Bay based on a bioenergetic model and acoustic measures of fish abundance. Mar. Ecol. Prog. Ser., 98, 223-236.

MacKenzie, B.W. and Köster, F.W., 2004. Fish production and climate: Sprat in the Baltic Sea. Ecology, 85(3), 784-794.

Mantua, N.J., Hare, S.R., Zhang, J., Wallace, J.M., Francis, R.J., 1997. A Pacific

interdecadal climate oscillation with impacts on salmon production. Bulletin of American Meteorological Society, 78(6), 1997.

Marshall, J., Kushnir, Y., Battisti, D., Chang, P., Czaja, A., Dickinson, R., Hurrell, J.W., McCartney, M., Saravanan, R., Visbeck, M., 2001. North Atlantic climate variability: phenomena, impacts and mechanisms. Intern. J. Clim., 21, 1863-1898.

Mayer, A.L., Rietkerk, M., 2004. The dynamic regime concept for ecosystem management and restoration. Bioscience, 54(11), 1013-1020.

Megrey, B.A., Hinckley, S., 2001. Effect of turbulence on feeding of larval fishes: a sensitivity analysis using an individual-based model. ICES J. of Mar. Sci. 58, 1015–1029.

Megrey, B.A., Rose, K.A., Klumb, R.A., Hay, D.E., Werner, F.E., Eslinger, D.L., Smith, S.L., 2007. A bioenergetic-based population dynamics model of pacific herring *(Clupea harengus pallasi)* coupled to a lower trophic lever nutrient-plankton-zooplankton model: Description, calibration, and sensitivity analysis. Ecol. Modell., 202, 144-164.

Mihnea, P.E., 1985. Effect of pollution on phytoplankton species. Rapp. Comm. Int. Mer. Medit., 29(9), 85-88.

Mikaelyan, A.S., 1997. Long-term variability of phytoplankton communities in open Black Sea in relation to environmental changes. In: Sensitivity to change: Black Sea, Baltic Sea and North Sea (Ozsoy, E., Mikaelyan, A. S., eds.), NATO ASI Series 2: Environment-Vol. 27. Kluwer Academic Publishers, Dordrecht, The Netherlands, 105-116.

Moncheva, S., Krastev, A., 1997. Some aspects of phytoplankton long-term alterations off Bulgarian Black Sea Shelf. In: Sensitivity to change: Black Sea, Baltic Sea and North Sea (Ozsoy, E., Mikaelyan, A. S., eds.), NATO ASI Series 2: Environment-Vol. 27. Kluwer Academic Publishers, Dordrecht, The Netherlands, 79-94.

Niermann, U., Kıdeyş, A.E., Kovalev, A.V., Melnikov, V., and Belokopytov, V., 1999. Fluctiations of pelagic species of the open Black Sea during 1980-1995 and possible teleconnections. In: Environmental Degredation of the Black Sea: Challenges and Remedies (Besiktepe, S., Unluata, U., Bologa, A., eds.), NATO ASI Series-B: Environmental Security 56, Kluwer Academic Publishers, Dordrecht, The Netherlands, 147-174.

Niermann, U., Bingel, F., Gorban, A., Gordina, A.D. and others, 1994. Distribution of anchovy eggs and larvae (*Engraulis encrasicolus* Cuv.) in the Black Sea in 1991-1992. ICES J. Mar. Sci., 51, 395-406.

Nissling, A., 2004. Effects of temperature on egg and larval survival of cod (*Gadus morhua*) and sprat (*Sprattus sprattus*) in the Baltic Sea - implications for stock development. Hydrobiologia, 514, 515-123.

Oğuz, T., 2005a. Longterm impacts of anthropogenic and human forcing on the reorganisation of the Black Sea ecosystem. J. Oceanogr., 18 (2), 112-121.

Oğuz, T., 2005b. Black Sea ecosystem response to climatic variations. J. Oceanogr., 18(2), 122-133.

Oğuz, T., 2007. Nonlinear response of Black Sea pelagic fish stocks to over-exploitation. Mar. Ecol. Prog. Ser., 345, 211-228.

Oğuz, T., Beşiktepe, S., 1999. Observations on the Rim Current structure, CIW formation and transport in the western Black Sea. Deep Sea Res.I, 46, 1733-1753.

Oğuz, T., Gilbert, D., 2007. Abrupt transitions of the top-down controlled Black Sea pelagic ecosystem during 1960-2000: Evidence for regime-shifts under strong fishery exploitation and nutrient enrichment modulated by climate-induced variations. Deep-Sea Res. I, 54, 220-242.

Oğuz, T., Ivanov, L. I., Beşiktepe, S., 1998. Circulation and hydrographic characteristics of the Black Sea during July 1992. In: Ecosystem Modeling as a Management Tool for the Black Sea (Ivanov, L.I., Oguz, T., eds.), NATO ASI Series 2: Environment-Vol. 47. Kluwer Academic Publishers. Dordrecht, The Netherlands, 69-92.

Oğuz, T., Malanotte-Rizzoli, P., Ducklow, H.W., 2001a. Simulations of phytoplankton seasonal cycle with multi-level and multi-layer physical ecosystem models: The Black Sea example. Ecol. Modell., 144, 295-314.

Oğuz, T., Dippner, J.W., Kaymaz, Z., 2006. Climatic regulation of the Black Sea hydro-meteorological and ecological properties at interannual-to-decadal time scales. J. Marine Systems, 60, 235-254.

Oğuz, T., Salihoğlu, B., Fach, B., 2008a. A coupled plankton-anchovy population dynamics model assessing nonlinear controls of anchovy and gelatinous biomass in the Black Sea. Mar. Ecol. Prog. Ser., 369, 229-256.

Oğuz, T., Salihoğlu, B., Fach, B., 2008b. Invasion dynamics of the alien ctenophore Mnemiopsis leidyi and its impact on anchovy collapse in the Black Sea. J.

Plankton Res., 30(12), 1385-1397.

Oğuz, T., Ducklow, H. W., Purcell J. E., Malanotte-Rizzoli, P., 2001b. Modeling the response of top-down control exerted by gelatinous carnivores on the Black Sea pelagic food web. J. Geophys. Res., 106, 4543-4564.

Oğuz, T., Cokacar, T., Malanotte-Rizzoli, P., Ducklow, H.W., 2003. Climatic warming and accompanying changes in the ecological regime of the Black Sea during 1990s. Global Biogeochem. Cycles, 17(3), 1088, doi:10.1029/2003.

Oğuz, T., Tuğrul, S., Kıdeyş, A. E., Ediger, V., Kubilay, N., 2005c. Physical and biogeochemical characteristics of the Black Sea. In: The Global Coastal Ocean-Interdisciplinary Regional Studies and Synthesis (Robinson, A.R., Brink, K.H., eds.), THE SEA Series, 14(33), Harvard University Press, Cambridge, MA, 1331-1369.

Ojaveer, E., 1998. Influence of long-term climate fluctuations on marine organisms: preliminary results. In: Climate change studies in Estonia (Kallaste, T. and Kuldna, P., eds.), Stockholm Environment Institute-Tallinn. International Institute for Environmental Technology and Management, Ministry of the Environment, Tallinn, Republic of Estonia.

Özsoy, E., Ünlüata, U., 1997. Oceanography of the Black Sea: a review of some recent results. Earth Sci. Rev., 42, 231-272.

Pavlovskaya, P.N., 1955. Survival of the Black Sea anchovy at the early stages of development. In: Proc. Azov-Black Sea Mar. Sci. Res. Inst. Fish. Oceanogr. 16, pp. 99–120.

Porumb, F., 1989. The influence of eutrophication on zooplankton communities in the

Black Sea waters. Certerari Marine, 22, 233-246.

Prodanov, K., Mikhaylov, K., Daskalov, G., Maxim, K. and others, 1997. Environmental management of fish resources in the Black Sea and their rational exploitation. GFCM Study Rev., 68, 1-178.

Rayner, N.A., Parker, D.E., Horton, E.B., Folland, C.K., Alexander, L.V., Rowell, D.P., Kent, E.C., Kaplan, A., 2003. Global analyses of sea surface temperature, sea ice, and night marine air temperature since the late nineteenth century. J. Geophys. Res. 108.4407, doi:10.1029/2002JD002670.

Rose, K. A., Tyler, J. A., SinghDermot, D., Rutherford, A. S., 1996. Multispecies modeling of fish populations. In: Computers in Fisheries Research (Megrey, B., Moksness, E., eds.), Chapman and Hall, London, 195-221.

Rose, K.A., Cowan, J.H., Clark, M.E., Houde, E.D., Wang, S.B., 1999. An individual-based model of bay anchovy population dynamics in the mesohaline region of Chesapeake Bay. Mar. Ecol. Prog. Ser., 185, 113-132.

Rothschild, B.J., 1986. Dynamics of Marine Fish Populations. Cambridge, Mass: Harvard University Press.

Samsun, O., Samsun, N., Kalayci, F., Bilgin, S., 2006. A study on recent variations in the population structure of European anchovy (*Engraulis encrasicolus* L., 1975) in the southern Black Sea. Ege Univ J Fish Aquat Sci, 23, 301–306.

Satılmış, H.H., Gordina, A.D., Bat, L., Bircan, R., Culha, M., Akbulut, M., Kideys, A.E., 2003. Seasonal distribution of fish eggs and larvae off Sinop (the southern Black Sea) in 1999-2000. Acta. Oecol., 24, S275-280.

Scheffer, M., Carpenter, S., Folley, J.A., Folke, C., Walker, B., 2001. Catastrophic shifts

in ecosystems. Nature, 413, 591-596.

Shiganova, T. A., 1998. Invasion of the Black Sea by the ctenophore *Mnemiopsis leidyi* and recent changes in pelagic community structure. Fish. Oceanogr., 7, 305-310.

Shiganova, T.A., Bulgakova, Y.V., 2000. Effects of gelatinous plankton on Black Sea and Sea of Azov fish and their food resources. ICES J. Mar. Sci., 57, 641-648.

Shiganova, T. A., Mirzoyan, Z. A., Studenikina, E. A., Volovik, S. P. and others, 2001. Population development of the invader ctenophore *Mnemiopsis leidyi* in the Black Sea and other seas of the Mediterranean basin. J. Mar. Biol., 139, 431-445.

Shiganova, T. A., Dumond, H., Bulgakova, Y. V., Mikaelyan, A., Glazov, D. M., Bulgakova, Y. V., Musayeva, E. I., Sorokin, P. Y., Pautova, L. A., Mirzoyan, Z. A., Studenikina, E. I., 2004. Interactions between the invading ctenophores *Mnemiopsis leidyi* (A. Agassiz) and *Beroe ovata Mayer* 1912, and their influence on pelagic ecosystem of the Northeastern Black Sea. In: Aquatic Invasions in the Black, Caspian, and Mediterranean Seas (Dumont, H., Shiganova, T. A. and Niermann, U., eds.), NATO Science Series: 4, Earth and Environmental Sciences, Springer. Netherlands, 35, 33-70.

Shushkina, E.A., Musayeva, E.I., 1983. The role of jellyfish in the energy system of Black Sea lankton communities. Oceanology (Mosc), 23, 92-96.

Shushkina, E. A., Vinogradov, M. E., Lebedeva, L. P., Oguz, T., Nezlin, N. P., Dyakonov, V. Yu., Anokhina, L. L., 1998. Studies of structural parameters of planktonic communities of the open part of the Black Sea relevant to ecosystem modeling. In: Ecosystem Modeling as a Management Tool for the Black Sea vol.1 (Ivanov, L. I., Oguz, T., eds.), NATO Sci. Partnership Sub-ser., 2, Kluwer Academic Publishers, Massachusettes, 47, 311-326.

Slastenenko, E., 1956. Karadeniz Havzası Balıkları. Et ve Balık Kurumu Umum Müdürlüğü Yayınlarından, İstanbul, 711s.

Sorokin, Y.I., 2002. The Black Sea-Ecology and Oceanography. Backhuys Publishers, UNESCO Venice Office, Leiden, 875pp.

Tian Y, Akamine T, Suda M (2004) Modeling the influence of oceanic-climatic changes on the modelling of the dynamics of Pacific saury in the northwesterrn Pacific using a life cycle model. Fish Oceanogr ,13(Suppl 1), 125–137.

Tsiklon-Lukanina, E.A., Reznichenko, O.G., Lukasheva, T.A., 1991. Quantitative patterns of feeding of the Black Sea ctenophore *Mnemiopsis leidyi*. Oceanol., 31, 196-199.

Tsikhon-Lukanina, E.A., Reznichenko, O.G., Lukasheva, T.A., 1993. Level of fish fry consumption by *Mnemiopsis* in the Black Sea shelf. Okeanologiya, 33, 895-899.

Uçkun, D., Akalın, S., Togulga, M., 2005. Investigations of the age and growth of anchovy (*Engraulis encrasicolus* L., 1958) in Izmir Bay. Ege Univ J Fish Aquat Sci 22:281–285

Uysal, Z., Kıdeyş, A.E., Senichkina, L., Georgieva, L., Altukhov, D., Kuzmenko, L., Manjos, L., Eker, E., 1998. Phytoplankton patches formed along the southern Black Sea coast in spring and summer 1996. In: Ecosystem Modeling as a Management Tool for the Black Sea (Ivanov, L.I., Oğuz, T., eds.), NATO ASI Series 2: Environment-Vol. 47. Kluwer Academic Publishers. Dordrecht, The Netherlands, 151-162.

Ünlüata, U., Oğuz, T., Latif, M. A., Özsoy, E., 1989. On the physical oceanography of the Turkish Straits. In: The Physical Oceanography of Sea Straits (Pratt, L.J.,

eds.), NATO ASI Series, Kluwer Academics, Dordrecht, 25–60.

Wang, S.B., Cowan Jr., J.H., Rose, G.A. and Houde, E.D., 1997. Individual-based modeling of recruitment variability and biomass production of bay anchovy in mid-Chesapeake Bay. Journal of Fish Biology, 51 (Suppl. A), 101-120.

Ware, D.M., Thomson, R.E., 2005. Bottom-up ecosystem trophic dynamics determine fish production in the northeast Pacific. Science, 308(5726), 1280-1284.

Zaitsev, Yu.P., Aleksandrov, B.G., 1997. Recent man-made changes in the Black Sea ecosystem. In: Sensivity of North Sea, Baltic Sea and Black Sea to anthropogenic and Climatic Changes, (Özsoy, E., Mikaelyan, A., eds.), Kluwer Acad. Pub., Dordrecht, Netherlands, pp. 25–32.

Zaitsev, Yu. P., Mamaev, V., 1997. Marine biological diversity in the Black Sea: a study of change and decline. GEF Black Sea Environmental Programme, United Nations Publications, Istanbul, pp.208.

APPENDIX

Mathematical equations used in the model

In this section, explicit forms of the equations used in the model are described. The values of the control parameters are introduced in Table 2.1 to calibrate the model to the ecosystem conditions of late 70's. The parameter setting of the anchovy adults provided in Table 2.2, while parameters for the different larval stages are given in Table 2.3.

$$\frac{dP_{i,k}}{dt} = U_{i,k} - G^{Pi}_{Z1,k} - G^{Pi}_{Z2,k} - m_{Pi}P_{i,k} + M^{Pi}_{k} \quad \text{(A1a)}$$

$$\frac{dZ_{1,k}}{dt} = \varepsilon_{Z1}\left[\sum_{i=1}^{3} G^{Pi}_{Z1,k} + G^{Z2}_{Z1,k}\right] - G^{Z1}_{Z3,k} - \underline{\tilde{C}^{Z1}_{A,k}} - m_{Z1}Z_{1,k} + M^{Z1}_{k} \quad \text{(A1b)}$$

$$\frac{dZ_{2,k}}{dt} = \varepsilon_{Z2}\sum_{i=1}^{3} G^{Pi}_{Z2,k} - G^{Z2}_{Z1,k} - G^{Z2}_{Z3,k} - \underline{\tilde{C}^{Z2}_{A,k}} - m_{Z2}Z_{2,k} + M^{Z2}_{k} \quad \text{(A1c)}$$

$$\frac{dZ_{3,k}}{dt} = \varepsilon_{Z3}\left[\underline{\underline{\tilde{G}^{A}_{Z3,k=1}}} + \sum_{i=1}^{2} G^{Zi}_{Z3,k}\right] - m_{Z3}Z_{3,k} + \kappa_{Z3}(Z^{S}_{3,k} - Z_{3,k}) + M^{Z3}_{k} \quad \text{(A1d)}$$

$$Det\_flux = (1-\varepsilon_{Z1})\left[G^{Z2}_{Z1,k} + \sum_{i=1}^{3} G^{Pi}_{Z1,k}\right] + (1-\varepsilon_{Z2})\sum_{i=1}^{3} G^{Pi}_{Z2,k} \quad \text{(A1e)}$$

$$+ (1-\varepsilon_{Z3})\left[\underline{\underline{\tilde{G}^{A}_{Z3,k=1}}} + \sum_{i=1}^{2} G^{Zi}_{Z3,k}\right] + (1-\varepsilon_{A})\underline{\left(\tilde{C}^{Z1}_{A,k} + \tilde{C}^{Z1}_{A,k}\right)}$$

$$\frac{dN_{k}}{dt} = -\sum_{i=1}^{3} U_{i,k} + \alpha\{Det\_flux\} + \sum_{i=1}^{3} m_{Pi}P_{i,k} + M^{N}_{k} \quad \text{(A1f)}$$

Eq. A1a-f are applied to both two layers of the model; surface mixed layer (k=1) and sub-thermocline (k=2). Correspondingly, P_i denotes phytoplankton taxa while i representing diatoms (i=1), dinoflagellates (i=2) and small phytoplankton (i=3). Z_i represents size-structured zooplankton groups of microzooplankton and mesozooplankton for i=1,2, respectively. N is used to represent the nitrate concentration. The operator dt/d is for taking the time derivate of P and Z. *Det_flux* represents the

detritus flux, it calculates the unassimilated part of food consumed by the zooplankton groups and all anchovy age groups. All state variables are tracked in mmol N/m^{-3}.

In Eq. A1a, phytoplankton biomass density is represented by the flux between growth function (U_i), grazing pressure exerted by microzooplankton and mesozooplankton (G_{Zj}^{Pi}), mortality rate (m_{Pi}) and vertical exchange between the upper and lower layer (M^{Pi}). The growth term is limited by temperature limitation function. In Eqs. A1b-c, the biomass density of microzooplankton and mesozooplankton varies due to phytoplankton ingestion, grazing pressure exerted by gelatinous carnivores (G_{Z3}^{Zi}), consumption by all cohorts of age-0 class and adult anchovy age class populations ($\tilde{C}_A^{Zi}$), mortality rate (m_{Zi}) and diffusive exchanges between the model layers (M^{Zi}). Moreover, microzooplankton is in mesozooplankton food diet and grazed by mesozooplankton (G_{Z1}^{Z2}).

Biomass of gelatinous species changes temporally (Eq. A1d) via their predation on anchovy eggs and larvae ($\tilde{G}_{Z3}^{A}$), microzooplankton and mesozooplankton (G_{Z3}^{Zi}), basal mortality rate and vertical migratory exchanges between the model layers (M^{Z3}). The source term, $Z_{3,k}^{S}$, is used to parameterize young gelatinous species transport from the shelf by the circulation provided that the temperature exceeds 15 °C and κ_{Z3} denotes the lateral transport rate.

The parameter ε_{Zi} in Eq. (A1b-d) is used to denote the fraction of the digested and assimilated food ingested by zooplankton groups after the losses due to excretion and respiration are eliminated.

N_c in the mixed layer and sub-thermocline layers changes over time (Eq. A1f), due to uptake by phytoplankton, recycling of the unassimilated food and of dead planktonic material, diffusive fluxed within the model layers and from the subsurface source layer (M_k^N). According to Eq. A1f, nitrate recycles partially within the euphotic layer and the rest of it sinks down to deep layers. The remineralization process is modeled implicitly, by prescribing the subsurface nitrate concentration (N_c) externally

as the control (forcing) variable in order to allow for increased amounts of nutrient feedback to the euphotic layer during eutrophication periods. Subsurface nitrate concentration (N_c) is supplied via diffusive and entrainment fluxes, and drives the nutrient cycling and primary production in the model.

The underlined terms in Eq. A1b-d, represent the anchovy and gelatinous carnivore feeding on microzooplankton and mesozooplankton and portion of recycled unassimilated zooplankton food, to establish the dynamic coupling between the lower trophic level and higher trophic level.

Mathematical formulation of anchovy population growth model

$$X_e = \left[\sum_{i=1}^{3} S \times E_g \times (0.5 X_i \times W_i) \times f_e(T_1)/w_{egg}\right] + X_{oe} \qquad \text{(A2)}$$

Eq. A2 calculates the total number of produced healthy eggs in the mixed layer by adult anchovy during the spawning season (June to August). Here, X_e denotes population density and W_i denotes weight of an individual adult anchovy in age classes, i=1,2,3.

Furthermore, $f_e(T_1)$ represents the limitation of temperature on egg production. And also, X_{oe} denotes the independent daily egg production constant (0.5 eggs m^{-2}) that is designed to introduce a cohort unless the temperature exceeds 20°C to start egg production at the beginning of spawning season.

$$\frac{dX_A}{dt} = (m_f + m_n) X_A \qquad \text{(A3a)}$$

Eq. A3a represents the time evolution of anchovy population density (X_A) of a random cohort of age-0 or each adult year classes (in nr. m^{-3}). Thus, m_f and m_n are the respective fishing and natural mortality rates.

$$m_n = m_b + m_l X_A + r_{Z3}^A Z_{3,k=1} \qquad \text{(A3b)}$$

In Eq. 3b, the natural mortality is defined as the sum of linear and quadratic terms (Fulton et al., 2003; Tian et al., 2004). The first one is the basal mortality rate (m_b) and used to represent stable or average environmental conditions and changes with respect to different age classes. It also represents all non-predatory losses. The quadratic density-dependent terms denote predation mortality exerted by (1) piscivores that are not explicit in the model but increase with increasing anchovy numbers and by (2) gelatinous carnivores grazing on eggs and larvae in the mixed layer. Parameter r_{Z3}^{A} expresses the temporal gelatinous carnivore clearance rate (in m^3 mgC^{-1} d^{-1}) and $Z_{3,k=1}$ is the gelatinous biomass density in the mixed layer.

Mathematical formulation of the weight growth model

$$\frac{dW_A}{dt} = (\varepsilon_A C_A - R_A - E_g) \times W_A \qquad \text{(A4)}$$

Eq. A4 represents the weight growth of 0-age anchovy which starts with the beginning of early larval period. The right hand side of the equation describes the difference between the realized consumption rate ($\varepsilon_A C_A$), losses due to total respiration (R_A) and individual spawner's weight loss rate due to reproduction (E_g), in units d^{-1}.

$$C_A^{Z_i} = c_1 \times W_A^{-c_2} \times f(T) \times f(\overline{Z_i}) \qquad \text{(A5a)}$$

In Eq. A5a, $C_A^{Z_i}$ denotes the consumption of herbiviorous and omnivorous zooplankton by an anchovy individual, by using maximum rate of consumption (c_1) (in mgC d^{-1}), anchovy weight, water temperature and microzooplankton and mesozooplankton biomass density where c_2 represents the weight dependence of consumption. Moreover, $f(\overline{Z_i})$ represents the cumulative feeding on zooplankton in the

euphotic layer.

$$\overline{Z_i} = \frac{h_1 Z_{i,k=1} + h_2 Z_{i,k=2}}{h_1 + h_2} \qquad \text{(A5b)}$$

In Eq. A5b, $\overline{Z_i}$ denotes euphotic later mean biomass density of microzooplankton and mesozooplankton, for i=1,2 respectively.

$$f(\overline{Z_i}) = \frac{s_i \overline{Z}_i^2}{K_{ZA}^2 + \sum_{j=1}^{j=2} s_j \overline{Z}_j^2} \qquad \text{(A5c)}$$

Then, the sigmoidal type of function with which $\overline{Z_i}$ calculated is given in Eq. A5c. In this case, K_{ZA} is the half-saturation constant of anchovy consumption on prey, s_j is the food preference coefficient of anchovy on zooplankton.

$$f(T) = \sum_{k=1}^{2} \frac{h_k}{h_1 + h_2} f_k(T_k) \quad \text{and} \quad f_k(T_k) = Q_{10Z}^{(T_k - T_{\max})/T_{Z_{ref}}} \qquad \text{(A5d)}$$

In Eq. A5d, the temperature limitation function in the euphotic zone is given, where $f(T)$ expresses the weighted sum of limitation exerted on the mixed layer and on the sub-thermocline as making use of relative thickness of relative layers $f_k(T_k)$.

Then, $Q_{10Z}^{(T_k - T_{\max})/T_{Z_{ref}}}$ is used to introduce unity to the mixed layer temperature providing that it never exceeds 25 °C. Thus, keeping the temperatures for the mixed layer always between the optimal ranges and let them remain at sub-optimal (7°C) for the sub-thermocline.

$$R_A = r_1 \times W_A^{-r_2} \times f(T) \times A_F \qquad \text{(A6)}$$

In Eq. A6, the respiration (R_A) comprises the summation of routine and active metabolic losses (Luo and Brandt, 1993). Respiration equation involves maximum rate of routine respiration (r_1) at optimal temperature, exponent for weight dependence of respiration (r_2), overall temperature limitation function for the euphotic zone ($f(T)$) and activity factor constant (A_F).

Mathematical formulation of the lower trophic level model

$$f_k(T_k) = Q_{10P}^{(T_k - T_{\max})/T_{P_{ref}}} \qquad \text{(A7)}$$

Eq. A7 is the explicit for of the phytoplankton temperature limitation function ($f_k(T_k)$), where $T_{\max}$=25°C, Q_{10P}=1.5 and T_{Pref}=15°C.